DOT/FAA/AR-11/27

Air Traffic Organization
NextGen & Operations Planning
Office of Research and
Technology Development
Washington, DC 20591

Analysis of Suppression Effects on Aviation Fuel Fires Around an Aircraft

November 2011

Final Report

This document is available to the U.S. public through the National Technical Information Services (NTIS), Springfield, Virginia 22161.

This document is also available from the Federal Aviation Administration William J. Hughes Technical Center at actlibrary.tc.faa.gov.

U.S. Department of Transportation
Federal Aviation Administration

NOTICE

Technical Report Documentation Page

1. Report No.	2. Government Accession No.	3. Recipient's Catalog No.
DOT/FAA/AR-11/27		

4. Title and Subtitle	5. Report Date
ANALYSIS OF SUPPRESSION EFFECTS ON AVIATION FUEL FIRES AROUND AN AIRCRAFT	November 2011
	6. Performing Organization Code
7. Author(s)	8. Performing Organization Report No.
Joseph L. Scheffey, Robert L. Darwin, and Sean Hunt	
9. Performing Organization Name and Address Hughes Associates, Inc. 3610 Commerce Drive, Suite 817 Baltimore, MD 21227-1652	10. Work Unit No. (TRAIS)
	11. Contract or Grant No. DTFACT-05-D-00012
12. Sponsoring Agency Name and Address U.S. Department of Transportation Federal Aviation Administration Air Traffic Organization Operations Planning Office of Aviation Research and Development Washington, DC 20591	13. Type of Report and Period Covered Final Report
	14. Sponsoring Agency Code AAS-300

15. Supplementary Notes

The Federal Aviation Administration Airport Technology Research & Development Branch COTR was Dr. Satish Agrawal.

16. Abstract

This report describes the details of a theoretical analysis of the firefighting agent amounts carried by aircraft rescue and firefighting (ARFF) equipment. The report is a detailed heat transfer and suppression analysis of fuel spill fires on exposed aircraft. This analysis addressed various factors in assessing current ARFF agent requirements. The amount of firefighting agent necessary to prevent interior aircraft ignition and allow for safe egress is presented for representative fuel spill fire scenarios and ARFF arrival times. The scenarios consider wind conditions, aircraft and fuel spill sizes, aircraft skin thickness, and aircraft insulation/construction. For example, fires burning in wind conditions will have a different flame shape and flame length than a fire burning under calm conditions with all other parameters held constant. The analysis also found that the time required to melt the aluminum skin is strongly dependent on the exposure heat flux and on the skin thickness but not on the insulation thickness.

The evaluation of the firefighting agent amount effect on the success of aircraft egress for a given fire scenario must address a number of elements, such as fire effects on egress, ARFF effects on the fire through the agent amount carried, and the relevant fire scenario parameters for the fire, aircraft, and passengers.

17. Key Words	18. Distribution Statement
Aircraft rescue and firefighting, AFFF, NFPA 403, Aircraft survivability, Aviation jet fuel, Composites, Radiation calculations, Heat transfer	This document is available to the U.S. public through the National Technical Information Service (NTIS), Springfield, Virginia 22161. This document is also available from the Federal Aviation Administration William J. Hughes Technical Center at actlibrary.tc.faa.gov.

19. Security Classif. (of this report)	20. Security Classif. (of this page)	21. No. of Pages	22. Price
Unclassified	Unclassified	99	

TABLE OF CONTENTS

LIST OF FIGURES

LIST OF TABLES

LIST OF ACRONYMS

AGA	American Gas Association
ARFF	Aircraft Rescue and Firefighting
FAA	Federal Aviation Administration
NFPA	National Fire Protection Association

EXECUTIVE SUMMARY

To improve the effectiveness of aircraft rescue and firefighting (ARFF) equipment, the Federal Aviation Administration reviewed the current methodology for calculating the total amount of firefighting agent required to combat aircraft crash fires. The approach was to review the historical basis of the calculations, review the loss history of aircraft accidents, and conduct a hazard analysis. The methodology was then assessed based on this analysis. The overall analysis is contained in a technical report, "A Technical Review of Methodologies for Calculating Firefighting Agent Quantities Needed to Combat Aircraft Crash Fires" (DOT/FAA/AR-11/29). The current report is a complementary report detailing the heat transfer and agent calculation analysis presented in the above-mentioned report. The current report provides the detailed technical analysis and calculations for analyzing the suppression effects on aviation fuel fires, which may threaten an aircraft and its occupants.

The current method for determining firefighting agent quantities required at an airport is based on the concept of a critical area, a rectangular box defined by the aircraft's length and fuselage width. Aircraft size and construction materials have evolved to an extent that the concept of a critical area, the fire area that requires immediate fire suppression, should be reassessed. This analysis addressed various factors in assessing current ARFF agent requirements to determine if the critical area concept was still a valid approach.

This report details the heat transfer and suppression analysis of fuel spill fires on exposed aircraft. The amount of firefighting agent necessary to prevent interior aircraft ignition and allow for safe egress is presented for representative fuel spill fire scenarios and ARFF arrival times. The scenarios consider different wind conditions, aircraft and fuel spill sizes, aircraft skin thickness, and aircraft insulation/construction. The analysis supports the overall conclusion that the critical area concept is still valid, subject to modifications to address new aircraft construction materials.

1. INTRODUCTION.

To improve the effectiveness of aircraft rescue and firefighting (ARFF) equipment, the current methodology for calculating the total amount of firefighting agent required to combat aircraft crash fires was analyzed. The approach was to review the historical basis of the calculations, review the loss history of aircraft accidents, and conduct a hazard analysis. The methodology was then assessed based on the results of this analysis. The overall analysis is contained in a technical report, "A Technical Review of Methodologies for Calculating Firefighting Agent Quantities Needed to Combat Aircraft Crash Fires" (DOT/FAA/AR-11/29) [1]. The current report is a complementary analysis to this report, which provides the detailed technical analysis and calculations for analyzing the suppression effects on aviation fuel fires.

The original methodology was developed in the 1970s by aviation experts studying crash data and using rudimentary radiation heat transfer estimates. The approach used a combination of factors involving the thermal threat to passengers, both within the aircraft and escaping outside the aircraft. The length of the aircraft was established as an important dimension of the critical area, based in part on the exposure potential to passengers still within the aircraft. The width of the potential fuel spill fire away from the aircraft, exposing escaping passengers, was more difficult to quantify. Ultimately, the width was established based partly on the relationship of potential radiant heat to escaping passengers, and partly on the amount of actual firefighting agent used at incidents. This resulted in the practical critical fire area needed to be suppressed.

This report addresses factors that can contribute to suppression requirements, including aircraft size, fuel load, passenger load, wind, and fuselage materials. It was concluded that there is no general correlation of the fuel and passenger loads between aircraft across different sized airports. The only trend is a general increase in these loads as aircraft size increases. It was determined that there is no quantitative method to predict how much fuel will spill in a crash, when it will ignite, at what rate it spills, or what total quantity is ultimately involved. An approach was adopted where the fire size was assumed to be unlimited. The agent required to protect occupants was calculated based on existing test data on foam fire suppression and thermal effects on passengers in an intact aircraft that crashed at an airport. This report provides the detailed thermal effects and heat transfer calculations.

This analysis starts with the characterization of a fire scenario. Given the range of aircraft types, airport configurations, and accident types, a large number of fire scenarios are possible. The types of fires considered in this report were fuel spill fires around an aircraft involving fuel that originates from the aircraft, which impedes egress. This is the basic concept embodied in National Fire Protection Association (NFPA) 403, a nationally recognized standard that addresses ARFF services at airports [2]. Scenarios involving storage tanks, secondary aircraft, or structures were not considered since they do not currently form the basis for the required agent amounts.

A large number of variables can affect egress from an aircraft exposed to a fuel fire, for example, whether or not there is a fire inside the aircraft, the severity of any impact, the structural integrity of the aircraft, the number of occupants, aircraft construction, local weather conditions, ARFF response time, and ground contours. A number of these variables may be eliminated from consideration because the egress would be unaffected by the actions of ARFF. For example,

where the aircraft fuselage is structurally breached and the fire immediately spreads into the aircraft. In such cases, the number of survivors depend on the occupants ability to escape before full involvement of the aircraft interior.

It is important to clarify the following terms used in this analysis.

- A fire scenario is treated as a single fire incident with a fixed set of parameters. A scenario would represent the timeline associated with a single aircraft fire incident under a given set of assumptions.

- A parameter is a component of a fire scenario that can vary, either because conditions can vary or because of uncertainty in the appropriate value. The parameters include wind conditions, fire location, aircraft size, ARFF arrival time, and amount of suppression agent that is brought by ARFF.

- The word target is used to describe what is being exposed to the source fire; it is typically the aircraft itself but may also be a passenger. A target may also have a range of parameters associated with it, such as the aircraft skin thickness, the aircraft skin material, the aircraft insulation thickness, the aircraft height, and the orientation of the target surface relative to the fire.

2. APPROACH.

The evaluation of the suppression agent available to the ARFF on the success of aircraft egress for a given fire scenario requires addressing a number of elements:

- Fire effects on egress

- ARFF effects on the fire through the agent amount carried

- The relevant fire scenario parameters for both the fire and the target

To describe the fire effects on egress, both the fire exposure and the conditions that could prevent egress need to be quantified. The fire exposure includes the exposure temperature and the heat flux to the target considered. The fire explosure is related to the fire size, the flame height, and the fire diameter or width. Empirical methods described by Shokri and Beyler [3], Mudan [4 and 5], Muñoz, et al. [6], and the Society of Fire Protection Engineers [7] are used as the basis for making these estimates. The effects of the fire exposure on egress are evaluated by considering the response of the target, or the aircraft, to the predicted exposure for a given fire scenario. This is done using the heat transfer model HEATING [8] and various full-scale test data for aircraft fire exposures [9-11].

The conditions that prevent egress are considered in terms of occupants located inside the aircraft and occupants that are exterior to the aircraft. This is typically referred to as the performance criteria in a performance-based design [12 and 13]. For occupants inside the aircraft, interior ignition is a reasonably conservative benchmark for assessing the egress potential (see section 3). Once ignition inside the aircraft has occurred, the amount of time available for egress can be less than 1 minute, and the amount of agent carried by ARFF becomes a secondary parameter.

Passengers outside the aircraft would be those that have successfully exited and are attempting to move to a safe area. It is assumed in this analysis that such passengers move within 1 m (3 ft) of the aircraft exterior and parallel to the fuselage.

The goal of the study was to link ARFF agent amounts to its egress success. A quantitative relationship between an agent amount and its effect on the fire is required. This is found by assuming a conservative extinguishing effectiveness of the agent of 5.2-L agent/m² of fire (0.13-gal agent/ft² of fire) [14]. For first responding units, a 60-second delivery time is also assumed, consistent with current requirements. This information effectively allows for an offset distance between the fire and the aircraft to be imposed, possibly over a 60-second period, once the first responding units arrive. By increasing the offset distance, the fire exposure boundary conditions change, and as a result, the target response and the egress conditions are affected.

The analysis is implemented by considering the first responding units and subsequent units separately. The first responding units are assumed to be focused on suppressing the fire with their available capacity (Q_1); the second responding units are assumed to provide additional suppression so that occupants can safely leave the aircraft and move to a safe area (Q_2). The first responding units are considered successful if they create conditions that remove any hazards to the aircraft occupants remaining in the aircraft. This means that subsequent response units only need to suppress the fire to allow passengers to escape.

As previously noted, many parameters can affect the severity of the fire as well as the response of the target to the fire exposure. Table 1 summarizes the key parameters considered in this analysis and provides the range of values considered. The ranges are based on available data for large commercial aircraft and airport crash fire and rescue departments and are not necessarily bounding. The ranges provide a significant cross-cut through the parameter space and their consideration provides sufficient insight toward addressing the goal of this study.

Table 1. Fire Scenario and Aircraft Parameter Ranges

Parameter	Range	Basis
Aircraft length	27-73 m (89-240 ft)	Range of large commercial aircraft addressed by NFPA 403 [2].
Aircraft external elevation	0-6 m (0-20 ft)	Estimated range of values for large aircraft tested [9 and 11].
Aircraft skin material	Aluminum or composite	Welker [15], Sarkos [16], and Marker [17]
Aircraft skin thickness	0.5-2.5 mm (0.02-0.1 in.)	Welker [15], Sarkos [16], and Marker [17]
Aircraft insulation thickness	0-10 cm (0-4 in.)	Welker [15] and Marker [17]
Aircraft skin orientation relative to fire exposure	Any angle	Due to various curves about the fuselage and wing structure, all surface angles are considered.

Table 1. Fire Scenario and Aircraft Parameter Ranges (Continued)

Parameter	Range	Basis
Maximum initial suppression agent amount	18,900 L (5,000 gal)	Reasonable upper bound based on NFPA 403 [2].
Wind	0-8.9 m/s, any direction (0-20 mph, any direction)	High crosswind speed that may occur on airport site
Passenger elevation	0-1.8 m (0-6 ft)	A person is assumed to extend from the ground to the average height for a person.
Passenger skin orientation relative to the fire	Any angle	Due to various curves on the surface of persons, all surface angles are considered.
ARFF arrival time	1-4 minutes	Higher and lower than NFPA 403 [2] current requirements.

3. PERFORMANCE CRITERIA.

A critical component to assessing the adequacy of suppression agent amount is the characterization of the fire effects on the aircraft and its occupants. When the fire effects are sufficiently characterized, a direct means of assessing the benefits of suppressing varying fractions of the fire becomes available. Therefore, a minimum amount of suppression agent necessary to prevent a certain outcome, if preventable, may be determined for any given scenario.

Assuming the goal of suppressing an exposure fire is to prevent further harm to the aircraft occupants, the fire effect of interest is the tenability within the aircraft and along the escape route outside the aircraft. Tenability is typically treated as a multicomponent parameter within an enclosure involving the temperature, incident heat flux, visibility, oxygen concentration, toxic gas concentrations, and irritant gas concentrations [18]. Outside an enclosure, the tenability component of interest is typically just the incident heat flux since there must be some displacement between the exposed person, the fire, and the fire plume for a tenable condition to exist.

Although current egress requirements for aircraft specify that all occupants must be able exit the aircraft within 90 seconds, conditions outside the aircraft could prevent or limit the escape process. In addition, because occupants may be injured or immobile, assuming occupants leave the aircraft within 90 seconds may not be a conservative approach.

Full-scale test data on aircraft indicate that once interior ignition has occurred, conditions within the cabin could become untenable within 60 seconds [9, 10, 11, and 19]. It is important to note that this does not mean conditions will always become untenable in such a short time, rather, that it is possible under the right circumstances. Whether or not conditions become untenable involve numerous parameters that are not explicitly considered in this analysis: the location where interior ignition occurs, the number of exits that are open, the material first ignited, the availability of combustibles in the area of ignition, etc. Fire tests on passenger rail cars, which are configured similarly to a moderate-sized aircraft cabin, indicate that once ignition has

occurred, flashover conditions could occur in less than 60 seconds [20]. In these tests, flashover is identified by a rapid increase in the heat release rate. This provides further evidence that once interior ignition has occurred, egress could be severely impacted in less than 60 seconds.

For a direct exposure to the occupants, as would be the case once they have exited the aircraft, there are two types of approaches typically taken. The simplest approach is to assume a steady-state exposure value. Based on data presented by Purser [18] and Babrauskas [21], an incident heat flux of 2.5 kW/m² (0.22 Btu/s-ft²) corresponds to a reasonable tenability limit for radiant exposures. This value is conservatively assumed in this analysis. The second approach involves an integrated or dose-type model, which has precedent in reference 14. Such an approach assumes that passengers can be exposed to higher heat fluxes for shorter times and that the product of the exposure time to the heat flux is more or less constant. This approach is significantly more complex but would result in a shorter fire offset distance and, hence, less suppression agent for successful exterior egress. The difference in the predicted agent amount that would be computed from either method is not expected to be significant enough to warrant a more detailed analysis of the direct heat flux exposures to aircraft occupants.

The performance criteria used in this analysis can be summarized as follows:

- Interior ignition: if interior ignition is prevented by the first responding units, the scenario outcome is deemed successful.

- Direct occupant exposure: incident heat flux exposure to an aircraft passenger outside the aircraft along the assumed egress route is 2.5 kW/m². The amount of agent necessary to provide an offset distance that creates this condition is determined, and if the total amount of agent available is equal to or greater than this quantity, the scenario outcome is successful.

4. FUEL SPILL FIRES.

The primary or initial exposure fire considered in this analysis is a fuel spill fire exterior to the aircraft. The fuel is assumed to spill from the aircraft and spread in an area adjacent to and around the aircraft. Fires that originate within the aircraft are not considered as they could lead to rapid flashover conditions [10, 11, 12, and 20] and successful egress of the aircraft occupants would depend strongly on parameters other than the amount of suppression agent brought by the initial response team.

4.1 FUEL SPILL FIRE CHARACTERISTICS.

4.1.1 Fuel Spill Configuration and Dimensions.

One of the most significant parameters associated with a fuel spill fire around an aircraft is the spill area. This is because other parameters from which the exposure and interior ignition potential are determined are based on the assumed fuel spill area and shape. Certainly, each fuel spill incident will essentially be unique as it depends on the fuel amount, the location of the fuel spill, the rate at which the fuel is spilled, the local ground conditions, and even the actions of the pilot with regard to positioning the plane in cases where it is still mobile. A number of possible fuel spill configurations around an aircraft are shown in figures 1a through 1f. The configuration

shown in figure 1a is the worst-case exposure scenario. The aircraft is entirely within the fuel pool, possibly due to fuel spilling from all sources on the aircraft and an unfavorable ground contour. Figure 1b shows the configuration observed in actual aircraft incidents, which is a common configuration used for full-scale tests [10, 11, 19, and 22]. This configuration typically arises when fuel leaks from one wing area and the ground contours divert the fuel away from the aircraft. Note that the fuel spill offset distance from the aircraft can be as little as zero. Figure 1c shows a variation of the configuration shown in figure 1b in which the fuel leaks from both wings, and the ground is contoured such that fuel flows away from the aircraft in two directions. This configuration essentially represents a double, simultaneous failure of the wing fuel tanks, possibly due to the impact and adverse ground contour. In this case, the exposure to the aircraft can be characterized by the configuration shown in figure 1b; however, the calculations relating to the amount of suppression agent would need to be revised.

The configuration shown in figure 1d is also a variation of figure 1b. In this case, fuel can leak from one or both wing tanks and the ground is contoured such that the fuel flows toward and away from the front of the aircraft. This configuration is essentially bound by the configuration shown in figure 1b.

The configurations shown in figures 1e and 1f represent more severe exposures to the aircraft. However, they can arise under less general ground contours and are less likely configurations than those shown in figures 1a through 1d. As such, they are not considered in this evaluation.

The configurations shown in figures 1g and 1h are dynamic fuel spills. In these cases, the fuel leaks from the aircraft and forms a growing liquid pool either toward or away from the aircraft. The 1985 incident at the Manchester, United Kingdom airport was, initially, a variation of the configurations shown in figures 1g and 1h [22]. Dynamic fuel spills are expected to be bound by the static configurations since the fuel spill area, fire size, flame height, and exposure heat flux are increasing.

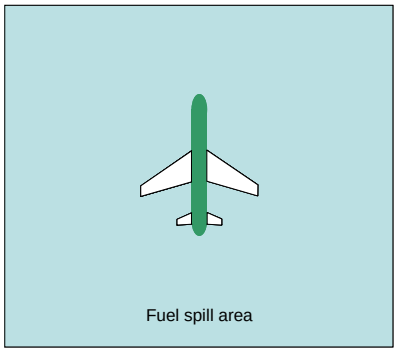

Figure 1a. Fuel Spill Surrounding the Aircraft

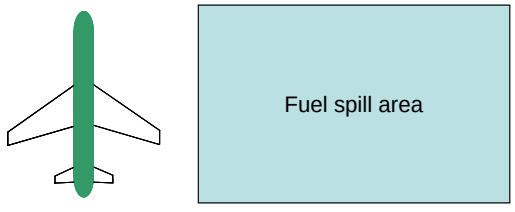

Figure 1b. Fuel Spill Adjacent to the Aircraft on One Side

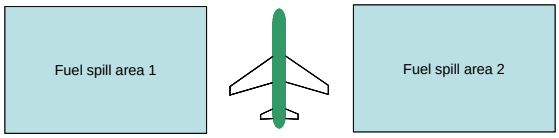

Figure 1c. Fuel Spill Adjacent to the Aircraft on Two Sides

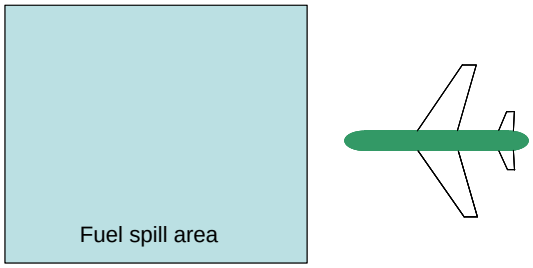

Figure 1d. Fuel Spill in Front of the Aircraft

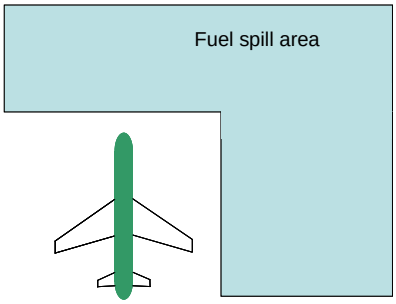

Figure 1e. Fuel Spill Adjacent to and in Front of the Aircraft

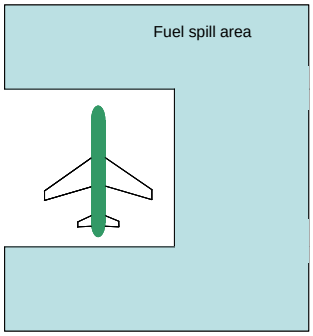

Figure 1f. Fuel Spill Adjacent to, in Front of, and Behind the Aircraft

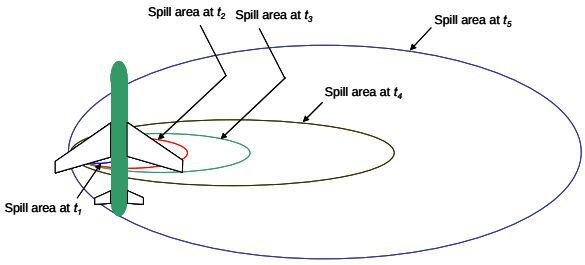

Figure 1g. Dynamic Fuel Spill Immersing the Aircraft

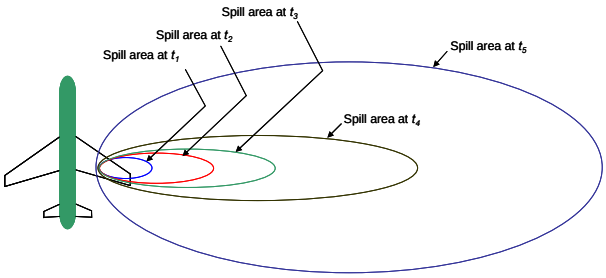

Figure 1h. Dynamic Fuel Spill Adjacent to the Aircraft

The fuel spill area, the fuel spill dimensions, and the fuel spill offset distances from the aircraft associated with the fuel spill configurations shown in figures 1a through 1f can vary also with time. The amount of fuel involved, ground contour, ground porosity, drainage capacity, and fuel spill rate, among other things, could lead to different fuel spill sizes and offset distances, given a configuration. To limit the number of scenarios to a manageable but reasonably bounding subset, a number of assumptions were made with regard the fuel spill dimensions, which are as follows:

- The characteristic dimension of any fuel spill is the length of the aircraft involved, L_a (m (ft)). This dimension is the diameter of the fuel spill fire, if the aircraft is immersed, or the width of the fuel spill fire adjacent to the aircraft, if the fuel spill is offset from the

aircraft. The aircraft lengths were between 27.1 and 73.2 m (89 and 240 ft), as described in table 1. This assumption is consistent with the dimensions compiled from actual incidents by Cohn, et al. [23].

- The fuel spill area is static, except for suppression effects. The fuel is assumed to have spilled from the aircraft and formed a pool that does not increase in size or spread toward the aircraft.

- The extent of the fuel spill away from the aircraft is unlimited when there is an initial offset between the fuel spill and the aircraft. When the aircraft is assumed to be fully immersed, a finite extent is assumed; otherwise, suppression efforts would have no effect on the exposure near the aircraft.

- Fuel spills initially offset from the aircraft are located on one side of the aircraft only.

- Adequate fuel is available to form the postulated fuel spill areas and to allow the scenario to persist as necessary in the analysis.

The consequence of the aforementioned assumptions is that only the configurations shown in figures 1a and 1b are considered. Other configurations are expected to be (1) bound by those considered, (2) extensions of those considered, or (3) too specific to the local ground conditions to warrant further analysis. The fuel spill configurations and the relevant dimensions for the two cases are shown in figure 2a for a scenario that immerses an aircraft, and in figure 2b for a fuel spill fire initially offset from the aircraft at a distance of S_i (m (ft)).

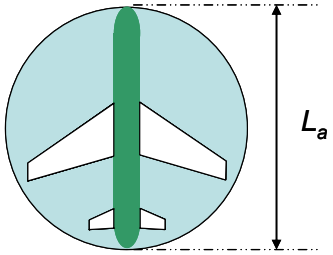

Figure 2a. Assumed Dimensions for a Fuel Spill Fire That Immerses an Aircraft

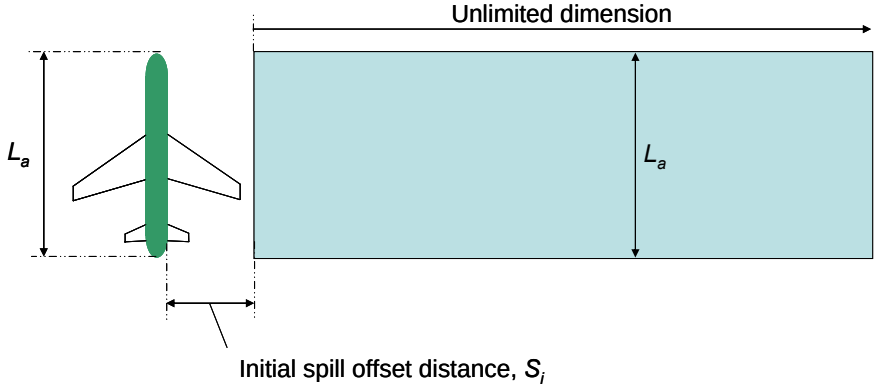

Figure 2b. Assumed Dimensions of an Initial Fuel Spill Fire Offset From Aircraft

The only dynamic modifications to the fuel spill area considered in this calculation during the postulated fire scenarios are those associated with the suppression actions of ARFF. As noted in section 2, the suppression agent is assumed to have an extinguishing capacity of 5.2 L agent/m² of fire (0.13 gal agent/ft² of fire) [14]. This is equivalent to 0.19 m² of fire area suppressed per liter of agent applied (7.7 ft² of fire area suppressed per gallon of agent applied). The first responding unit is assumed to apply their entire amount of agent at a constant rate over a 60-second period, as described in section 2. This led to a linear reduction in the fuel fire area or a linear increase in the fire offset distance from the aircraft between the time the agent was first applied and the time the initial agent amount was depleted. Consideration of the dynamic effects on the fuel spill area or offset distance due to additional responding units was not considered since the focus would change to life safety (i.e., egress away from the aircraft) rather than the prevention of interior aircraft ignition.

Suppression effects for fuel spill fires that immerse the aircraft are assumed to reduce the diameter such that the fuel spill area decreases in proportion to the amount of agent applied (see figure 3). The fuel spill fire area as a function of time may be computed using the following equation.

$$A(t) = A_i - \frac{V_A}{\Delta t_A} k_A t \qquad \frac{V_A}{\Delta t_A} k_A t < A_i$$

$$A = 0 \qquad \frac{V_A}{\Delta t_A} k_A t \geq A_i \tag{1}$$

where A is the fuel spill fire area (m² (ft²)) at t (seconds) after suppression has begun, A_i is the initial fuel spill fire area (m² (ft²)), V_A is the agent amount carried by the first responding units (m³ (ft³)), Δt is the time interval over which the initial amount of agent is applied (60 seconds), and k_A is the suppression capacity of the agent (189 m² fire area suppressed/m³ agent applied (58 ft² fire area suppressed/ft³ agent applied)). Equation 1 applies to the first responding units. Further reductions in area are possible as additional units arrive and bring more suppression agent. Figure 4 depicts the fuel spill fire area as a function of time for a 73.2-m (240-ft)-long aircraft fuel spill fire and different agent amounts brought by the first responding units. The results are similar for other aircraft lengths. Although other means of suppressing such fires are possible (upwind, from the aircraft outward, etc.), there is limited opportunity to prevent interior aircraft ignition when the aircraft is immersed by the fire, regardless of the suppression tactics, as discussed in section 6.

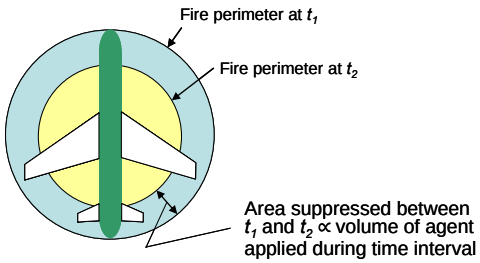

Figure 3. Fuel Spill Fire Area During Suppression Activities for Immersed Aircraft Scenarios

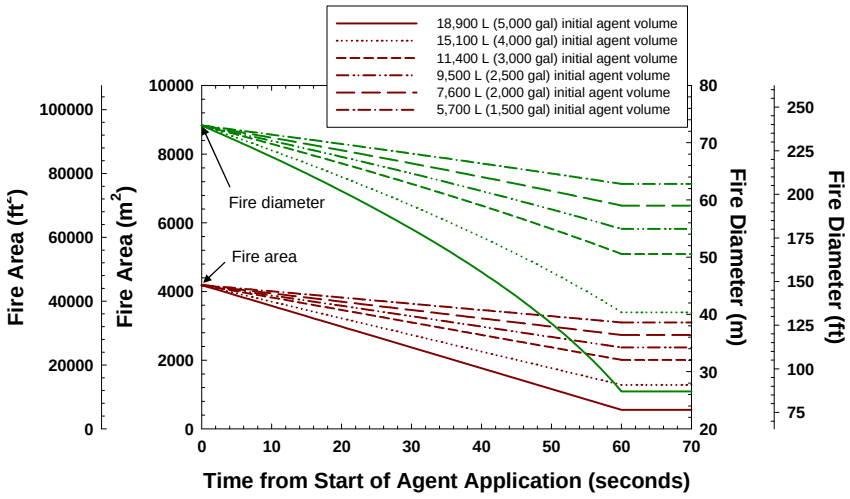

Figure 4. Dynamic Fuel Spill Fire Area due to Suppression by First Responding Unit (Fully Immersed Aircraft—73.2 m (240 ft) Long)

Suppression effects for fuel spill fires that are offset from the aircraft are assumed to increase the offset distance in proportion to the amount of agent applied (see figure 5). The offset distance as a function of time may be computed using the following equation assuming the agent is supplied at time zero.

$$S_a(t) = S_{a,i} + \frac{1}{L_a}\frac{V_A}{\Delta t_A}k_A t \tag{2}$$

where $S_a(t)$ is the fuel spill fire offset distance (m (ft)) at t (seconds) after suppression has begun, and $S_{a,i}$ is the initial fuel spill fire offset distance (m (ft)). Equation 2 applies to the first responding units. Further increases in the offset distance and complete suppression of the fire become possible as additional units arrive and bring more suppression agent.

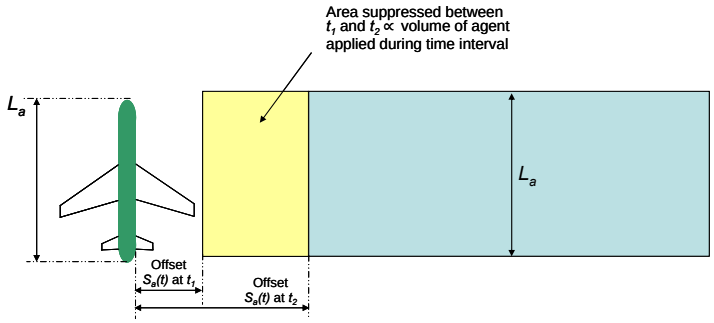

Figure 5. Offset Fuel Spill Fire Area During Suppression Activities

Figure 6 depicts the fuel spill fire area as a function of time for a 27-m (89-ft)- and a 73.2-m (240-ft)-long aircraft fuel spill fire and different agent amount brought by the first responding units. The results show that for a given agent amount, the offset distances are increased the most for smaller aircraft. This indicates that the required agent amount is to some extent proportional to the length of the aircraft, consistent with the current NFPA 403 approach.

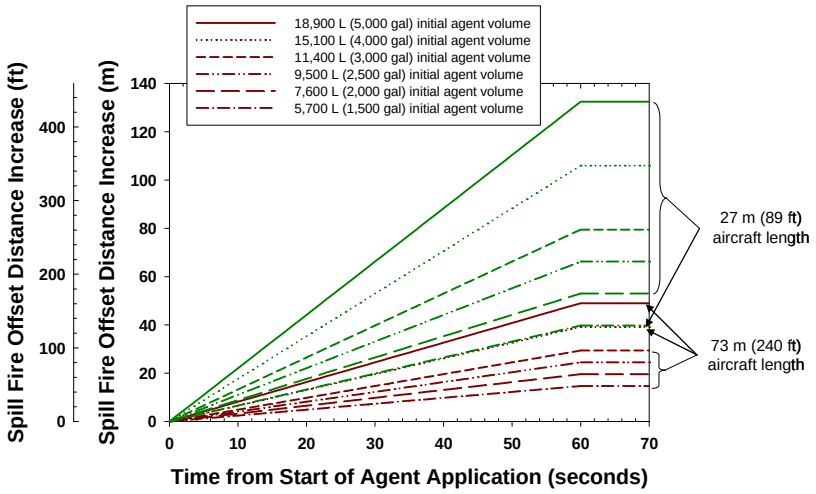

Figure 6. Dynamic Fuel Spill Fire Area due to Suppression by First Responding Unit (Two Fully Immersed Aircraft—27 m (89 ft) and 73 m (240 ft) Long)

4.1.2 Fuel Combustion and Physical Properties.

This research focused on fuel combustion and physical properties, including the heat of combustion, the burning rate, the heat release per unit area, and the density. There is little variation in these properties among the various aviation fuels [24 and 25]. However, the properties of JP-5 were assumed in this evaluation because this fuel has a somewhat greater heat release rate per unit area among the aviation fuels. Table 2 summarizes the data for deep-pool burning (greater than 2.5 mm (0.1 in.)) [26] of JP-5. Shallow-pool burning is not postulated in this evaluation but would normally be characterized using a burning rate and heat release rate per unit area that is one-fifth of the deep-pool burning [26].

Table 2. Fuel Combustion Properties for JP-5

Heat of Combustion, ΔH_c (kJ/kg (Btu/lb))	Burning Rate, $\dot{m}''$ (kg/s (lb/s))	Heat Release Rate per Unit Area, $\dot{q}''$ (kW/m² (Btu/s-ft²))	Density, ρ (kg/m³ (lb/ft³))
43,000 (18,500)	0.054 (0.119)	2320 (204)	810 (50.5)

4.1.3 Fire Size.

The fire size is used to determine the flame length, which, in turn, is used to determine whether flames impinge on the aircraft, and to determine the exposure heat flux. The fire size is, in general, a function of the fuel spill area, as follows [24]:

$$\dot{Q} = \dot{q}'' A_f \tag{3}$$

where $\dot{Q}$ is the heat release rate (kW), $\dot{q}''$ is the heat release rate per unit area (kW/m² (Btu/s-ft²)), and A_f is the fuel spill area (m² (ft²)).

In this evaluation, fuel spill fire incidents that do not immerse the aircraft are treated as essentially unrestricted in terms of their extent beyond the aircraft. This creates some difficulty in assessing the fuel spill area parameter. To circumvent this difficulty, two fuel spill areas are considered: one associated with an axisymmetric pool having an effective diameter equal to the width of the aircraft and one associated with a line fire having a width equal to the length of the aircraft (see figure 7).

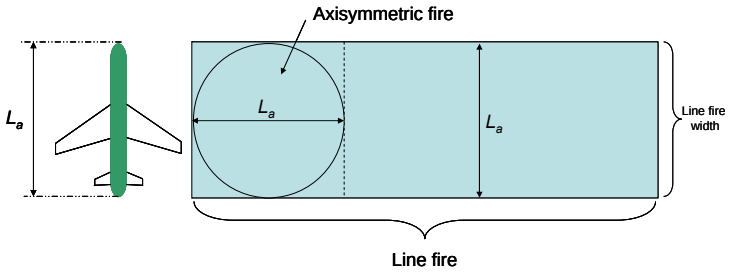

Figure 7. Fuel Spill Fire Areas Used to Compute Heat Release Rate Parameters

The relevant parameter for line fires is the heat release rate per unit area. This is given by the following equation [24].

$$\dot{Q}' = \dot{q}'' L_a \tag{4}$$

where $\dot{Q}'$ is the heat release rate per unit length of a line fire (kW/m (Btu/s-ft)) and L_a is the length of the aircraft (m (ft)), assumed to range between 27.1 and 73.2 m (89 and 240 ft), as described in sections 2 and 4.1.1.

The heat release rate and heat release rate per unit area for aircraft lengths between 27.1 and 73.2 m (89 and 240 ft) computed using equations 3 and 4 is shown in figure 8. The figure indicates that the fire sizes can be on the order of 10,000 MW (9,480 MBtu/s) for large fuel spill areas with characteristic dimensions comparable to the length of a large aircraft.

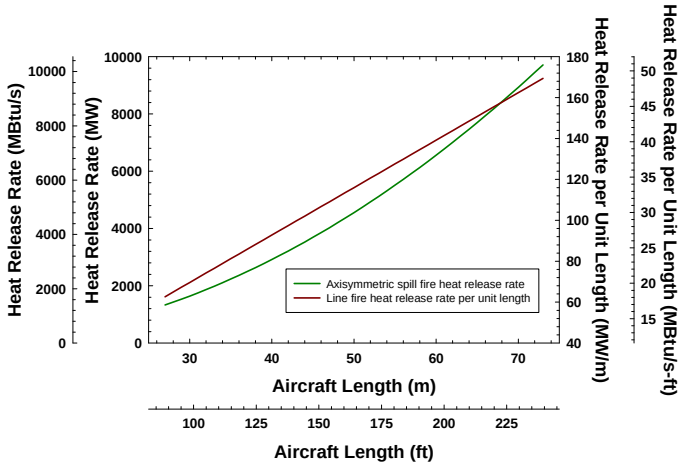

Figure 8. Fuel Spill Fire Heat Release Rate as a Function of the Characteristic Dimension (the Aircraft Length)

Equations 3 and 4 yield the steady-state heat release rate or heat release rate per unit length, given a fuel spill width, which is assumed to be equal to the aircraft length. No consideration is given to the time needed for the fire to spread over the pool surface or for dynamic fuel spill areas resulting from spilling or spreading liquid fuel. The growth time for large fuel spill fires may be substantial. Webster [19] noted growth times on the order of 30-60 seconds for fuel spill fires in the 6- to 10-m (20- to 35-ft) range. Gottuk, et al. [26], suggests that the gas phase flame spread rate on liquid fuels is a function of the fuel temperature and flashpoint, which typically lies between 1.3 and 2.2 m/s (4.3 and 7.2 ft/s). Since the pool width is assumed to be equal to the aircraft width, the flame spread time over the largest pool widths (73.2 m (240 ft)) could approach 60 seconds, consistent with the observations of Webster [19] for smaller fires. Dynamic fuel spill fires include those for which the fuel is draining from the aircraft and spreading over the ground surface, according to the ground contours. These types of scenarios have been noted to occur and may result in a lower heat release rate fire but not necessarily shorter internal ignition times [22 and 23]. By ignoring the growth time and dynamic fuel spill characteristics, the predicted interior ignition times may be conservatively biased by as much as 1 minute or longer, especially for scenarios for which there are initial offset distances between the fire and the aircraft exterior.

4.1.4 Fuel Consumption.

The fuel mass loss rate per unit area is an input parameter for determining the flame height under various wind conditions and is a fuel combustion property. The total volumetric fuel loss rate and total fuel consumption are not directly used in the calculation but provide a means to compare the fuel amount needed to sustain a postulated scenario for a given amount of time against the fuel amount typically carried by an aircraft.

The total fuel mass loss rate for constant area axisymmetric fires is given by the following equation.

$$\dot{V} = \dot{m}'' A_f \rho \tag{5}$$

where $\dot{V}$ is the total fuel volumetric fuel loss rate (m^3/s (ft^3/s)), $\dot{m}''$ is the mass loss rate per unit area for the fuel (kg/s-m^2 (lb/s-ft^2)), A_f is the fuel spill fire area (m^2 (ft^2)), and ρ is the fuel density (kg/m^3 (lb/ft^3)). Similarly, the total volumetric fuel consumption at any time for the constant area axisymmetric fuel spill fire is given by the following equation:

$$V(t) = \dot{V} \Delta t \tag{6}$$

where V is the total amount of fuel consumed (m^3 (ft^3)) over the time interval Δt (seconds). The equations assume a static pool size, as described in section 4.1.1. Suppression activities are assumed to linearly reduce the fuel spill fire area over the time the suppression agent is applied when the aircraft is immersed in the pool. In this case, the fuel spill fire area A_f (m^2 (ft^2)) in equation 5 would be the linear function given by equation 1, and the total amount of fuel consumed could be determined by integrating equation 5 with respect to time. Table 3 summarizes the fuel consumption rate for constant area axisymmetric fires around various-sized aircraft. Figure 9 shows the fuel amount required to sustain axisymmetric fires as a function of

time. The figure indicates that the total amount required to sustain fires longer than about 5 minutes approaches the fuel capacity for many types of aircraft.

Table 3. Fuel Consumption Rates for Various-Sized Axisymmetric Fires

Aircraft Length/Characteristic Fire Dimension (m (ft))	Fire Area, A_f (m² (ft²))	Total Fuel Mass Loss Rate, $\dot{M}$ (kg/s (lb/s))	Total Fuel Mass Loss Rate, $\dot{V}$ (L/s (gal/s))
27.1 (89)	578 (6,220)	31.2 (68.6)	38.5 (10.2)
37.5 (123)	1,100 (11,880)	59.4 (130.7)	73.3 (19.4)
46.6 (153)	1,710 (18,390)	92.3 (203.1)	114 (30.2)
60.1 (197)	2,830 (30,480)	152.8 (336.2)	189 (50)
70.4 (231)	3,900 (41,910)	210.6 (463.3)	260 (67.8)
73.2 (240)	4,200 (45,240)	226.8 (499)	280 (74.1)

Fuel spill fire exposures adjacent to the aircraft are treated as either axisymmetric fires or line fires, whichever produces the most severe condition for a given scenario. The fuel consumption rate for the axisymmetric approach, which corresponds to the portion of the fire burning nearest the aircraft, is shown in table 3 and figure 9. The fuel consumption for a line fire varies with the actual extent; however, by assumption, the extent is undefined. The consumption rate for a line fire as a function of the extent is shown in figure 10. Comparing these results with the data shown in table 3 indicates that the consumption and, thus, the expected total fuel amount necessary to sustain the postulated fire increases rapidly with the extent of the line fire.

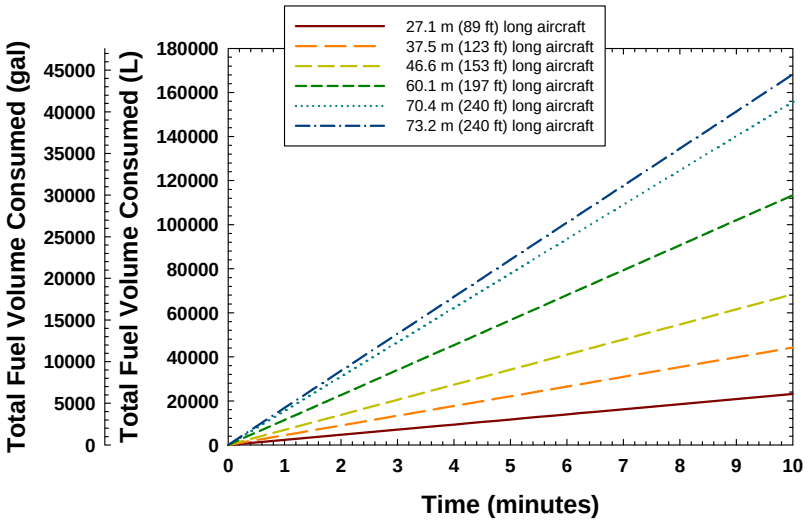

Figure 9. Total Fuel Consumption for Various-Sized Axisymmetric Aircraft Fires

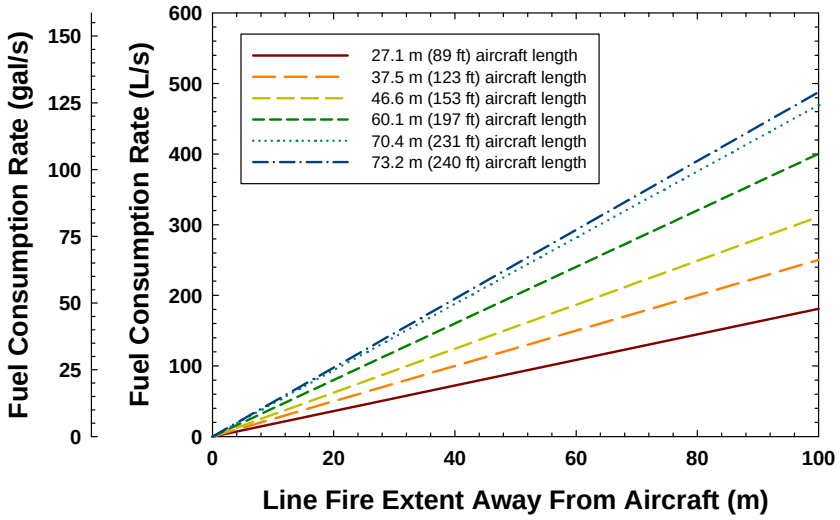

Figure 10. Fuel Consumption Rate for Line Fires

The fuel consumption estimates indicate that the amount of fuel necessary to sustain a large pool fire approaches the total amount of fuel carried by aircraft within several minutes. Fuel amounts are not explicitly accounted for in this calculation; instead, it is assumed an adequate amount of fuel is available to sustain the postulated fire. This introduces some additional conservatism when low fuel amount, long-duration fires, or favorable ground conditions are factors.

4.1.5 Flame Height.

The flame height or flame length is used to determine the shape of the flame and to assess whether the flames impinge on the aircraft fuselage under wind conditions (see section 4.1.7). As described in sections 4.1.6 and 4.2, the flame height is an input parameter for determining the view factor and, ultimately, the incident heat flux for scenarios where flame impingement on the aircraft is not postulated. The Mudan [4] method is used in this calculation because it provides the most conservative emissive power function for the fire sizes considered. The mean visible flame height correlation associated with this method is used [4 and 7].

$$H_{f,as} = 42D\left(\frac{\dot{m}''}{\rho_a\sqrt{gD}}\right)^{0.61} \tag{7}$$

where $H_{f,as}$ is the flame height for an axisymmetric pool fire (m (ft)), $\dot{m}''$ is the mass burning rate of the fire (kg/s (lb/s)), ρ_a is the ambient density (kg/m³ (lb/ft³)), g is the acceleration of gravity (m/s² (ft/s²)), and D is the diameter of the fire (m (ft)). Equation 7 was originally developed by Thomas [27] for wood-based fires but has been successfully used to predict the heat flux from hydrocarbon fuel fires having diameters on the order of 100 m (330 ft) [4 and 7].

Equation 7 is applicable to axisymmetric fires. For a line fire, as postulated for fuel spills adjacent to an aircraft, a greater flame height could result due to the reduced entrainment. The flame height in this case is given by the following equation [28].

$$H_{f,lin} = 0.034\dot{Q}'^{2/3} \qquad (SI)$$
$$H_{f,lin} = 0.255\dot{Q}'^{2/3} \qquad (English) \tag{8}$$

where $H_{f,lin}$ is the flame height for a line fire type approximation to the fuel spill area (m (ft)) and $\dot{Q}'$ is the heat release rate per unit area (kW/m (Btu/s-ft)), as given by equation 4. The Mudan method is correlated using the axisymmetric flame height of equation 8. Thus, to account for line fires while maintaining a conservative analysis, the flame height is taken as the maximum of equations 7 and 8.

$$H_f = \max(H_{f,as}, H_{f,lin}) \tag{9}$$

where H_f is the assumed flame height for fires offset from the aircraft (m (ft)). It is readily observed that equation 9 will conservatively skew the results toward a higher target heat flux since the emissive power of the fire described in section 4.1.6 is not decreased to account for the increased flame-emitting area.

Figure 11 shows the flame height predicted using equations 7 and 8 for a range of fire diameters or line fire widths (aircraft lengths). Also shown in figure 11 is the flame height predicted using the more general Heskestad [29] correlation for axisymmetric fires.

$$H_{f,as} = -1.02D + 0.23\dot{Q}^{0.4} \qquad (SI)$$
$$H_{f,as} = -1.02D + 0.77\dot{Q}^{0.4} \qquad (English) \tag{10}$$

where $\dot{Q}$ is the fire size (kW (Btu/s)), as given by equation 3. Figure 11 indicates that the line fire produces the greatest flame height for a given fire diameter over the range of interest. Also, the Heskestad [29] correlation and the Thomas [27] correlation agree reasonably well for the fire diameter range of interest and all are bound by the line fires. This provides further evidence of a conservative bias in the flame height approach for fuel spill fires that are offset from the aircraft.

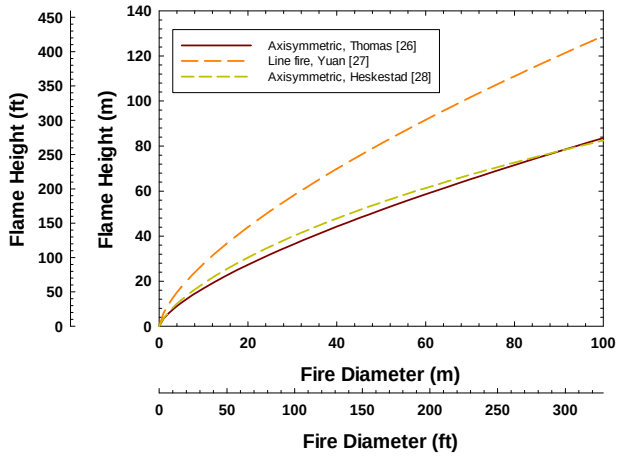

Figure 11. Predicted Flame Height for Axisymmetric and Line Fires as a Function of the Characteristic Dimension

4.1.6 Flame Emissive Power.

The emissive power of the fire is used to determine the incident heat flux for targets that are not within the flames (i.e., fuel spill offset configurations). The emissive power varies significantly over the flame surface both spatially and temporally, as shown in figure 12, for a 6-m (20-ft)-diameter diesel fuel fire [6]. Several features are apparent in this figure, such as:

- The peak emissive power is about 140 kW/m² (12.3 Btu/s-ft²) in a small region near the fire centerline between 10% and 30% of the flame height.
- The emissive power is effectively triangular or conical in shape.
- Over half of the region above the base of the fire and below the flame tip has an emissive power below 20 kW/m² (1.8 Btu/s-ft²).

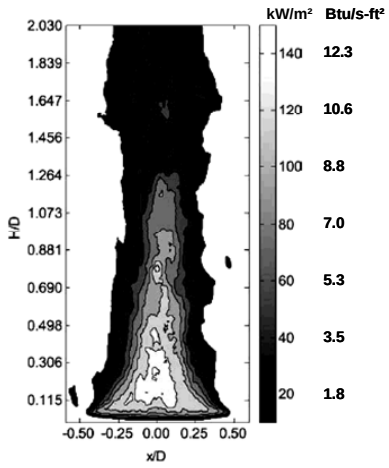

Figure 12. Spatial Variation of the Emissive Power Over the Flame Surface for a 6-m (20-ft)-Diameter Diesel Pool Fire [6]

Because the emissive power of the flame is a complex function of space and time, an effective or average emissive power is typically assumed for radiation heat transfer computations [3, 4, and 30]. The effective emissive power may be regarded as a time averaged value over an assumed flame shape, typically a cylinder or a cone. Mudan [5] correlated the effective emissive power from large pool fires assuming a cylindrical flame shape having a height as determined using equation 7 [4 and 7].

$$E = E_f \exp(-kD) + E_s(1 - \exp(-kD) \tag{11}$$

where E is the emissive power (kW/m² (Btu/s-ft²)), E_f is the maximum flame emissivity (120 kW/m² (10.6 Btu/s-ft²)), k is an extinction coefficient (0.12 m^{-1} (0.037 ft^{-1})), D is the fire diameter (m (ft)), and E_s is the soot or smoke emissivity (20 kW/m² (1.8 Btu/s-ft²)). The Mudan method is used because it provides the most conservative estimate of the emissive power among those available for the large size aircraft. The emissive power as a function of the fire diameter as predicted using equation 11 is shown in figure 13. This equation is applied to line type fires using the line fire width as the diameter.

Other detailed methods that are correlated against smaller-sized pool fire data may predict significantly lower emissive powers at large diameters. The emissive power predicted by the Shokri and Beyler [3] method given by the following is shown in figure 13.

$$E = 58 \cdot 10^{-0.00823D} \qquad (SI)$$
$$E = 55 \cdot 10^{-0.0025D} \qquad (English) \tag{12}$$

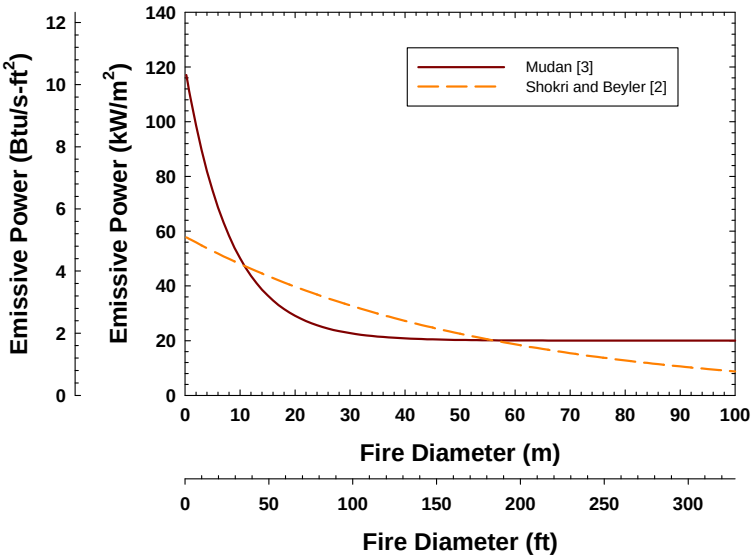

Figure 13. Effective Emissive Power of Pool Fire Flames as a Function of the Fire Diameter

The Shokri and Beyler emissive power correlation is somewhat more conservative than the Mudan correlation [4] for fire diameters between approximately 12 and 55 m (39 and 180 ft), which includes the lower range of the aircraft sizes considered. However, for the larger aircraft, which much of the analysis is focused on, the Mudan model is more apt. The Shokri and Beyler model would not predict failure for fires greater than approximately 100 m (328 ft) since the incident heat flux is below the threshold value for interior ignition (see section 5).

The emissive power for large-diameter fires may be significantly reduced when compared to small-diameter fires due to soot and smoke obscuration [4 and 7]. Data for very large fires (~50-100 m (~164-332 ft) in diameter) suggest that the average emissive power may be as low as 20 kW/m² (1.8 Btu/s-ft²) due to smoke obscuration [4 and 7]. Figure 13 shows that this effect is adequately addressed by equation 11. The decreasing emissive power with increasing fire diameter or, conversely, the increasing emissive power with decreasing fire diameter may create counterintuitive results: small-diameter, localized fire exposures could result in internal aircraft ignition sooner than a large-diameter fire for small offset distances. As the offset distance increases, the view factor and, thus, the incident heat flux at the aircraft rapidly decrease. The distance at which a large-diameter fire becomes more severe will vary from scenario to scenario. However, the small-diameter fires would be readily suppressed by the agent amount carried by the first responding units; any increase in agent amount would not affect the outcome of the scenario. As such, small, localized fire exposures are not considered in detail in this calculation (see section 7).

4.1.7 Wind Effects.

Fires burning in wind conditions have a different flame shape and flame length than a fire burning under calm conditions with all other parameters held constant [5, 6, and 7]. Figure 14 shows the effects of wind on a fuel spill fire, as well as the key parameters of interest. When there is a steady wind with a characteristic velocity, u_w (m/s (ft/s)), the flame will tilt an angle, θ, (radians (degrees)) relative to the vertical axis above the fire centerline, C_L. The original flame length, H_L, (m (ft)) will also be reduced to $\bar{F}_L$ (m (ft)) due to the different mixing conditions [6 and 7]. It is possible that the flames adhere to the ground surface near the base via a flame drag phenomenon [7 and 27]. This phenomenon is not expected to significantly affect the results of this analysis since multiple target heights are considered and thus is ignored.

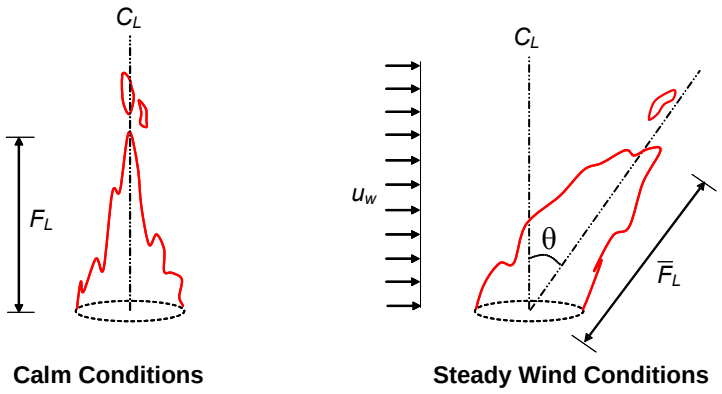

Figure 14. Effect of Wind on a Fuel Spill Fire

The method for determining the flame tilt and modified flame length under wind conditions is that proposed by the American Gas Association (AGA) for large hydrocarbon pool fires [7 and 31]. The flame length is given by the following equation for axisymmetric pool fires [7].

$$\bar{F}_L = 55D\left(\frac{\dot{m}''}{\rho_a\sqrt{gD}}\right)^{0.67}\left(u^*\right)^{-0.21} \tag{13}$$

where $\bar{F}_L$ is the flame length under wind conditions (m (ft)) and u^* is a nondimensional wind speed parameter (–). The nondimensional wind speed parameter is given by the following equation [7].

$$u^* = \frac{u_w}{\left(\frac{g\dot{m}''D}{\rho_a}\right)^{1/3}} \tag{14}$$

where u_w is the wind speed (m/s (ft/s)), g is the acceleration of gravity (m/s² (ft/s²)), $\dot{m}''$ is the mass loss rate per unit area of the burning fuel (kg/s-m² (lb/s-ft²)), D is the effective fire diameter (m (ft)), and ρ_a is the ambient air density (kg/m³ (lb/ft³)).

The deflection angle relative to the fire centerline is given by the following equation [7].

$$\theta = \begin{cases} 0 & u^* \le 1 \\ \cos^{-1}\left(\frac{1}{\sqrt{u^*}}\right) & u^* > 1 \end{cases} \tag{15}$$

Figure 15 shows the flame length as a function of the fire diameter and the wind speed for ranges considered in this analysis. Figure 16 shows the deflection angle as a function of the fire diameter and wind speed for various fire diameters. It is clear that for low wind speeds and large fire diameters little deflection is expected. However, once the wind is sufficiently strong to cause a deflection, the deflection angle rapidly increases with rising wind speed.

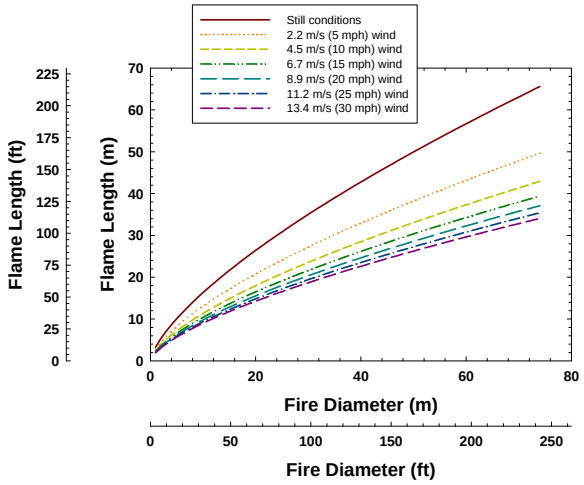

Figure 15. Flame Length vs the Assumed Fire Diameter for Various Wind Conditions

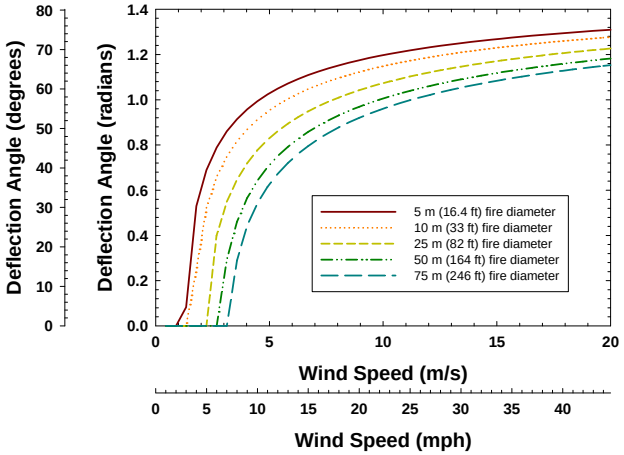

Figure 16. Flame Deflection Angle vs the Assumed Fire Diameter for Various Wind Conditions

Because the deflection angle may be steep, it is possible that pool fires with a substantial offset could still result in flame impingement on the aircraft. This phenomenon was observed in the 1985 aircraft fire incident at Manchester airport [22]. Figure 17 depicts the geometry considered

where the maximum aircraft height is $H_{p,m}$ (m (ft)), the fire offset distance is S (m (ft)), and the flame deflection angle with respect to the ground is α (radians (degrees)). Flame impingement is assumed if both of the following conditions are met.

$$\bar{F}_L > \frac{1}{\sin\alpha} S$$

$$\bar{F}_L < \frac{1}{\sin\alpha} H_{p,m} \tag{16}$$

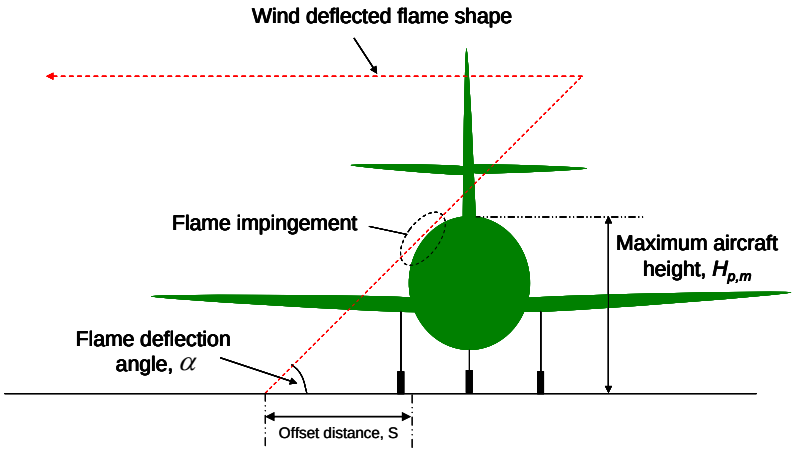

Figure 17. Flame Impingement due to Wind

The deflected-flame approach developed by the AGA is applicable to axisymmetric pool fires. Such fires are considered in this analysis only when the aircraft is immersed. In these cases, the effects of wind are not material since an increase in the exposure conditions would not be postulated; the aircraft is already assumed to be exposed to the most adverse conditions.

When the fire is offset from the aircraft, it is treated as either an axisymmetric or a line type fire, whichever is most severe. When treated as an axisymmetric fire, whether by artifice or because the fuel spill extent is limited, the AGA method would be applicable or bounding.

When treated as a line type fire, the deflection angle is expected to decrease when the wind direction is parallel to the fire length. This is because the effective diameter would be much larger which tends to reduce the deflection angle. Nevertheless, figure 15 shows that the effect of the diameter on the deflection angle decreases with very large diameter fires indicating the application of this method to line fires would not be overly conservative. The flame length for a line type fire in wind conditions is calculated assuming the same flame length reduction fraction determined for the analogous axisymmetric pool.

$$\bar{F}_{L,lin} = \frac{\bar{F}_L}{H_{f,as}} H_{f,lin} \tag{17}$$

where $\bar{F}_{L,lin}$ is the flame length for the line fire under wind conditions (m (ft)); $H_{f,as}$ is the axisymmetric flame height (m (ft)) under calm conditions, as defined in section 4.1.5; and $H_{f,lin}$ is the line fire flame height (m (ft)) under calm conditions, as defined in section 4.1.5.

The wind is assumed to be steady and directed towards the aircraft. Other wind directions would be bound by either the calm conditions or the direction considered. Variable wind speeds would be less severe than assuming an upper-bound, steady wind speed since the deflection angle, and thus the heat flux, would oscillate between a maximum and minimum value. The maximum value corresponds to the upper-bound, steady wind speed used in this analysis.

4.2 AIRCRAFT OR PASSENGER FIRE EXPOSURE.

The aircraft fire exposure is the temperature and thermal radiation boundary conditions at the exterior surface of the aircraft. These boundary conditions may be constant or transient, the latter arising when the fire location varies as a result of suppression actions. Spatial and temporal variations that arise from a steady or quasi-steady fire are not considered; instead, the most severe values at any location on the exterior of the aircraft are used as the basis for evaluating interior ignition.

Two types of fire exposures are considered: (1) complete immersion of the aircraft in the fire and (2) flame impingement on the aircraft and a heat flux from a fire that is offset from the aircraft. Flame impingement scenarios result in both a convection and thermal radiation boundary condition, although full-scale data are available for the total incident heat flux, which includes both components. A fire that is offset from the aircraft is assumed to radiate heat only; the offset distance is assumed to be sufficient such that the air layer adjacent to the aircraft is essentially at ambient temperature. For fires with substantial offset distances, this is clearly a good assumption. As the fire offset distance decreases, the interaction of the airflows caused by the fire and the aircraft may result in the flame deflecting and attaching at the aircraft surface. For relatively small fires (~100 kW (95 Btu/s)), offset distances of several centimeters (inches) to about 0.5 m (1.6 ft) is sufficient to prevent flame attachment [32]. Whether these offset distances apply to the fire sizes considered in this analysis is not apparent. Given this, the minimum offset distance considered in this evaluation is 0.5 m (1.6 ft). It should be recognized that this distance may still result in flame attachment. Additional data would be needed to resolve the transition from complete flame separation to flame attachment as the offset distance decreases.

4.2.1 Immersion Fire Exposure Conditions.

The maximum average heat flux for objects immersed in large-scale pool fires varies from approximately 75 to 120 kW/m² (6.6 to 10.6 Btu/s-ft²) [3], where the fluxes are temporally averaged. Small calorimeter measurements suggest the maximum average heat flux could be as high as 170 kW/m² (15 Btu/s–ft²) [3]. Peak values at specific locations could approach 200-240 kW/m² (17.6-21.1 Btu/s-ft²). Lattimer [33] reports peak incident heat fluxes to various immersed objects on the order of 200 kW/m² (17.6 Btu/s-ft²). These peak values are consistent with various full-scale measurements of aircraft sections exposed to large pool fires [9, 11, and 19], although the average values at fixed locations tended to span a wider range (40-150 kW/m² (3.5-13.2 Btu/s-ft²)). Lower values appear to correspond to heat flux measurements outside the

flame impingement zone. The higher values correspond to flame impingement; as such, a value of 150 kW/m² (13.2 Btu/s-ft²) is the assumed heat flux boundary condition for portions of the aircraft that are immersed in the fire or that are subject to flame impingement.

4.2.2 Offset Fire Exposure Conditions—Constant Separation.

The incident heat flux at the surface of the aircraft, or to an escaping passenger, for offset fires is due to thermal radiation. The basic equation for determining the heat flux is given by the following [3].

$$\dot{q}''_{inc}(S,\hat{g}) = E(D)\cdot F(S,\hat{g}) \tag{18}$$

where $\dot{q}''_{inc}$ is the incident heat flux (kW/m² (Btu/s-ft²)), E is the emissive power of the fire (kW/m² (Btu/s-ft²)) as determined using equation 11, D is the fire diameter or line fire width (m (ft)), F is the view factor between the fire and a location on the aircraft (–), S is the offset distance (m (ft)), and $\hat{g}$ is the set of parameters that characterize the flame shape (flame height, cylindrical, tilted cylinder) and target orientation (–). The transmissivity of the intervening medium is conservatively ignored in equation 18.

The most adverse view factor configuration is not obvious since the exposure may be treated as a line fire or an axisymmetric fire, the target surface on the aircraft may be elevated up to 6 m (20 ft), and the target surface may be rotated at any angle. Given this, four configurations are considered. These are shown in figures 18a through 18d for calm conditions.

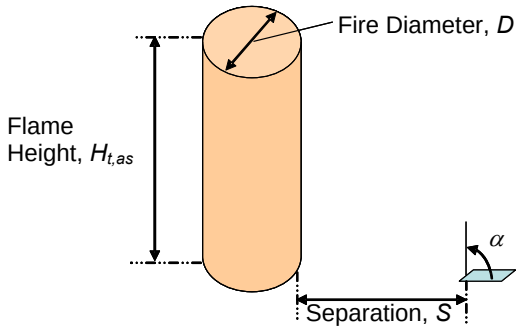

F_1, Ground-based target rotated so that view factor is maximized (axisymmetric fire exposure)

Figure 18a. View Factor Configuration for a Ground-Based Target With an Assumed Axisymmetric Exposure—No Wind

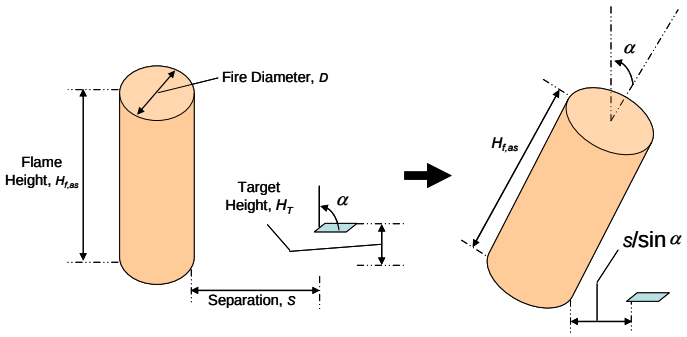

F_2, Elevated target rotated so that view factor is maximized (axisymmetric fire exposure)

Figure 18b. View Factor Configuration for an Elevated Target With an Assumed Axisymmetric Exposure—No Wind

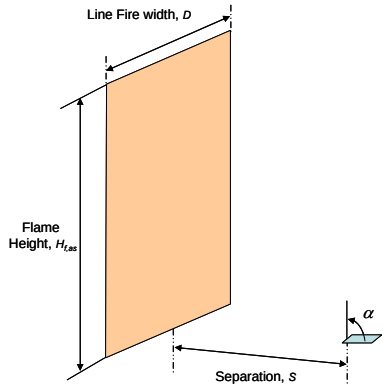

F_3, Ground-based target rotated so that view factor is maximized (line fire exposure)

Figure 18c. View Factor Configuration for a Ground-Based Target With an Assumed Line Fire Exposure

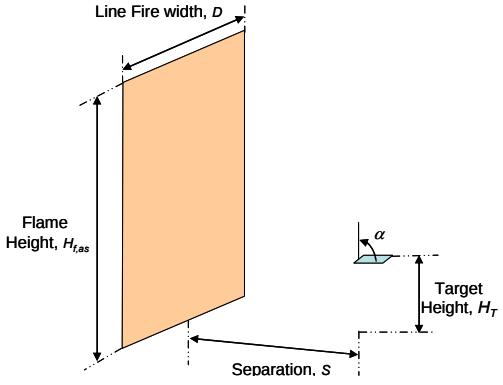

F_4, Elevated target rotated so that view factor is maximized (line fire exposure)

Figure 18d. View Factor Configuration for an Elevated Target With an Assumed Line Fire Exposure

The first view factor, F_1, assumes the target is on the ground and is rotated to maximize the view factor. The rotation angle resulting in the maximum view factor varies with the flame height, fire diameter, and separation distance, but it is not necessary to compute it directly. Instead, the horizontal and vertical components are determined as follows [3 and 7]:

$$F_{1,H} = \frac{B - \frac{1}{L}}{\pi\sqrt{B^2 - 1}} \tan^{-1}\left(\sqrt{\frac{(B+1)(L-1)}{(B-1)(L+1)}}\right) - \frac{A - \frac{1}{L}}{\pi\sqrt{A^2 - 1}} \tan^{-1}\left(\sqrt{\frac{(A+1)(L-1)}{(A-1)(L+1)}}\right)$$

$$F_{1,V} = \frac{1}{\pi L} \tan^{-1}\left(\frac{h}{\sqrt{L^2 - 1}}\right) - \frac{h}{\pi S} \tan^{-1}\left(\sqrt{\frac{L-1}{L+1}}\right) + \frac{Ah}{\pi L\sqrt{A^2 - 1}} \tan^{-1}\left(\sqrt{\frac{(A+1)(L-1)}{(A-1)(L+1)}}\right)$$

$$A = \frac{h^2 + L^2 + 1}{2S} \qquad (19)$$

$$B = \frac{1 + L^2}{2L}$$

$$L = \frac{2S}{D}$$

$$h = \frac{2H_{f,as}}{D}$$

where $F_{1,H}$ is the horizontal component of the view factor (–) and $F_{1,V}$ is the vertical component (–). The maximum view factor for this configuration is given by the following equation [7].

$$F_1 = \sqrt{F_{1,v}^2 + F_{1,H}^2} \qquad (20)$$

where F_1 is the view factor (–) for the configuration shown in figure 18a. The behavior of the view factor function described by equations 19 and 20 is shown in figure 19. As expected, the view factor essentially decreases in proportion to $1/S^2$ at large distances [7].

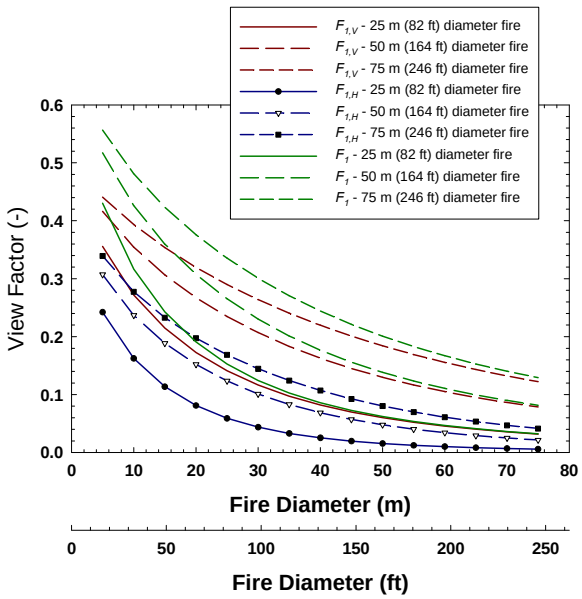

Figure 19. View Factor Between an Axisymmetric Fire and a Ground-Based Target (Equations 19 and 20)

The second view factor, F_2, assumes the target is elevated and possibly rotated. If the target is not rotated, F_2 is determined using the vertical component of the view factor described by equation 19 but applied to the upper and lower portions of the fire when it is split at the target height. If the target is rotated, the view factor is determined using the following equations [4 and 5].

$$\pi F_2 = \tan^{-1}\left(\frac{1}{D}\right) + \frac{\sin\theta}{C}\left[\tan^{-1}\left(\frac{ab - F^2\sin\theta}{FC}\right) + \tan^{-1}\left(\frac{F\sin\theta}{C}\right)\right] \tag{21a}$$

$$-\left[\frac{a^2 + (b+1)^2 - 2(b+1+ab\cdot\sin\theta)}{AB}\right]\tan^{-1}\left(\frac{AD}{B}\right)$$

with

$$a = \bar{F}_{L,as} / r$$

$$b = (S + r) / r$$

$$A = \sqrt{a^2 + (b+1)^2 - 2a(b+1)\cdot \sin\theta}$$

$$B = \sqrt{a^2 + (b-1)^2 - 2a(b-1)\cdot \sin\theta} \qquad (21b)$$

$$C = \sqrt{1 + (b^2 - 1)\cdot \cos^2\theta}$$

$$D = \sqrt{(b-1)/(b+1)}$$

$$F = \sqrt{b^2 - 1}$$

where r is the radius of the fire (m (ft)) and θ is the tilt angle of the target with respect to the fire (radians (degrees)). If the separation is such that the target is effectively above the fire, the flame height is extended, and equation 21b is applied twice: once to the extended fire and once to the virtual extension. F_2 is the difference between these two values. As the rotation angle increases, larger portions of the fire are truncated and the effective separation distance increases. Thus, the angle at which the view factor is most severe is not necessarily the maximum tilt angle. Indeed, it is typically about 0.04 to 0.08 radians (5 to 10 degrees). Figure 20 shows the behavior of this view factor function. As expected, for a fixed distance, the view factor increases relative to the still condition (zero tilt) fire with the greatest deviation where the nondimensional distance parameter b in equation 21b is approximately 5.

The third view factor, F_3, assumes the target is on the ground and is rotated to maximize the view factor. The rotation angle resulting in the maximum view factor varies with the flame height, line fire width, and separation distance, but it is not necessary to compute it directly. Instead, the horizontal and vertical components are determined as follows [7].

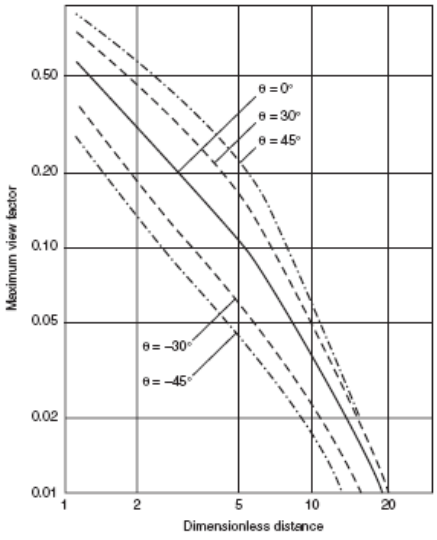

Figure 20. View Factor for a Tilted Cylinder Configuration Used to Approximate an Elevated and Rotated Target Exposed to an Axisymmetric Fire

$$F_{3,V} = \frac{1}{\pi}\left[\frac{X}{\sqrt{1+X^2}}\tan^{-1}\left(\frac{Y}{\sqrt{1+X^2}}\right)+\frac{Y}{\sqrt{1+Y^2}}\tan^{-1}\left(\frac{1}{a+\sqrt{1+Y^2}}\right)\right]$$

$$X = \frac{W}{2S} \tag{22a}$$

$$Y = \frac{H_{f,lin}}{S}$$

$$F_{3,H} = \frac{1}{\pi}\left[\tan^{-1}\left(\frac{1}{Y}\right)+AY\tan^{-1}(A)\right]$$

$$X = \frac{2H_{f,lin}}{W} \tag{22b}$$

$$Y = \frac{2S}{W}$$

$$A = \frac{1}{\sqrt{X^2+Y^2}}$$

where $F_{3,H}$ is the horizontal component of the view factor (–), $F_{3,V}$ is the vertical component (–), and W is the width of the line fire (m (ft)), equal to D in figures 18c and 18d. Equations 22a and 22b assume the target is located midway between the width of the line fire. The behavior of

equations 22a and 22b is shown in figure 21 for the range of diameters considered in this evaluation. The maximum view factor shown in figure 21 is somewhat more severe than the view factor computed, assuming a cylindrical shape for the fire sizes shown at close separations, though the horizontal and vertical components behave quite differently from one another. The large view factor is primarily at near distances where the edge effects become significant—for the cylinder, the edge curves away, whereas in the flat plat approximation, it does not.

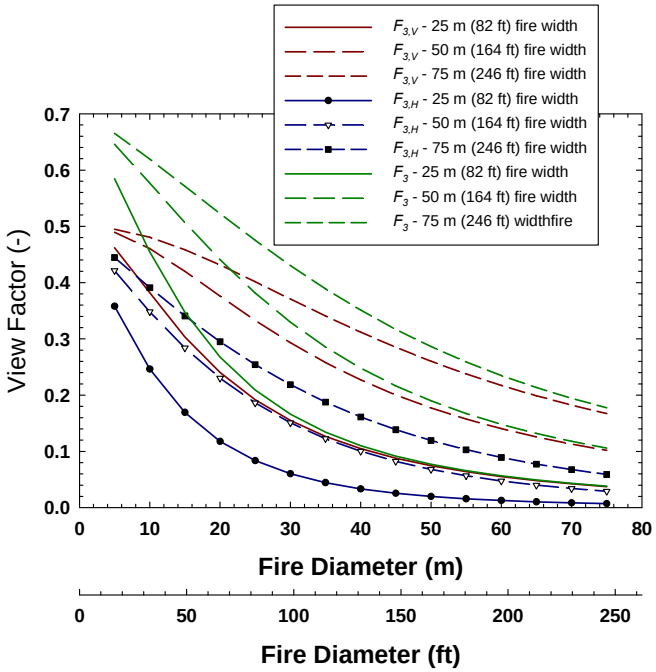

Figure 21. View Factor Between an Axisymmetric Fire and a Ground-Based Target (Equations 22a and 22b)

The fourth view factor, F_4, uses the same view factor equations as F_3. When the target is vertical, $F_{3,V}$ is computed for the upper and lower portions of the flame when divided at the target heath. The total view factor, F_4, is then the sum of the upper and lower portions. When the target is rotated, the offset distance is modified for the portions in view using the following equation [34].

$$F_4 = \cos\alpha F_{3,V} \tag{23}$$

The view factor that is used for any given fire exposure is the maximum of the four configurations shown in figures 18a through 18d, or

$$F(S,\hat{g}) = \max(F_1, F_2, F_3, F_4) \tag{24}$$

where F_1, F_2, F_3, and F_4 are determined using the aforementioned methods. The target height is varied at 0.3-m (1-ft) increments from 0 to 6 m (0 to 20 ft) to determine the largest value over the exposed surface of the aircraft.

4.2.3 Offset Fire Exposure Conditions—Variable Fire Separation.

Variable fire separations are assumed for fires initially offset from the aircraft after the first responding units apply suppression agent. The offset distance is assumed to increase linearly in proportion the amount of agent discharged in accordance with the following extension of equation 2.

$$S_a(t) = S_{a,i} \qquad (t < t_{arr})$$

$$S_a(t) = S_{a,i} + \frac{1}{L_a}\frac{V_A}{\Delta t_A}k_A t \qquad (t_{arr} < t < t_{arr} + 60) \tag{25}$$

$$S_a(t) = S_{a,i} + \frac{V_A k_A}{L_A} \qquad (t > t_{arr} + 60)$$

where $S_a(t)$ is the fuel spill fire offset distance from the aircraft exterior (m (ft)) at t (seconds) after suppression has begun, $S_{a,i}$ is the initial fuel spill fire offset distance (m (ft)), t_{arr} is ARFF arrival time (seconds), V_A is the agent amount carried by the first responding unit (m³ (ft³)), Δt is the time interval over which the initial amount of agent is applied (60 seconds), k_A is the suppression capacity of the agent (189 m² of fire area suppressed/m³ agent applied (58 ft² of fire area suppressed/ft³ of agent applied)), and L_A is the aircraft length (fire diameter or width) (m (ft)). This gives rise to a view factor and an incident heat flux that is dependent on time in addition to the parameters already discussed. Because ARFF is assumed to increase the offset distance (see section 4.1), the diameter or fire width does not change. Thus, the emissive power of the fire remains constant during the suppression period.

A typical example of the variable view factor and incident heat flux for an ARFF response time of 1 minute is shown in figures 22 through 24. A transient exposure curve is uniquely associated with a fire scenario given an agent amount, ARFF response time, and initial offset distance, $S_{a,i}$.

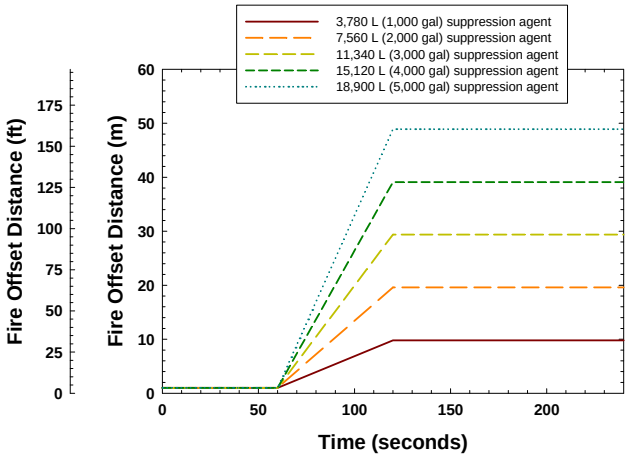

Figure 22. Offset Distance as a Function of Time due to ARFF Suppression Actions for a Scenario With a 1-m (3-ft) Initial Offset Distance and a 73-m (240-ft) Fire Diameter

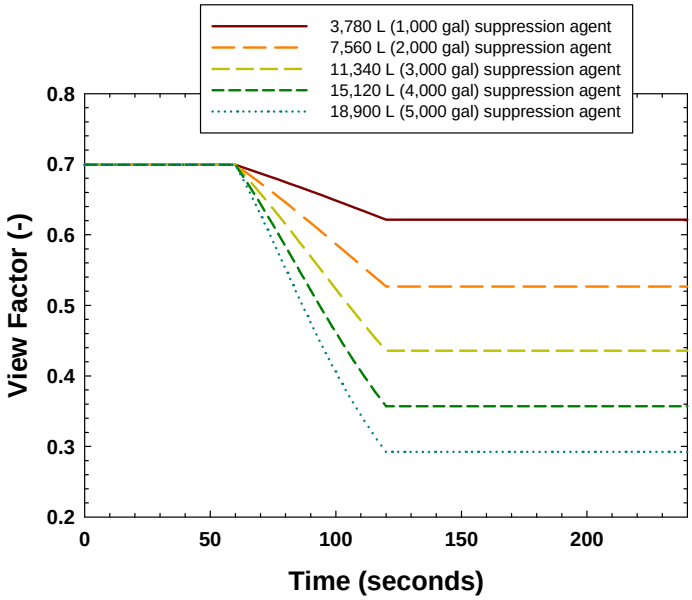

Figure 23. View Factor as a Function of Time due to ARFF Suppression Actions for a Scenario With a 1-m (3-ft) Initial Offset Distance and a 73-m (240-ft) Fire Diameter (Ground-Based Target)

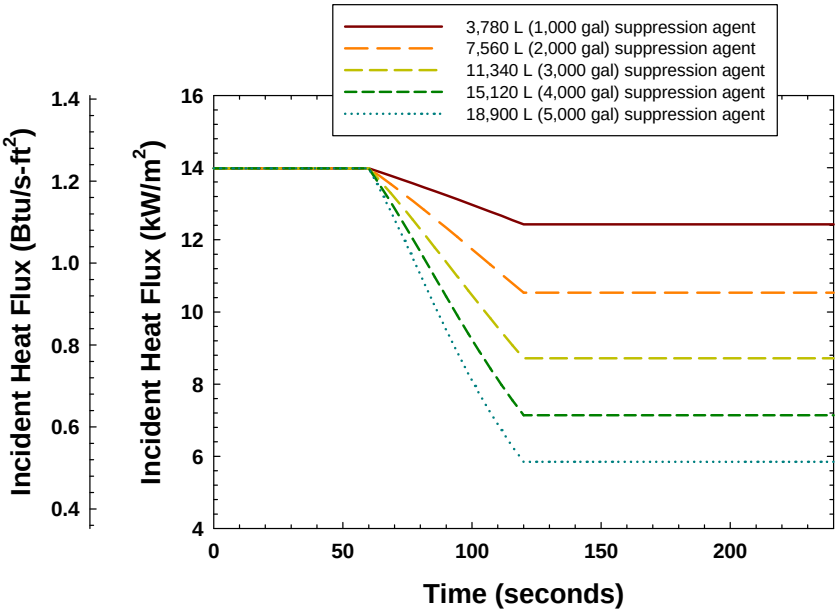

Figure 24. Incident Heat Flux as a Function of Time due to ARFF Suppression Actions for a Scenario With a 1-m (3-ft) Initial Offset Distance and a 73-m (240-ft) Fire Diameter (Ground-Based Target)

5. INTERIOR AIRCRAFT IGNITION.

5.1 HIGH HEAT FLUX FIRE EXPOSURES.

Tenability conditions within the aircraft can be linked to the time at which ignition occurs. As such, an approach for determining the ignition time for a specific fire exposure is one focus of this analysis. Previous attempts at estimating the damage time for an aircraft, assumed to be synchronous with interior aircraft ignition, have focused on determining the time at which the skin of the aircraft melts [15 and 16]. These studies considered only aircraft immersed in pool fires, which represented severe fire exposure conditions. Typically, the ignition time has been assumed to be equal to the time the skin melts plus an offset to account for flame penetration through the insulation, which may be as short as 10 to 15 seconds [15 and 17]. Fire propagation into the aircraft through other pathways, such as the windows, door gaps, and the outflow valves, are typically comparable to the propagation time through the skin [9, 19, and 35].

This type of approach is useful for predicting possible interior ignition when the exposure conditions are severe, given a melting temperature for the aluminum skin of about 649°C (1200°F) [15 and 16]. The types of exposures that are capable of melting the aircraft skin can be estimated using a steady-state heat balance at the skin surface [36 and 37]:

$$\dot{q}''_{inc} - \dot{q}''_{cond} - \dot{q}''_{conv} - \dot{q}''_{rad} = 0 \tag{26}$$

where $\dot{q}''_{inc}$ is the incident or exposure heat flux (kW/m² (Btu/s-ft²)), $\dot{q}''_{cond}$ is the conduction losses into the aircraft across the skin surface (kW/m² (Btu/s-ft²)), $\dot{q}''_{conv}$ is the convective losses to the surrounding air (kW/m² (Btu/s-ft²)), and $\dot{q}''_{rad}$ is the thermal radiation losses to the surroundings (kW/m² (Btu/s-ft²)). Assuming the convection and conduction losses are minor and that the surface can be treated as an approximate black body, the minimum incident heat flux that can melt the aluminum skin can be estimated as follows [36].

$$\dot{q}''_{inc,m} = \sigma T^4_{s,melt} \tag{27}$$

where $\dot{q}''_{inc,m}$ is the minimum incident heat flux needed to melt aluminum aircraft skin (kW/m² (Btu/s-ft²)), σ is the Stefan-Boltzmann constant (5.67×10^{-11} kW/m²-K^4 (4.76×10^{-13} Btu/s-ft²-°R^4)), and $T_{s,melt}$ is the melting temperature of the aluminum skin (649°C or 922 K (1200°F or 1659°R)). The minimum flux needed to melt the skin, $\dot{q}''_{inc,m}$, is about 40 kW/m² (3.5 Btu/s-ft²).

5.1.1 Aluminum Aircraft Skin-Melting Ignition Model.

A reasonable model for assessing interior ignition under high heat flux exposures (i.e., greater than about 40 kW/m² (3.5 Btu/s-ft²)) predicts the time the aircraft skin melts and then applies a time differential to account for flame penetration through the insulation. Based on available full- and small-scale test data, a realistic but conservative time differential for flame penetration after the skin melts is 10 seconds [9, 10, 11, 15, 17, and 19].

The time at which the aircraft skin melts, given an incident heat flux exposure, is calculated using the heat transfer model HEATING (version 7.3) [8]. HEATING (version 7.3) is a finite difference computer model that can calculate the transient temperature distribution within a solid exposed to combinations of prescribed convection, radiation, temperature, and heat flux boundary conditions [8]. HEATING has been validated and verified for calculating the temperature rise in concrete, steel, and insulation systems exposed to fire and is well-suited for this application [38, 39, and 40].

The incident heat flux is assumed to be spatially constant over a large enough area so that the conduction is one-dimensional. Furthermore, the exposure is assumed constant with respect to time for a given fire size and offset distance; transient oscillations about a mean value are not considered, but variations in the exposure that could arise from suppression actions are included in the model. Bounding heat flux values are used in this analysis such that situations where the incident heat flux is not spatially constant would be bound by the results of the one-dimensional analysis. Figure 25 depicts a modeled aircraft skin-insulation system. The key parameters are

- the thickness of the aircraft skin, δ_s (m (ft))
- the thickness of the insulation, δ_i (m (ft))
- the boundary conditions on both the exposed and unexposed surfaces
  - the exposure heat flux $\dot{q}_i''(x=0,t)$ (kW/m² (Btu/s-ft²))
  - the heat losses at the exposed surface $\dot{q}_{l,e}''(x=0,t)$ (kW/m² (Btu/s-ft²))
  - the heat losses at the unexposed surface $\dot{q}_{l,u}''(x=\delta_s+\delta_i,t)$ (kW/m² (Btu/s-ft²))

where x is the spatial coordinate (m (ft)) and t is the temporal coordinate (seconds). This approach is consistent with previous attempts at estimating the melting time [15 and 16] but represents an improvement by including the transient conduction flux through the system (i.e., $\dot{q}_{cond}''$ in equation 26) and the thermal radiation and convection losses at the unexposed face (i.e., $\dot{q}_{l,u}''(x=\delta_s+\delta_i,t)$ in figure 25).

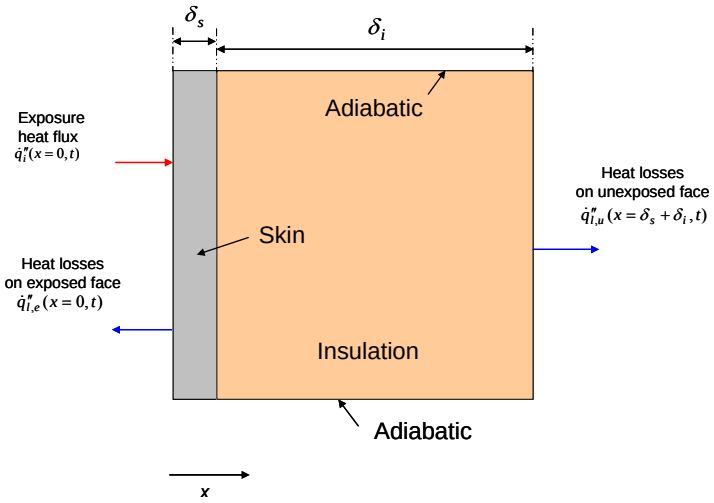

Figure 25. One-Dimensional Modeled Aircraft Skin-Insulation System

The thermal material properties needed to predict the transient response of the aluminum and insulation to prescribed boundary conditions are the thermal conductivity, heat capacity, density, and emissivity of the surfaces involved. Although these properties may be temperature or spatially dependent, constant but conservative values are assumed. Such variations in the material properties for the aluminum skin do not affect the results given. Since the thermal conductivity is so much larger than the insulation, the material is essentially at a uniform temperature. Consideration of different insulation thicknesses provides insight into the sensitivity of the model to conduction losses and, thus indirectly, the assumed thermal properties for the insulation. Table 4 lists the properties assumed in this analysis.

Table 4. Thermal Material Properties for the Aluminum-Insulation System Used to Estimate the Aircraft Skin-Melting Time [15 and 36]

Material	Thermal Conductivity (W/m-°C (Btu/s-ft-°F))	Heat Capacity (J/kg-°C (Btu/lb-°F))	Density (kg/m³ (lb/ft³))	Emissivity (–)
Aluminum	177 (0.028)	883 (0.211)	2787 (174)	0.9
Fiberglass insulation	0.03 (4.82×10^{-6})	835 (0.2)	32 (2)	0.9

The energy absorbed by the aluminum melting process is included in the heat capacity over the melting temperature range of 482° to 649°C (900° to 1200°F) [15]. Given a heat of formation of 394 kJ/kg (170 Btu/lb), the effective heat capacity over this temperature interval is 3240 J/kg-°C (0.776 Btu/lb-°F).

The heat losses consist of both thermal radiation and convection. The thermal radiation heat losses apply regardless of the exposure type and are determined using the following equation [36]

$$\dot{q}''_{r,l} = \varepsilon\sigma T_s^4 \tag{28}$$

where $\dot{q}''_{r,l}$ is the radiant heat flux loss on the exposed or unexposed surface (kW/m² (Btu/s-ft²)), ε is the surface emissivity (–), and T_s is the surface temperature (K (°R)). The emissivity parameter is assumed to be 0.95 based on conservative approximation of surfaces, including those that are painted, have carbon deposition, or are weathered [36 and 37].

For immersion fire exposures, there is no convection loss component since the heat flux boundary condition includes the convection component. For fires that are offset from the aircraft and for unexposed surfaces, the convection is determined from the following equation [36 and 41].

$$\dot{q}''_{conv} = h(T)\left(T_s - T_\infty\right) \tag{29}$$

where $\dot{q}''_{conv}$ is the convective heat loss on the respective surface (kW/m² (Btu/s-ft²)) and T_∞ is the ambient temperature (°C (°F)). The convection coefficient is determined assuming free convection from a vertical plate and is given by the following equation [36].

$$h = 1.32\Delta T^{1/3} \qquad (SI)$$
$$h = 5.3\times10^{-5}\Delta T^{1/3} \qquad (English) \tag{30}$$

where h is the convection coefficient (W/m²-°C (Btu/s-ft²-°F)), and ΔT is the temperature difference between the wall surface and the surrounding air (°C (°F)). The convection coefficient from other orientations could be somewhat lower but is nearly the same [36]. The resulting coefficients for the surface temperatures of interest range from zero to 13 W/m²-°C (6.4×10^{-4} Btu/s-ft²-°C) when the surface temperature is equal to the aluminum melting temperature of 649°C (1200°F).

Forced convection conditions can arise on the exterior boundary when there is moderately strong wind [36, 37, and 41]. The convection coefficient can increase to as high as 20 W/m²-°C (9.8×10^{-4} Btu/s-ft²-°C) for a 13.4-m/s (30-mph) wind [37 and 41]. Because this is approximately equal to the values already assumed, forced convection is conservatively ignored when wind is considered.

5.1.2 Aluminum Aircraft Skin-Melting Model Results.

5.1.2.1 Constant Heat Flux Exposures.

The peak incident heat flux at the surface of the aircraft will vary with distance between the exposure and the skin but may also vary with time if the fire is being suppressed as noted previously. Each scenario considered is, therefore, unique. However, by fixing the separation distance, the melting time versus the exposure flux may be computed for various skin and insulation thickness combinations. These results are shown in figures 26 through 28 for aluminum skin and insulation thicknesses typical of aircraft. The ignition time based on a 10-second delay after the aluminum skin has melted is also shown in the figures. Figure 29 shows the aluminum skin-melting time for two skin thicknesses and insulation backing thicknesses.

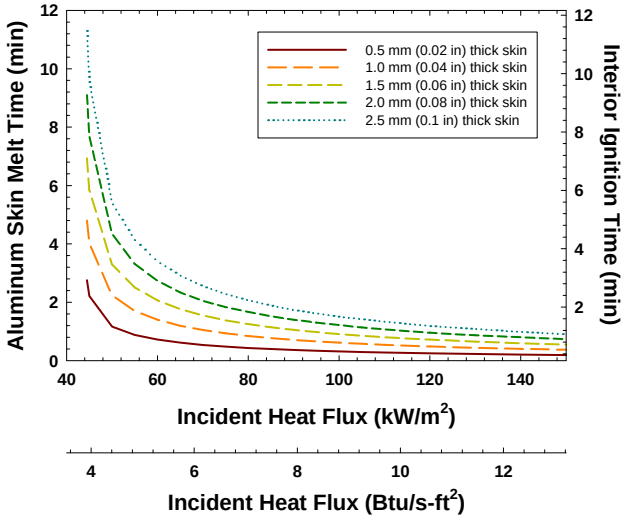

Figure 26. Aircraft Skin-Melting Time vs the Incident Heat Flux With 2.5 cm (1 in.) of Fiberglass Insulation Backing

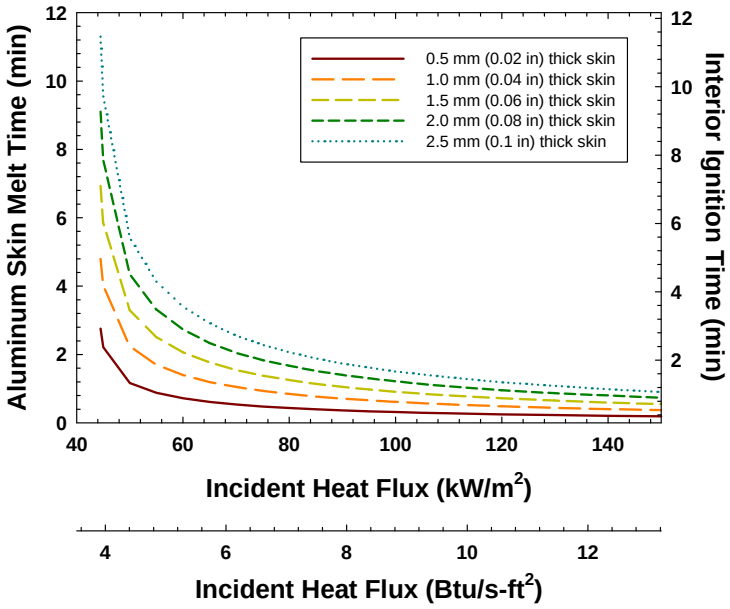

Figure 27. Aircraft Skin-Melting Time vs the Incident Heat Flux With 5.1 cm (2 in.) of Fiberglass Insulation Backing

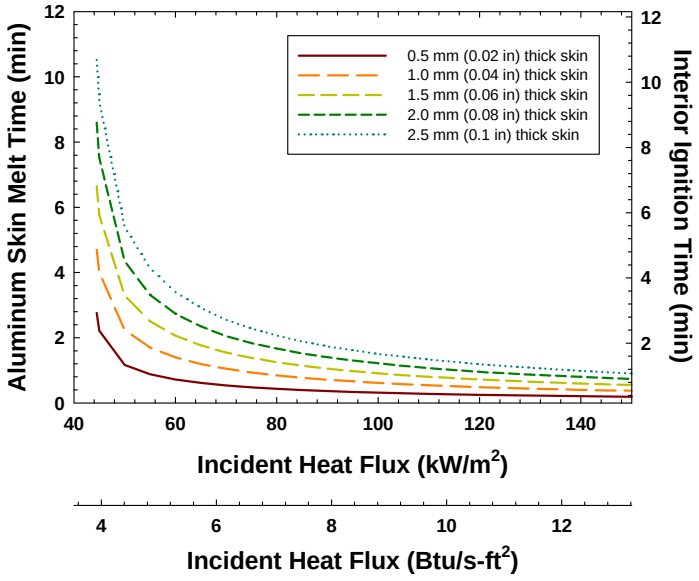

Figure 28. Aircraft Skin-Melting Time vs the Incident Heat Flux With 10 cm (4 in.) of Fiberglass Insulation Backing

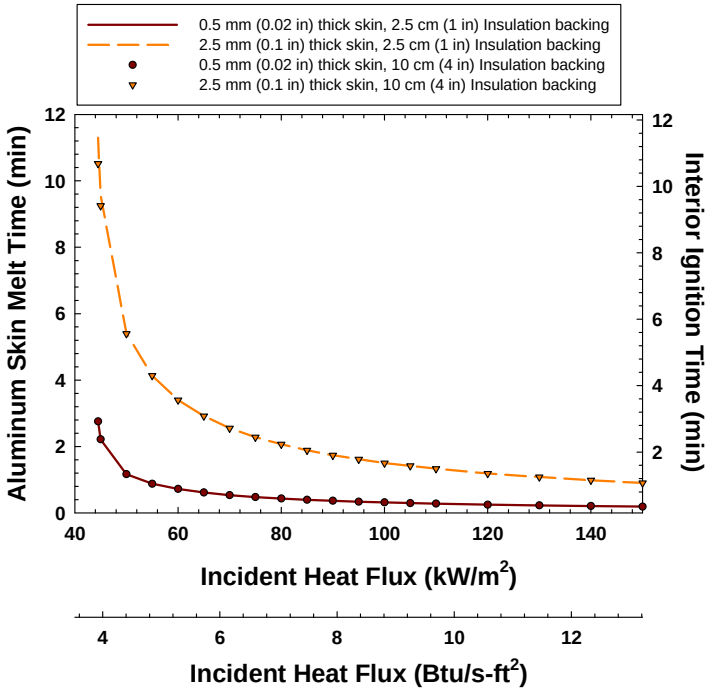

Figure 29. Aircraft Skin-Melting Time vs the Incident Heat Flux With 2.5 cm (1 in.) and 10 cm (4 in.) of Fiberglass Insulation Backing

Figures 26 through 29 indicate that the minimum heat flux that can melt the skin is approximately 44.5 kW/m² (3.9 Btu/s-ft²), slightly greater than 40 kW/m² (3.5 Btu/s-ft²). The difference is due to the inclusion of the conduction and convection heat loss terms within the model. Figure 29 shows that the assumed thickness of the fiberglass insulation has, at most, a minor effect on the predicted skin-melting times, and only at heat fluxes close to the threshold value of 44.5 kW/m² (3.9 Btu/s-ft²), suggesting that the conduction losses through the skin-insulation system are minor. Since conduction losses are minor, variations in the material properties of the fiberglass with respect to temperature have an insignificant effect on the results, thus confirming the original constant property assumption.

Figures 26 through 29 show that the time required to melt the aluminum skin is strongly dependent on the exposure heat flux and on the skin thickness but not on the insulation thickness. Average peak heat fluxes for objects immersed in fires can range between 120 and 150 kW/m² (10.6 and 13.2 Btu/s-ft²) with instantaneous peak values approaching 200 kW/m² (17.6 Btu/s-ft²) [3, 10, and 19]. The skin-melting time under these conditions is predicted to be between 15 and 60 seconds, depending on the flux and skin thickness. These values compare well with observed data that range between 30 and 60 seconds for complete immersion at the peak fire size [9, 16, 17, and 19].

The transient response of the aluminum skin and insulation exposed to a constant incident heat flux is shown in figure 30 for a typical case. The plot shows that the aluminum skin is essentially at a uniform temperature and that the rate of temperature increase slows substantially when the aluminum skin reaches a temperature of about 482°C (900°F), the temperature at which the melting process is assumed to begin. Figure 30 shows a case in which the aluminum aircraft skin is exposed to the minimum flux capable of melting through the aluminum skin, which is

defined by a temperature of 649°C (1200°F) at the aluminum-insulation interface. It is apparent from the linear temperature profile through the insulation that steady-state conditions have nearly been reached after being exposed for 6 minutes [36].

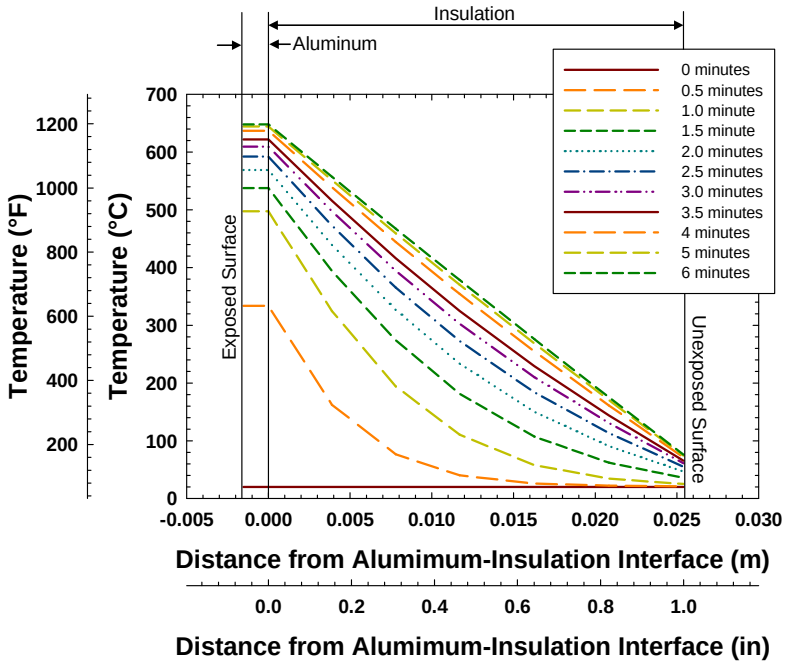

Figure 30. Temperature Profiles at Various Times Within Skin-Insulation System: 1.5-mm (0.06-in.)-Thick Skin, 2.5-cm (1-in.) Fiberglass Insulation, and a 44.5-kW/m² (3.9-Btu/s-ft²) Incident Flux

A model developed by Welker [15] for predicting the aircraft skin temperature compared reasonably well with full-scale test data [15]. Two aluminum cylinders, one with a 0.5-mm (0.02-in.)-thick skin and one with a 2.3-mm (0.09-in.)-thick skin were exposed to a hydrocarbon pool fire. The interiors were insulated with 1.3 cm (2 in.) of Kaowool™, having a thermal conductivity of 0.1 W/m-°C (1.6×10^{-5} Btu/s-ft²-°F) [15]. An effective radiant exposure flux of 98 kW/m², a flame temperature of 1093°C (2000°F), and a convection coefficient of 28.4 kW/m²-°C (1.39×10^{-3} Btu/s-ft²-°F) was deduced [15]. The aluminum skin temperatures as a function of time, as calculated by Welker and measured in the test series, are shown in figure 31 for the two cylinder skin thicknesses. Also shown are the predicted temperatures using the HEATING model described in section 5.1.1, assuming a heat capacity and density for the Kaowool insulation as listed in table 4 for the fiberglass insulation. Figure 31 indicates that the HEATING model produces results similar to the Welker model with somewhat improved prediction of the initial temperature rise likely due to the inclusion of a transient rather than a steady-state conduction term.

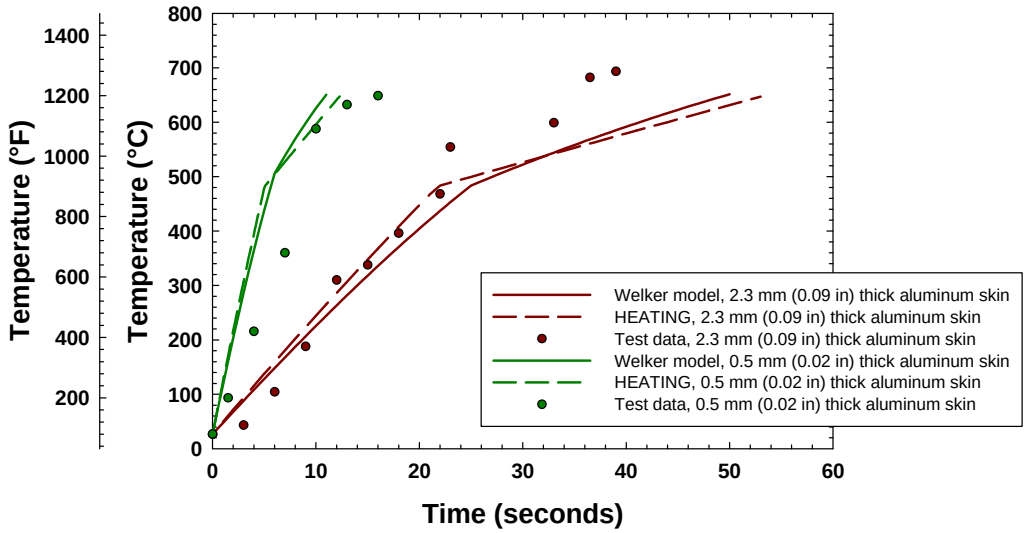

Figure 31. Aluminum Skin Temperatures for Full-Scale Test Configuration—Welker and HEATING Models

5.1.2.2 Time-Varying Heat Flux Exposures.

Because the aluminum skin is essentially at a constant temperature, a decreasing heat flux caused by fire suppression activities results in either a reduced rate of temperature increase or a temperature decrease of the aluminum skin. If the heat flux decreases below the threshold value of 44.5 kW/m² (3.9 Btu/s-ft²) and remains below this value and the skin has not melted, it will not melt at any subsequent time.

5.1.3 Aluminum Aircraft Skin-Melting Model Summary.

A model for predicting the time a high heat flux exposure can cause interior aircraft ignition involves predicting the time the aircraft skin entirely melts. A 10-second time delay to account for flame penetration through the insulation is added based on observations of full-scale tests. An assessment of various parameters, including the skin thickness and insulation backing thickness, indicate that the model is not sensitive to the assumed insulation thickness within the 2.5- to 10-cm (1- to 4-in.) range typical of aircraft configurations [9 and 19]. The results are sensitive to the assumed skin thickness as this serves as the primary heat sink for the exposure boundary condition. For consistency and the purpose of this evaluation, an insulation backing thickness of 2.5 cm (1 in.) was assumed.

5.2 LOW HEAT FLUX FIRE EXPOSURES.

Heat flux exposures lower than approximately 40 kW/m² (3.5 Btu/s-ft²), characteristic of fires that are offset from the aircraft, can still cause the interior aircraft ignition even though the aircraft skin may not melt through. This observation is apparent in light of the critical or minimum ignition heat flux for common combustible materials such as plastics or cellulosic products, typically between 9 and 45 kW/m² (0.8 and 4.1 Btu/s-ft²) [30, 42, and 43]. Based on equation 27, the ignition temperature for these types of materials under a radiant exposure is between 360° and 670°C (680° and 1238°F) [43]. Clearly, incident heat fluxes lower than

44.5 kW/m² (3.9 Btu/s-ft²), the threshold flux for melting aluminum skin, could cause portions of the aircraft interior to reach or exceed these temperatures after some time interval.

5.2.1 Thermal Penetration Ignition Model.

A heuristic means of assessing whether or not ignition from low heat fluxes could cause ignition for finite time intervals is deduced from full-scale test data of aircraft and aircraft panels presented by Webster [9 and 19]. The results of six full-scale fire tests on aluminum skin aircraft, including the time at which interior aircraft ignition was observed or detected and the likely propagation paths, are summarized by Webster [9 and 19]. To use this data for low heat flux fire exposures, it is noted that aircraft insulation is typically wrapped in a Tedlar® (polyvinyl chloride polymer) moisture barrier [17] and that a reasonable estimate of the depth of degradation of the interior insulation corresponds to the upper performance limit for the Tedlar, or 204°C (400°F) [44]. Using the HEATING model described in section 5.1.1, the depth of the 204°C (400°F) isotherm within the insulation may be estimated for each of the six full-scale tests. These results are summarized in table 5, where 2.5 cm (1 in.) of fiberglass insulation backing and a peak incident heat flux of 150 kW/m² (13.2 Btu/s-ft²) are assumed [19]. The exposure heat flux is linearly increased from 0 kW/m² (0 Btu/s-ft²) to the peak value of 150 kW/m² (13.2 Btu/s-ft²) over the time to reach the peak fire size. Since the time to reach the heat flux profile varies from case to case, each test represents a unique heat flux profile. The results shown in table 5 indicate that the isotherm depth is fairly uniform at the time of ignition, having an average value of about 1.2 cm (0.47 in.) for a wide range of skin thicknesses, heat flux profiles, and ignition times. This suggests that when the 204°C (400°F) isotherm penetrates 1.2 cm (0.47 in.) into the insulation, it is reasonable to assume interior ignition is possible regardless of the incident heat flux.

Table 5. Summary of Full-Scale Aluminum Skin Fuselage Tests and Estimated Depth of the 204°C (400°F) Isotherm Within the Fiberglass Insulation

Test	Skin Thickness (mm (in.))	Time for Fire to Reach Peak Size (seconds)	Interior Ignition Time (seconds)	Predicted 204°C (400°F) Isotherm Depth in Insulation (cm (in.))
1	1.6 (0.063)	50	94	1.4 (0.56)
2	1.3 (0.05)	30	71	1.3 (0.50)
3	1.6 (0.063)	35	50	0.075 (0.30)
4	1.5 (0.06)	40	86	1.4 (0.54)
5	2.0 (0.08)	25	70	1.1 (0.44)
6	1.6 (0.063)	25	75	1.3 (0.51)

It is worth noting that the unexposed surface temperature limit for fire barriers is 164°C (325°F), and this temperature is meant to approximate the temperature at which Class A combustible materials adjacent to the barrier could ignite [45]. Using this heuristic model, a possible ignition mechanism would be that Class A combustible materials, which are adjacent to the exposed surfaces, including the insulation binders and moisture barriers, could ignite due to high temperatures. If sufficient amount of the moisture barrier have degraded, gases and flames can pass through the boundary and into the cabin upon ignition.

5.2.2 Thermal Penetration Ignition Model Results.

5.2.2.1 Constant Heat Flux Exposures.

As with the high heat flux exposures, the peak incident heat flux at the surface of the aircraft will vary with distance between the exposure and the skin. It may also vary with time if the fire is being suppressed, as noted previously, resulting in unique scenarios. However, by fixing the separation distance, the ignition time versus the exposure heat flux may be computed for various skin and insulation thickness combinations. These results are shown in figures 32 through 34 for aluminum skin and insulation thicknesses typical of aircraft. Figures 32 through 34 indicate the minimum heat flux that could cause interior ignition, as predicted using the model described in section 5.2.1. This is approximately 9.59 kW/m² (0.84 Btu/s-ft²). This is remarkably close to the 9-kW/m² (0.79-Btu/s-ft²) minimum ignition heat flux for common Class A materials of [30, 42, and 43].

Figure 35 shows the predicted interior ignition time for two skin thicknesses and insulation backing thicknesses. This figure shows that the model is not sensitive to the backing thickness, except when the exposure is close to 9.59 kW/m² (0.84 Btu/s-ft²). This is not unexpected as the ignition times increase rapidly, which allow the unexposed boundary condition to have a greater influence on the temperature profile within the insulation. The short interval over which the model is sensitive to the backing thickness (i.e., ~0.5 kW/m² (0.044 Btu/s-ft²)) is small relative to the sensitivity of the offset distance to the flux produced.

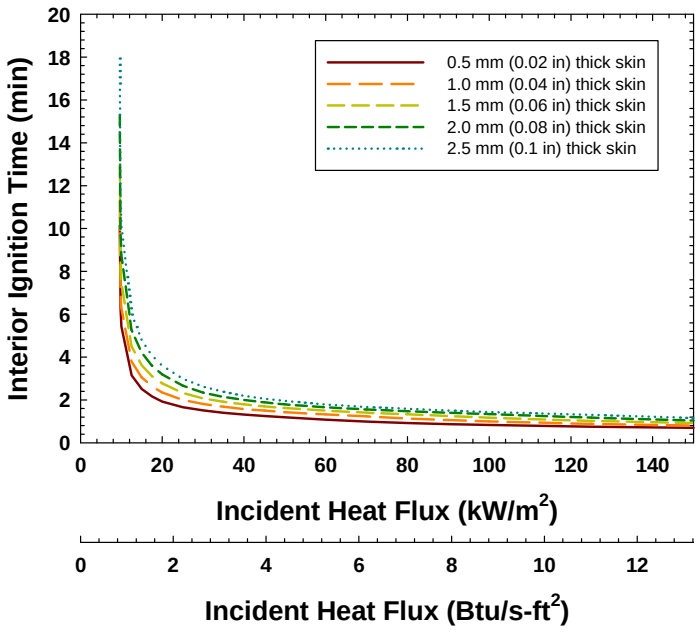

Figure 32. Aircraft Interior Ignition Time as Predicted From the Location of the 204°C (400°F) Isotherm vs the Incident Heat Flux With 2.5 cm (1 in.) of Fiberglass Insulation Backing

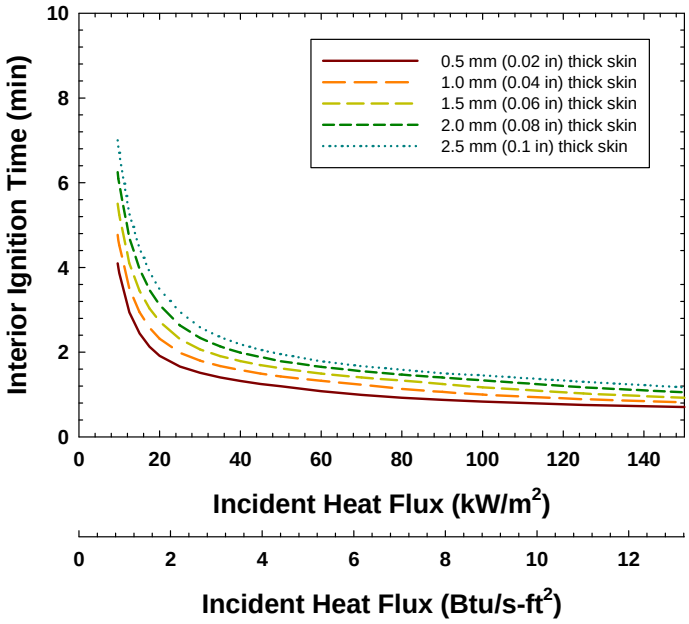

Figure 33. Aircraft Interior Ignition Time as Predicted From the Location of the 204°C (400°F) Isotherm vs the Incident Heat Flux With 5.1 cm (2 in.) of Fiberglass Insulation Backing

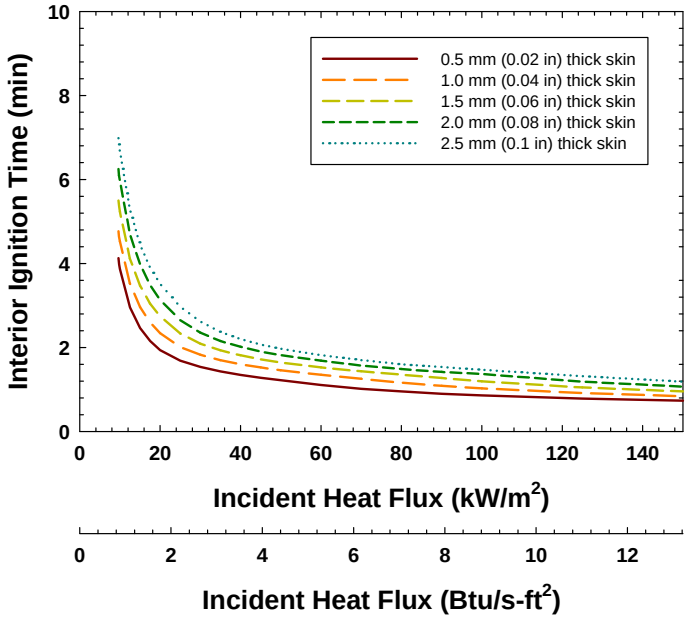

Figure 34. Aircraft Interior Ignition Time as Predicted From the Location of the 204°C (400°F) Isotherm vs the Incident Heat Flux With 10 cm (4 in.) of Fiberglass Insulation Backing

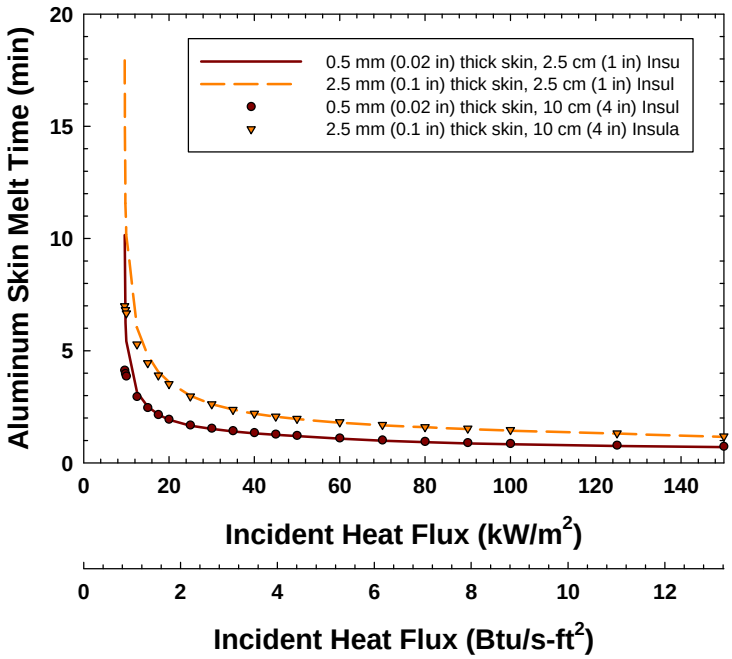

Figure 35. Aircraft Interior Ignition Time as Predicted From the Location of the 204°C (400°F) Isotherm vs the Incident Heat Flux for 2.5 cm (1 in.) and 10 cm (4 in.) of Fiberglass Insulation Backing

Figures 32 through 35 show that the predicted interior ignition time is strongly dependent on the exposure heat flux and on the skin thickness, but not on the insulation thickness in much the same manner as the skin-melting time. The shape of the heat flux versus ignition time curves resembles the shape of exposure flux versus ignition curves for typical combustible materials [42]. This suggests that the interior ignition model is essentially a combustible ignition model with the point of interest embedded within the solid rather than at the surface. It is also worth noting that the predicted ignition times are generally shorter than the skin-melting time for exposure fluxes between 45 and 60 kW/m² (4.0 and 5.3 Btu/s-ft²) and longer for exposure fluxes above 60 kW/m² (5.3 Btu/s-ft²).

The transient response of the aluminum skin and insulation exposed to a constant incident heat flux is shown in figures 36 and 37 for a low and a high incident exposure heat flux. The plots show that the aluminum skin is essentially at a uniform temperature regardless of the exposure flux and that the rate of temperature increase slows substantially when the aluminum skin approaches a temperature of approximately 482°C (900°F), the temperature at which the melting process is assumed to begin. The case shown in figure 37 indicates that the skin melts at a distance of 1.2 cm (0.47 in.), before the melting temperature is reached. The figures also show that for very low heat flux exposures, the unexposed boundary condition influences the temperature at the location of interest before ignition is predicted, whereas the reverse is true for high heat flux exposures.

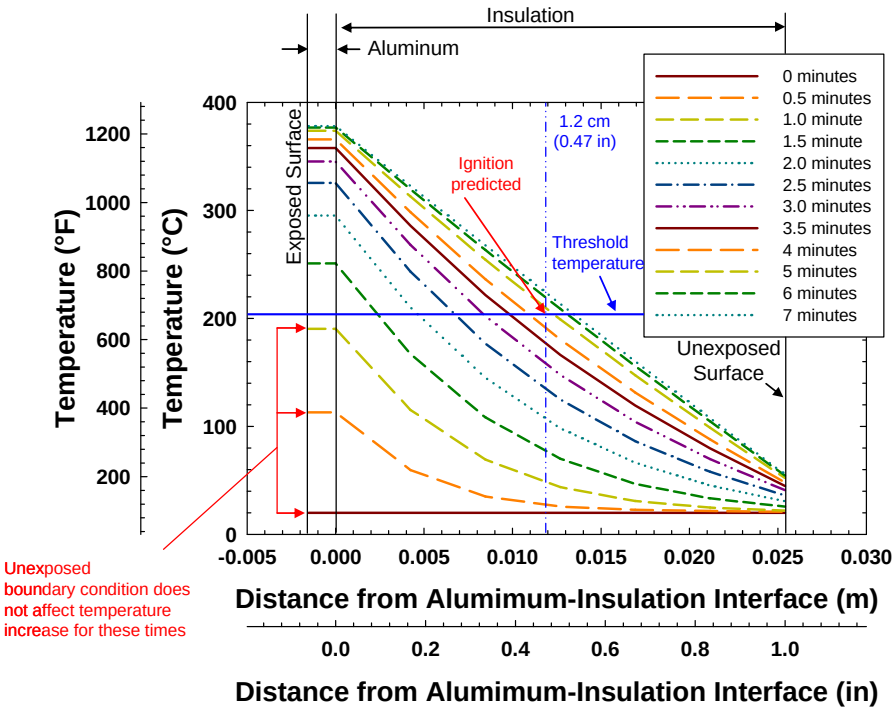

Figure 36. Temperature Profiles at Various Times Within the Skin-Insulation System: 1.5-mm (0.06-in.)-Thick Skin, 2.5-cm (1-in.) Fiberglass Insulation, and a 12.5-kW/m² (3.9-Btu/s-ft²) Incident Flux

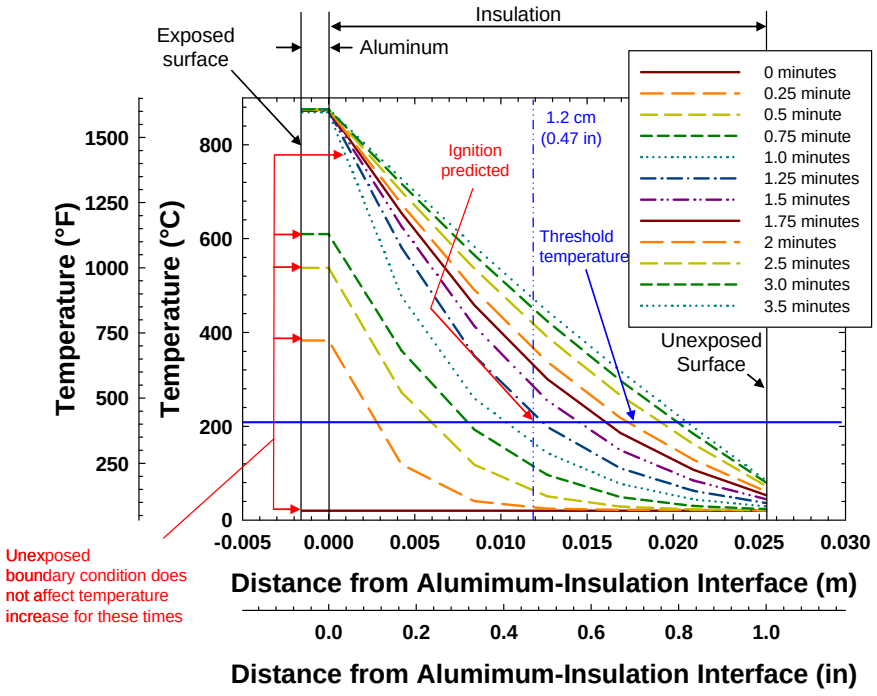

Figure 37. Temperature Profiles at Various Times Within the Skin-Insulation System: 1.5-mm (0.06-in.)-Thick Skin, 2.5-cm (1-in.) Fiberglass Insulation, and a 100-kW/m² (3.9-Btu/s-ft²) Incident Flux

5.2.2.2 Time-Varying Heat Flux Exposures.

Time-varying heat flux exposures affect the predicted ignition time somewhat differently than the skin-melting model because the point of interest is not at the surface. When the exposure heat flux decreases, the surface temperature either increases at a lower rate or decreases. If it increases, the system will behave as expected: all temperatures increase. If the skin surface temperature decreases, the temperature at interior points may still increase until the heat flow at that particular location reverses direction. This is because heat diffuses away from the point where the maximum temperature is located in two directions [46]; locations between the unexposed boundary and the point of maximum temperature may still experience a temperature increase due to this heat flow. The consequence of this phenomenon is that ignition may still be predicted even if the exposure heat flux is below the threshold value for ignition (9.59 kW/m² (0.84 Btu/s-ft²)). In essence, enough heat can be input into the system before ignition is predicted so that ignition is either unavoidable or small heat fluxes (i.e., <<9.59 kW/m² (0.84 Btu/s-ft²)) can reduce surface losses enough to cause ignition. Although this may be an artifact of the model approach, it can be viewed as a conservative means to account for ignition delays at low temperatures.

Figures 38 through 43 depict three possible responses of the temperature at a point 1.2 cm (0.47 in.) from the skin-insulation interface to variations in the exposure. Figures 38 and 39 depict a case where the temperature at the location of interest will increase beyond the critical value of 204°C (400°F), even though the heat flux exposure decreases to zero before ignition is predicted. Figure 38 shows the temperature distribution through the skin-insulation system at various times, and figure 39 shows the transient temperature at fixed locations. When the heat flux exposure decreases to zero at 1.8 minutes, the temperature at the location of interest is approximately 190°C (374°F). However, the peak temperature at this location is approximately 220°C (428°F), and this occurs at about 1 minute after the exposure has decreased to zero. For this particular case, ignition would be predicted at approximately 2.8 minutes.

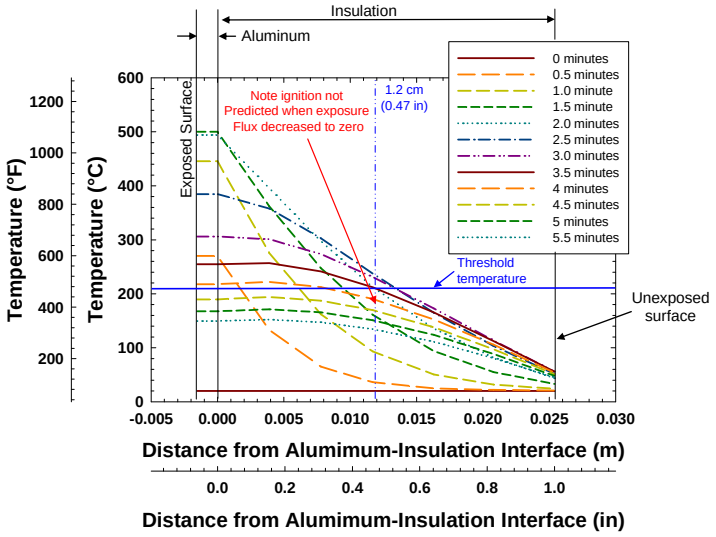

Figure 38. Temperature Profiles Through the Skin-Insulation System at Various Times for a 1.8-Minute, 35-kW/m² (3.1-Btu/s-ft²) Exposure Heat Flux and a Zero Postexposure Heat Flux—0.15-cm (0.06-in.)-Thick Aluminum Skin and 2.5 cm (1 in.) of Fiberglass Insulation

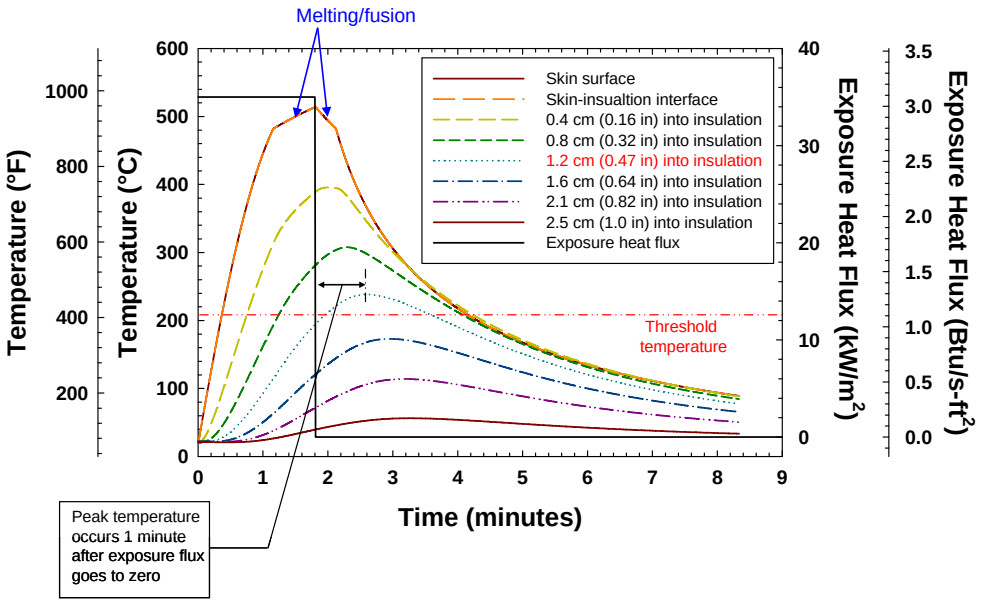

Figure 39. Transient Temperature Profiles at Fixed Locations in the Skin-Insulation System at Various Times for a 1.8-Minute, 35-kW/m² (3.1-Btu/s-ft²) Exposure Heat Flux and a Zero Postexposure Heat Flux—0.15-cm (0.06-in.)-Thick Aluminum Skin and 2.5 cm (1 in.) of Fiberglass Insulation

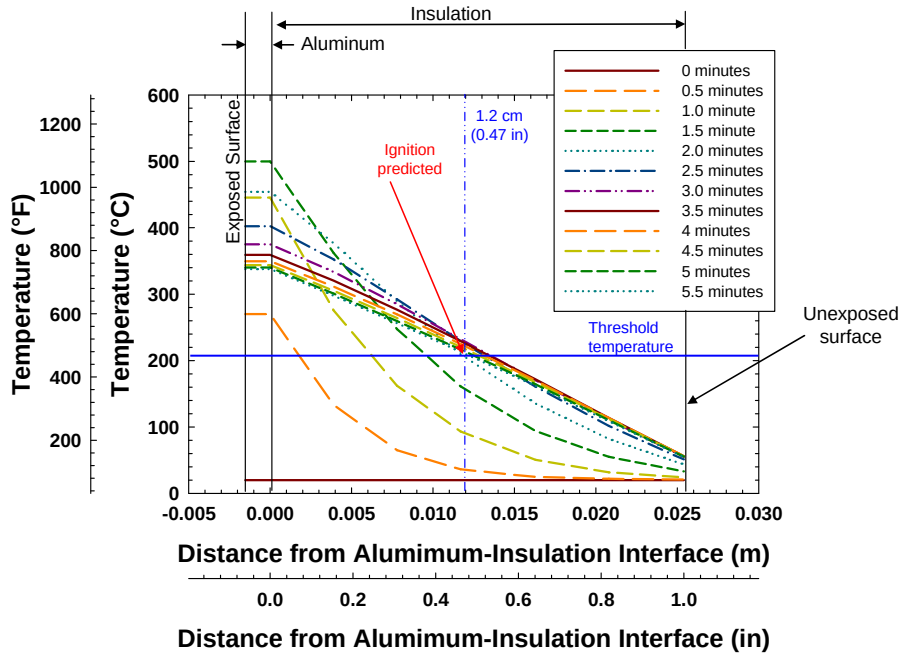

Figure 40. Temperature Profiles Through Skin-Insulation System at Various Times for a 1.5-Minute, 35-kW/m² (3.1-Btu/s-ft²) Exposure Heat Flux and a 9.59-kW/m² (0.84-Btu/s-ft²) Postexposure Heat Flux—0.15-cm (0.06-in.)-Thick Aluminum Skin and 2.5 cm (1 in.) of Fiberglass Insulation

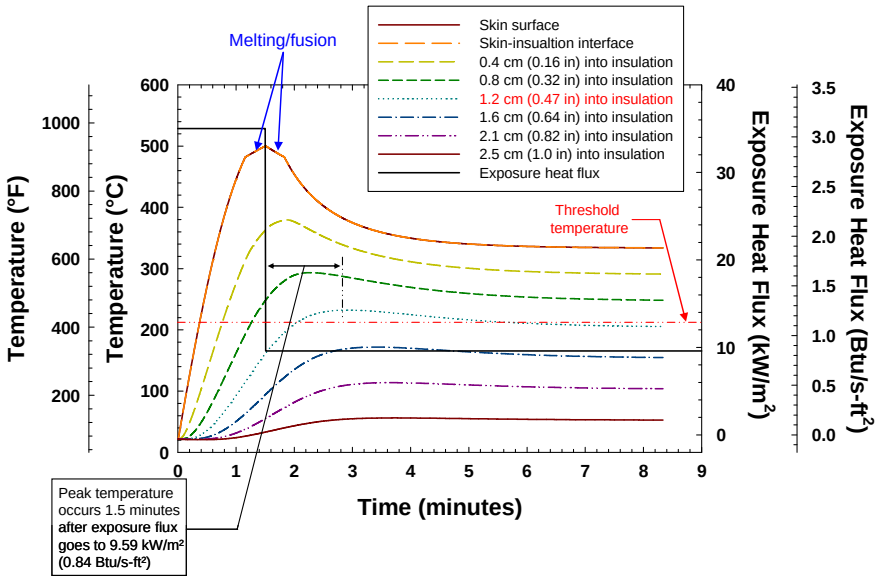

Figure 41. Transient Temperature Profiles at Fixed Locations in the Skin-Insulation System at Various Times for a 1.5-Minute, 35-kW/m² (3.1-Btu/s-ft²) Exposure Heat Flux and a 9.59-kW/m² (0.84-Btu/s-ft²) Postexposure Heat Flux—0.15-cm (0.06-in.)-Thick Aluminum Skin and 2.5 cm (1 in.) of Fiberglass Insulation

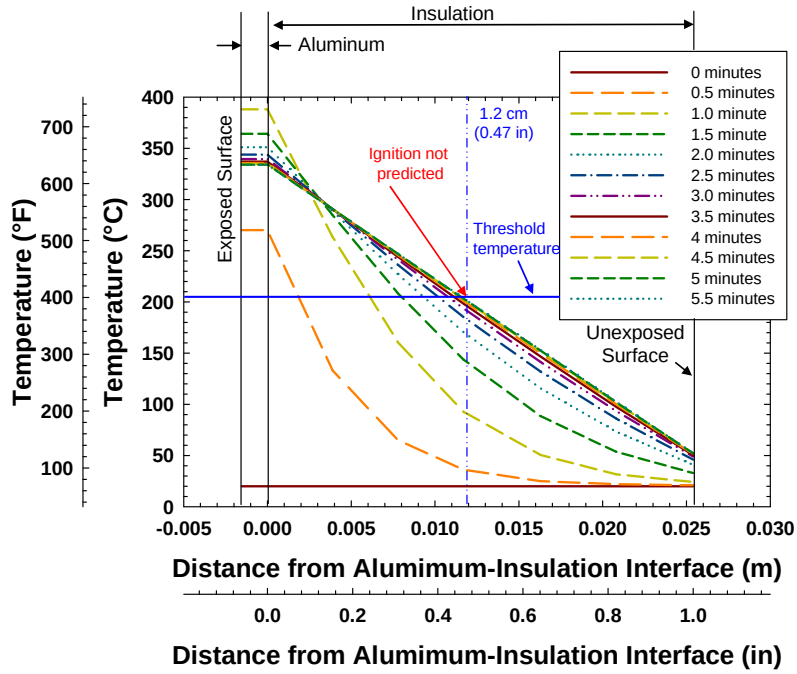

Figure 42. Temperature Profiles Through Skin-Insulation System at Various Times for a 0.83-Minute, 35-kW/m² (3.1-Btu/s-ft²) Exposure Heat Flux and a 9.59-kW/m² (0.84-Btu/s-ft²) Postexposure Heat Flux—0.15-cm (0.06-in.)-Thick Aluminum Skin and 2.5 cm (1 in.) of Fiberglass Insulation

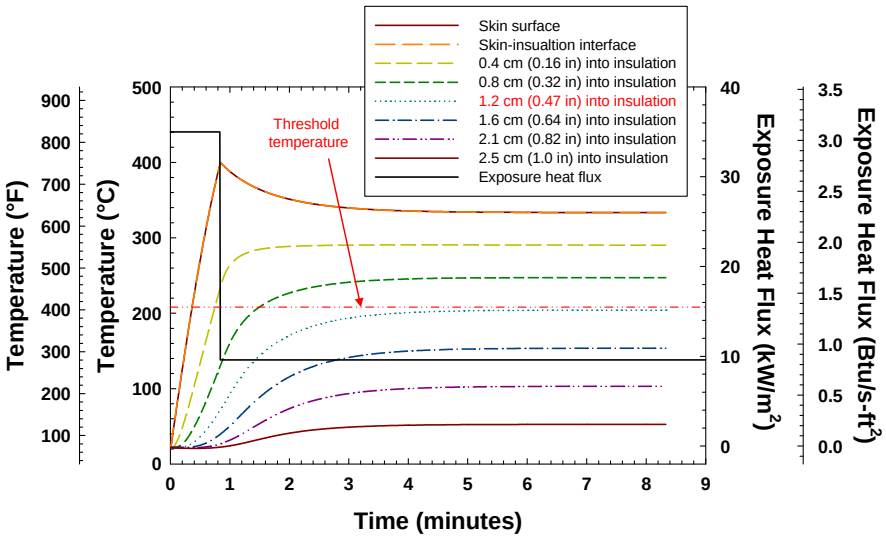

Figure 43. Transient Temperature Profiles at Fixed Locations in the Skin-Insulation System at Various Times for a 0.83-Minute, 35-kW/m² (3.1-Btu/s-ft²) Exposure Heat Flux and a 9.59-kW/m² (0.84-Btu/s-ft²) Postexposure Heat Flux—0.15-cm (0.06-in.)-Thick Aluminum Skin and 2.5 cm (1 in.) of Fiberglass Insulation

Figures 40 and 41 depict a case in which the temperature at the location of interest increases beyond the critical value of 204°C (400°F) and the heat flux exposure decreases to the minimum value for ignition, 9.59 kW/m² (0.84 Btu/s-ft²), before ignition is predicted. Figure 40 shows the temperature distribution through the skin-insulation system at various times, and figure 41 shows the transient temperature at fixed locations. When the heat flux exposure decreases to 9.59 kW/m² (0.84 Btu/s-ft²) at 1.5 minutes, the temperature at the location of interest is approximately 150°C (302°F). However, the peak temperature at this location is approximately 215°C (419°F), which occurs at approximately 1.5 minutes after the exposure has decreased to 9.59 kW/m² (0.84 Btu/s-ft²). The temperature at the location of interest decreases to the critical value of 204°C (400°F) after several minutes, as expected. For this particular case, ignition would be predicted at approximately 3 minutes.

Figures 42 and 43 depict a case in which the temperature at the location of interest does not increase beyond the critical value of 204°C (400°F) after the exposure heat flux decreases to the minimum value for ignition (9.59 kW/m² (0.84 Btu/s-ft²)). Figure 42 shows the temperature distribution through the skin-insulation system at various times, and figure 43 shows the transient temperature at fixed locations. When the heat flux exposure decreases to 9.59 kW/m² (0.84 Btu/s-ft²) at 0.8 minutes, the temperature at the location of interest is approximately 80°C (176°F). After several minutes, the temperature approaches the critical value of 204°C (400°F), as expected. For this particular case, ignition would not be predicted.

Figures 39 and 41 clearly show the effect that the heat of fusion for aluminum has on the temperature profiles. When the lower melting temperature is reached, the rate of increase slows sharply due to the absorption of heat associated with the melting process. This process is conservatively reversed during the cooling cycle, assuming that the softened or melted aluminum does not completely flow away from the area and solidifies. It is interesting to note that the heat

of fusion of the aluminum delays both the temperature increase and the temperature decrease at a fixed point, depending on the exposure boundary condition.

5.2.3 Thermal Penetration Ignition Model Summary.

A heuristic model for predicting the time a low heat flux exposure can cause interior aircraft ignition involves predicting the time the 204°C (400°F) temperature penetrates 1.2 cm (0.47 in.) into a 2.5-cm (1-in.)-thick fiberglass insulation backing. An assessment of various parameters, including the skin thickness and insulation backing thickness, indicates that the model is not sensitive to the assumed insulation thickness within the 2.5- to 10-cm (1- to 4-in.) range typical of aircraft configurations, except at exposure fluxes close to the minimum needed to cause ignition [9 and 19]. The ignition model is sensitive to the exposure heat flux range of approximately 0.5 to 1 kW/m² (0.044 to 0.088 Btu/s-ft²). This exposure heat flux range is not expected to result in significant differences in offset distances needed to prevent ignition, as determined in section 6. The results are also sensitive to the assumed skin thickness as this serves as the primary heat sink for the exposure boundary condition. An insulation backing thickness of 2.5 cm (1 in.) is assumed for consistency with the high heat flux model as well as the correlated test data.

The limiting heat flux capable of causing ignition is approximately 9.59 kW/m² (0.84 Btu/s-ft²), consistent with the lower critical ignition fluxes for Class A combustible materials [42 and 43]. Depending on the exposure boundary condition transient profile, ignition may still be predicted when the heat flux is lower than 9.59 kW/m² (0.84 Btu/s-ft²), since the location of interest is within the insulation system. This may be an artifact of the model approach, but it could be interpreted as the ignition delay expected when the temperature is close to but above the ignition temperature for the materials ignited.

5.3 IGNITION MODEL SUMMARY.

Two ignition models are used to predict the interior aircraft ignition potential, given an exposure profile. One model applicable to high heat flux exposures predicts ignition 10 seconds after the aluminum skin melts and is consistent with previous analysis approaches. A second model applicable to low heat flux exposures predicts ignition when the 204°C (400°F) isotherm penetrates 1.2 cm (0.47 in.) into a 2.5-cm (1-in.)-thick fiberglass insulation backing. The low heat flux model was developed to assess the ignition potential for exposure fires that would not melt the aluminum skin, and was deduced from typical aircraft construction materials and observations made in six full-scale fire tests of aircraft immersed in fuel fires. Both approaches have a lower ignition heat flux exposure threshold where the predicted ignition time diverges to infinity as the threshold is approached from higher heat fluxes. This is consistent with small-scale ignition tests for various combustible materials [42 and 43]. These thresholds are found to be 44.5 kW/m² (3.9 Btu/s-ft²) for the high heat flux model and 9.59 kW/m² (0.84 Btu/s-ft²) for the low heat flux exposure model. The overall potential for an exposure fire to cause interior aircraft ignition is predicted using both the high and low heat flux models as follows.

$$t_{ig}(Q_e'') = \min(t_{ig,1}(Q_e''), t_{ig,2}(Q_e'')) \tag{31}$$

where $t_{ig}(Q_e'')$ is the predicted ignition time ignition time (seconds) given an exposure heat flux profile Q_e'' (kJ/m² (Btu/ft²)), $t_{ig,1}(Q_e'')$ is the ignition time predicted using the high heat flux model (seconds), and $t_{ig,2}(Q_e'')$ is the ignition time predicted using the low heat flux model (seconds).

Figure 44 shows the ignition times for constant exposure fluxes, as predicted using equation 28 and the data in figures 26 and 32. Figure 44 indicates that the high heat flux model results in the minimum-predicted ignition time over the greatest exposure heat flux range when the skin is thin. It is possible that the limiting model changes one or more times over the period of interest for variable heat flux exposures.

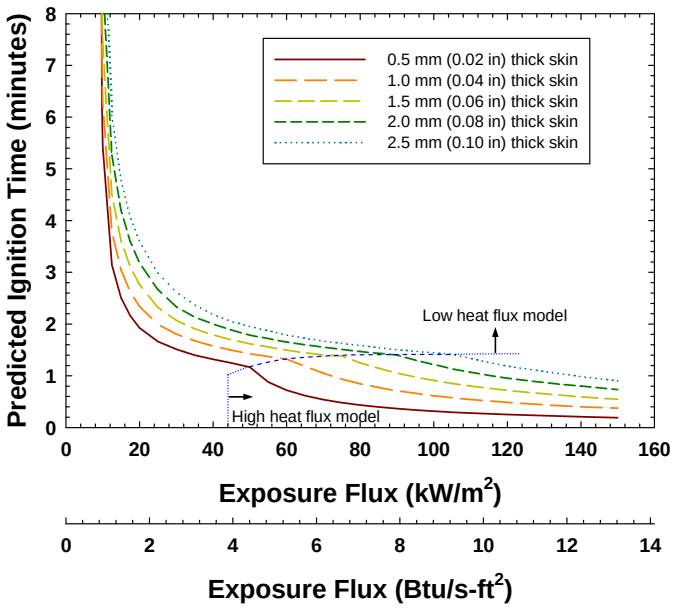

Figure 44. Predicted Interior Ignition Time for Constant Exposure Heat Fluxes

Because the focus of this analysis is on ignition prevention, equation 28 is actually inverted in this analysis so that the output is the most adverse heat flux exposure that does not result in ignition. The solution is the heat flux exposure that produces an infinite ignition time, which for practical purposes is greater than 20 minutes, as shown in figure 44. Since the initial response units are assumed to suppress the fire over 60 seconds, the agent amount (capacity to suppress) and the final offset between the fire and the aircraft are linked. This allows for a one-to-one correspondence between the agent amount and the exposure heat flux profile to be established such that an iterative solution for the most adverse heat flux exposure profile that does not cause ignition may be computed.

6. AIRCRAFT IMMERSION SCENARIOS.

Fire scenarios that immerse the aircraft can expose large portions of the fuselage to a heat flux of 150 kW/m² (13.2 Btu/s-ft²), as described in section 4. A thermal analysis of the interior ignition time under this exposure flux for aluminum skin aircraft shows that the ignition time will vary from approximately 10 to 60 seconds, depending on the skin thickness (see figure 45). This is less than the minimum assumed ARFF arrival time of 1 minute, and over 2 minutes less than the

current standard of 3 minutes. In addition, since ARFF needs 60 seconds to discharge the agent, the minimum flame impingement time at any location is 60 seconds, assuming immediate ARFF arrival. This suggests that for aluminum skin aircraft with the fuselage partially or fully immersed in the fuel spill fire, ARFF may have little opportunity to affect the egress time regardless of the agent amount carried.

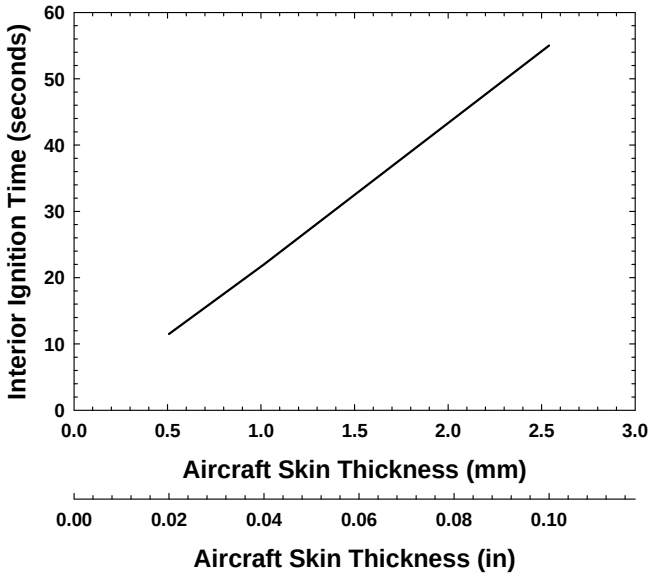

Figure 45. Interior Ignition Times for Fuel Spill Fire Scenarios That Immerse Some or all of the Aircraft

The analysis assumes that the exposure immediately reaches the maximum value of 150 kW/m² (13.2 Btu/s-ft²). This may not be entirely representative of the conditions, especially for very large fuel spill fires. Nevertheless, only a small portion of the aircraft needs to be in contact with the heat fluxes postulated for interior ignition to occur on the time scales shown in figure 45. It is possible that the fire would start before the aircraft stopped and the wind would blow the fire into contact with the fuselage as occurred during the Manchester aircraft incident [22].

Aircraft that are constructed of materials better able to resist thermal penetration may respond more favorably in a fuel spill fire immersion scenario [14 and 17]. If the thermal resistance of the fuselage is at least 60 seconds greater than ARFF arrival time, then interior ignition could be prolonged by ARFF and there would be some sensitivity to the agent amount. Section 7 provides some indication of ARFF's effect on fires offset from the aircraft; these results provide a sense of the distances and agent amount that would be involved for immersion scenarios involving aircraft fuselages that have some inherent fire resistance. Because the dominant aircraft material presently in use is aluminum, the results are constrained to those derived from figure 45. As such, if the aircraft is immersed in the flames, ARFF is not expected to be able to respond in sufficient time to prevent interior ignition and, thus, improve the chances for successful egress of the passengers. This is to say that prevention of interior ignition cannot be assured. Under actual circumstances, ARFF will respond and extinguish the exposing fire. The totally immersed aircraft condition is addressed in section 4.1.

7. NONIMMERSION SCENARIOS.

Eight aircraft and wind condition combinations were evaluated to assess the range of agent amount that would be necessary to allow for successful egress (see table 6). They represent the extremes for the aircraft dimensions, aircraft skin thickness and composition, and wind conditions using the methods described in section 4. The parameter ranges selected are expected to bracket the intermediate parameter values in terms of the agent amount required.

Table 6. Nonimmersion Scenario Groups Evaluated

Scenario Group	Aircraft Length (m (ft))	Aircraft Skin Material	Aircraft Skin Thickness (mm (in.))	Wind Speed (m/s (mph))	Wind Direction
1	73 (240)	0.5 (0.02)	Aluminum	0 (0)	No wind
2	48 (159)	0.5 (0.02)	Aluminum	0 (0)	No wind
3	27 (89)	0.5 (0.02)	Aluminum	0 (0)	No wind
4	73 (240)	2.5 (0.1)	Aluminum	0 (0)	No wind
5	73 (240)	0.5 (0.02)	Aluminum	8.9 (20)	Toward aircraft
6	73 (240)	2.5 (0.1)	Aluminum	8.9 (20)	Toward aircraft
7	73 (240)	0.5 (0.02)	Aluminum	8.9 (20)	Away from aircraft
8	73 (240)	Unspecified aircraft skin thickness	Composite aircraft skin material	0 (0)	No wind

The fire scenarios listed in table 6 assume that the characteristic diameter of the fire is equal to the length of the aircraft, as described in section 4. For any given incident, smaller-diameter fires are possible if the fuel spill amount is small or if ground contours are present. The analysis does not specifically consider smaller-diameter fires because the agent amount presently carried by ARFF is sufficient for complete extinguishment. Nevertheless, smaller-diameter fires could represent a class of exposures that are locally more severe than the large-diameter fires because

- the emissive power increases with decreasing diameter (see section 4.1.6).
- the flame deflection angle increases for a given wind speed as the diameter decreases (see section 4.1.7).

The view factor sharply decreases with distance for small-diameter fires, and this effect may partially offset the increased emissive power and flame deflection. Another offsetting factor is the lateral heat transfer due to the localized nature of the peak heat fluxes. However, for distances close to the aircraft, it should be noted that a small-diameter fire can cause interior ignition faster than a larger-diameter fire at the same position, but that the outcome is essentially independent of the agent amount. Consequently, only large-diameter fire scenarios are considered in detail in this section.

The results for each scenario in table 6 are presented in two types of tables. The first type of table provides the agent amount required to prevent ignition for different initial fuel spill fire

offset distances and ARFF arrival times. This type of table applies to the first responding units. The offset distances range from about a 0.5 m (1.6 ft) flame/aircraft separation to the distance at which ignition is not predicted. These distances vary among the scenarios. The assumed ARFF times range from 1 to 4 minutes. Also, the maximum initial amount of suppression agent brought by ARFF is 18,900 L (5,000 gal). When the solution yields a value greater than this, it is considered unsuccessful.

The second type of table summarizes the amount of additional agent required to allow for safe egress (movement away from the aircraft) for different offset distances and ARFF arrival times. The amount of agent necessary to prevent ignition is assumed to have been used initially. In cases where interior ignition is predicted, flame impingement is possible, or over 18,900 L (5,000 gal) of agent are required to prevent ignition, the agent amount shown in the second type of table is the total amount required to allow for safe egress. This may lead to some initially counterintuitive results: the agent amount can decrease, then increase, then decrease with an increasing offset distance. This is merely an artifact of the presentation; in all cases, the total amount of agent required to allow for safe egress decreases with increasing offset distance.

A graph that visually depicts the possible scenario outcomes accompanies the two aforementioned table types. The scenario outcomes are grouped into time regions for all initial fuel spill fire offset distances.

Eight scenarios were run depicting five time regions. These regions show the range of possible outcomes for all ARFF-initial fuel spill fire offset distances. These regions are described as follows:

- Time Region I: ARFF needs to extinguish the fire so that the offset distance results in an incident heat flux at the aircraft that is equal to 9.59 kW/m², the critical incident heat flux for interior aircraft ignition, as described in section 5.

- Time Region II: ARFF needs to extinguish the fire so that the offset distance results in an incident heat flux at the aircraft that is less than 9.59 kW/m².

- Time Region III: ARFF arrives before the aircraft ignites but suppressing some or all of the fuel spill fire does not prevent ignition.

- Time Region IV: ARFF arrives after the aircraft interior has ignited.

- Time Region V: The maximum incident heat flux at the aircraft is less than 9.59 kW/m²; thus, ignition is not predicted regardless of ARFF suppression actions.

In some cases, a sixth and seventh region are depicted that correspond to flame impingement and the transition to flame impingement, respectively. Ignition is unavoidable in either case so that no specific ignition estimates are shown for these regions.

Identifying which region applies to a particular scenario provides insight into the agent amount required to prevent ignition and to allow for safe egress. The interpretation of an event falling into Time Region IV or V is straightforward. The interpretation of an event falling in Time

Regions I, II, or III is not as intuitive and warrants additional explanation. Because a heat flux exposure of 9.59 kW/m² (0.84 Btu/s-ft²) would not result in interior ignition, the expectation is that suppressing a fuel spill fire so that the exposure heat flux equals this value would be an adequate measure. This is indeed the case for Time Region I, but it is not so for Time Regions II or III. In these regions, the exposure flux would either have to be reduced below 9.59 kW/m² (0.84 Btu/s-ft²) to prevent interior ignition or ignition is not preventable regardless of the area of fire suppressed. The reason for this result is that one criterion for ignition is the temperature at a fixed interior location within the aircraft skin-insulation boundary. Temperature changes due to boundary condition change that result in a temperature reduction do not immediately propagate into the skin-insulation boundary. Depending on the temperature distribution within the skin-insulation system, when the heat flux at the boundary decreases, the temperature at an interior point can still increase. The magnitude of this increase can be reduced by lowering the incident heat flux below the threshold value of 9.59 kW/m² (0.84 Btu/s-ft²), and if the temperature remains below the critical value of 204°C (400°F), then the event falls into Time Region II. If ignition still results when a zero heat flux is imposed, then the event falls into Time Region III. Figures 38 through 43 show the transient temperature distribution through the skin-insulation for cases that would fall into Time Regions II and III.

7.1 SCENARIO GROUP 1.

Scenario Group 1 involves a 73-m (240-ft)-long aircraft with a 0.5-mm (0.02-in.) aluminum skin. The wind speed is assumed to be zero. Some key features of this scenario group are as follows:

- Fire width/diameter: 73 m (240 ft)
- Maximum flame height: 81.2 m (266 ft) (line fire correlation)
- Maximum flame emissive power: 20.0 kW/m² (1.8 Btu/s-ft²)
- Heat release rate per unit width of the source fire: 170 MW/m (49,400 Btu/ft)
- Offset distance at which view factor reaches one: 2.15 m (7.1 ft)
- Distance at which heat flux is equal to 9.59 kW/m² (0.84 Btu/s-ft²): 19.1 m (63 ft)
- Distance at which heat flux is equal to 2.5 kW/m² (0.22 Btu/s-ft²): 87.5 m (287 ft)
- Maximum separation that can be developed using 18,900 L (5,000 gal) of suppression agent: 48.8 m (160 ft)

Figure 46 shows the possible outcomes for different ARFF arrival times as a function of the initial fire offsets. Tables 7 and 8 summarize the agent amount needed to prevent interior ignition and allow for safe passenger egress.

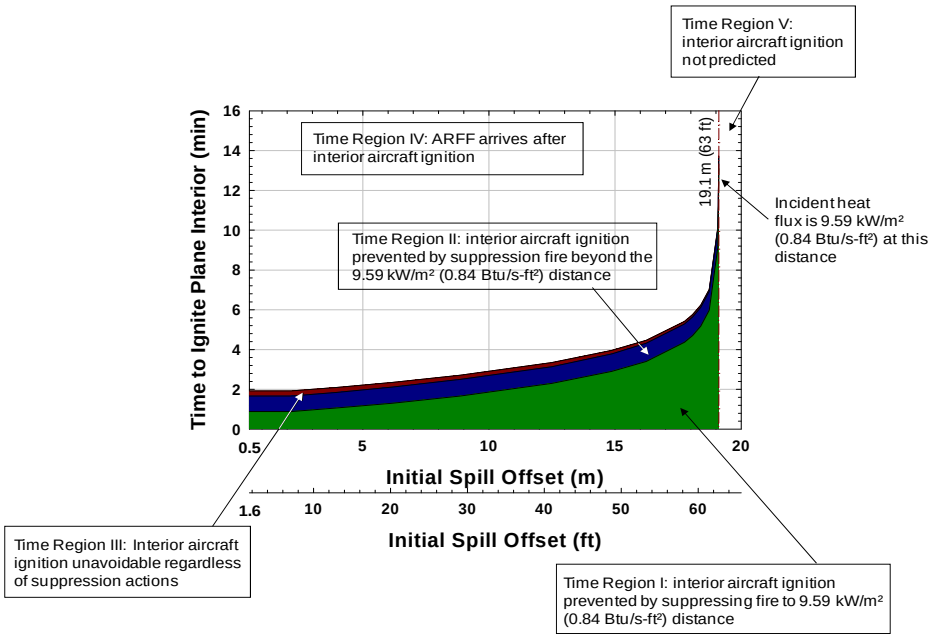

Figure 46. Response Time Regions for Scenario Group 1

Table 7. Suppression Agent Amount Needed to Prevent Interior Aircraft Ignition for Scenario Group 1

Initial Fuel Spill Offset (m (ft))	ARFF Arrival Time (min)						
	1.0	1.5	2.0	2.5	3.0	3.5	4.0
0.5 (1.6)	7450 L (1970 gal)	18,900+ L (5,000+ gal)	I.C.N.P	I.C.N.P	I.C.N.P	I.C.N.P	I.C.N.P
1 (3.3)	7250 L (1920 gal)	18,900+ L (5,000+ gal)	I.C.N.P	I.C.N.P	I.C.N.P	I.C.N.P	I.C.N.P
2 (6.6)	6680 L (1770 gal)	18,900+ L (5,000+ gal)	I.C.N.P	I.C.N.P	I.C.N.P	I.C.N.P	I.C.N.P
3 (9.8)	6290 L (1660 gal)	18,900+ L (5,000+ gal)	I.C.N.P	I.C.N.P	I.C.N.P	I.C.N.P	I.C.N.P
5 (16.4)	5440 L (1440 gal)	9,090 L (2,400 gal)	I.C.N.P	I.C.N.P	I.C.N.P	I.C.N.P	I.C.N.P
6 (19.7)	5070 L (1340 gal)	6,380 L (1,690 gal)	18,900+ L (5,000+ gal)	I.C.N.P	I.C.N.P	I.C.N.P	I.C.N.P
8 (26.2)	4300 (L) (1140 gal)	4, 300 (L) (1,140 gal)	13,250 L (3,500 gal)	18,900+ L (5,000+ gal)	I.C.N.P	I.C.N.P	I.C.N.P
10 (33)	3520 L (930 gal)	3,520 L (930 gal)	4,260 L (1,130 gal)	18,900+ L (5,000+ gal)	I.C.N.P	I.C.N.P	I.C.N.P
12 (39)	2750 L (730 gal)	2,750 L (730 gal)	2,750 L (730 gal)	4,930 L (1,300 gal)	18,900+ L (5,000+ gal)	I.C.N.P	I.C.N.P
14 (46)	1980 L (520 gal)	1,980 L (520 gal)	1,980 L (520 gal)	1,980 L (520 gal)	4,160 L (1,100 gal)	18,900+ L (5,000+ gal)	I.C.N.P

Table 7. Suppression Agent Amount Needed to Prevent Interior Aircraft Ignition for Scenario Group 1 (Continued)

Initial Fuel Spill Offset (m (ft))	ARFF Arrival Time (min)						
	1.0	1.5	2.0	2.5	3.0	3.5	4.0
16 (52)	1180 L (310 gal)	1,180 L (310 gal)	1,180 L (310 gal)	1,180 L (310 gal)	1,180 L (310 gal)	1,640 L (440 gal)	18,900+ L (5,000+ gal)
18 (59)	430 L (110 gal)	430 L (110 gal)	430 L (110 gal)	430 L (110 gal)	430 L (110 gal)	430 L (110 gal)	430 L (110 gal)
19.1 (63)	none	none	none	none	none	none	none

+over 18,900 L (5,000 gal) condition

Key:

I.C.N.P – Internal aircraft ignition cannot be prevented under the assumed conditions.

Green: Time Region I

Blue: Time Region II

Red: Time Region III or IV

Black: Time Region V

Table 8. Suppression Agent Amount Needed to Allow Passengers to Egress to a Safe Area for Scenario Group 1†

Initial Fuel Spill Offset (m (ft))	ARFF Arrival Time (min)						
	1.0	1.5	2.0	2.5	3.0	3.5	4.0
0.5 (1.6)	26,200 L (6,930 gal)	33,700 L (8,900 gal)‡	33,700 L (8,900 gal)	33,700 L (8,900 gal)	33,700 L (8,900 gal)	33,700 L (8,900 gal)	33,700 L (8,900 gal)
1 (3.3)	26,200 L (6,930 gal)	33,500 L (8,850 gal)‡	33,500 L (8,850 gal)	33,500 L (8,850 gal)	33,500 L (8,850 gal)	33,500 L (8,850 gal)	33,500 L (8,850 gal)
2 (6.6)	26,400 L (6,980 gal)	33,100 L (8,750 gal)‡	33,100 L (8,750 gal)	33,100 L (8,750 gal)	33,100 L (8,750 gal)	33,100 L (8,750 gal)	33,100 L (8,750 gal)
3 (9.8)	26,400 L (6,980 gal)	32,700 L (8,650 gal)‡	32,700 L (8,650 gal)	32,700 L (8,650 gal)	32,700 L (8,650 gal)	32,700 L (8,650 gal)	32,700 L (8,650 gal)
5 (16.4)	26,500 L (7,000 gal)	22,800 L (6,040 gal)	31,910 L (8,440 gal)	31,910 L (8,440 gal)	31,910 L (8,440 gal)	31,910 L (8,440 gal)	31,910 L (8,440 gal)
6 (19.7)	26,500 L (7,000 gal)	25,100 L (6,650 gal)	31,500 L (8,340 gal)‡	31,500 L (8,340 gal)	31,500 L (8,340 gal)	31,500 L (8,340 gal)	31,500 L (8,340 gal)
8 (26.2)	26,500 L (7,000 gal)	26,500 L (7,000 gal)	17,500 L (4,630 gal)	30,750 L (8,140 gal)‡	30,800 L (8,140 gal)	30,800 L (8,140 gal)	30,800 L (8,140 gal)
10 (33)	26,500 L (7,000 gal)	26,500 L (7,000 gal)	25,700 L (6,810 gal)	30,000 L (7,930 gal)‡	29,900 L (7,930 gal)	29,900 L (7,930 gal)	29,900 L (7,930 gal)
12 (39)	26,500 L (7,000 gal)	26,500 L (7,000 gal)	26,500 L (7,000 gal)	24,300 L (6,420 gal)	29,200 L (7,730 gal)‡	29,200 L (7,730 gal)	29,200 L (7,730 gal)
14 (46)	26,500 L (7,000 gal)	26,500 L (7,000 gal)	26,500 L (7,000 gal)	26,500 L (7,000 gal)	24,300 L (6,420 gal)	28,400 L (7,520 gal)‡	28,400 L (7,520 gal)
16 (52)	26,500 L (7,000 gal)	26,500 L (7,000 gal)	26,500 L (7,000 gal)	26,500 L (7,000 gal)	26,500 L (7,000 gal)	25,800 L (6,880 gal)	27,700 L (7,320 gal)‡

Table 8. Suppression Agent Amount Needed to Allow Passengers to Egress to a Safe Area for Scenario Group 1† (Continued)

Initial Fuel Spill Offset (m (ft))	ARFF Arrival Time (min)						
	1.0	1.5	2.0	2.5	3.0	3.5	4.0
18 (59)	26,500 L (7,000 gal)	26,500 L (7,000 gal)	26,500 L (7,000 gal)	26,500 L (7,000 gal)	26,500 L (7,000 gal)	26,500 L (7,000 gal)	26,500 L (7,000 gal)
19.1 (63)	26,500 L (7,000 gal)	26,500 L (7,000 gal)	26,500 L (7,000 gal)	26,500 L (7,000 gal)	26,500 L (7,000 gal)	26,500 L (7,000 gal)	26,500 L (7,000 gal)
20 (66)	26,100 L (6,910 gal)						
25 (82)	24,180 L (6,400 gal)						
30 (98)	22,240 L (5,880 gal)						
35 (115)	20,310 L (5,370 gal)						
40 (131)	18,370 L (4,860 gal)						
50 (164)	14,510 L (3,838 gal)						
60 (197)	10,640 L (2,810 gal)						
70 (230)	6,770 L (1,791 gal)						
80 (262)	2,900 L (770 gal)						
85 (279)	970 L (260 gal)						
87.5 (287)	none						

†No initial agent assumed for table 7 I.C.N.P and 18,900$^+$ L (5,000$^+$ gal) cases.
‡ Table 7 18,900$^+$ L (5,000$^+$ gal) case.
Key:
I.C.N.P – Internal aircraft ignition cannot be prevented under the assumed conditions.
Green: Time Region I
Blue: Time Region II
Red: Time Region III or IV
Black: Time Region V

7.2 SCENARIO GROUP 2.

Scenario Group 2 involves a 48-m (159-ft)-long aircraft with a 0.5-mm (0.02-in.) aluminum skin. The wind speed is assumed to be zero. Some key features of this scenario group are as follows:

- Fire width/diameter: 48 m (159 ft)
- Maximum flame height: 61.7 m (202 ft) (line fire correlation)
- Maximum flame emissive power: 20.4 kW/m² (1.79 Btu/s-ft²)
- Heat release rate per unit width of the source fire: 113 MW/m (32,700 Btu/ft)
- Offset distance at which view factor reaches one: 1.55 m (5.1 ft)
- Distance at which heat flux is equal to 9.59 kW/m² (0.84 Btu/s-ft²): 15.2 m (50 ft)

- Distance at which heat flux is equal to 2.5 kW/m² (0.22 Btu/s-ft²): 63 m (207 ft)
- Maximum separation that can be developed using 18,900 L (5,000 gal) of suppression agent: 73 m (239 ft)

Figure 47 shows the possible outcomes for different ARFF arrival times as a function of the initial fire offsets. Tables 9 and 10 summarize the agent amount needed to prevent interior ignition and allow for safe passenger egress.

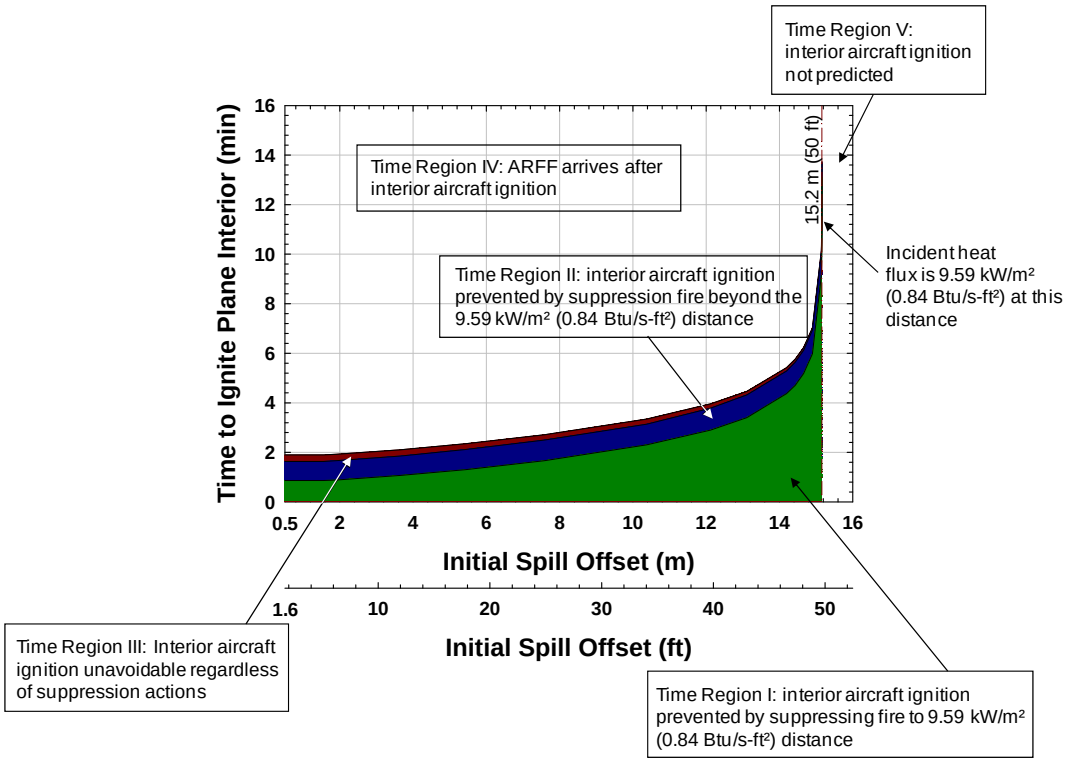

Figure 47. Response Time Regions for Scenario Group 2

Table 9. Suppression Agent Amount Needed to Prevent Interior Aircraft Ignition for Scenario Group 2

Initial Fuel Spill Offset (m (ft))	ARFF Arrival Time (min)						
	1.0	1.5	2.0	2.5	3.0	3.5	4.0
0.5 (1.6)	4040 L (1070 gal)	18,900^{+} L (5,000^{+} gal)	I.C.N.P	I.C.N.P	I.C.N.P	I.C.N.P	I.C.N.P
1 (3.3)	3840 L (1020 gal)	18,900^{+} L (5,000^{+} gal)	I.C.N.P	I.C.N.P	I.C.N.P	I.C.N.P	I.C.N.P
2 (6.6)	3460 L (90 gal)	18,900^{+} L (5,000^{+} gal)	I.C.N.P	I.C.N.P	I.C.N.P	I.C.N.P	I.C.N.P
3 (9.8)	3110 L (820 gal)	9,670 L (2,560 gal)	I.C.N.P	I.C.N.P	I.C.N.P	I.C.N.P	I.C.N.P

Table 9. Suppression Agent Amount Needed to Prevent Interior Aircraft Ignition for Scenario Group 2 (Continued)

Initial Fuel Spill Offset (m (ft))	ARFF Arrival Time (min)						
	1.0	1.5	2.0	2.5	3.0	3.5	4.0
5 (16.4)	2490 L (660 gal)	2,450 L (660 gal)	18,900+ L (5,000+ gal)	I.C.N.P	I.C.N.P	I.C.N.P	I.C.N.P
7.5 (25)	1960 L (520 gal)	1,960 L (520 gal)	3,780 L (1,000 gal)	18,900+ L (5,000+ gal)	I.C.N.P	I.C.N.P	I.C.N.P
10 (33)	1320 L (350 gal)	1,320 L (350 gal)	1,320 L (350 gal)	2,240 L (590 gal)	18,900+ L (5,000+ gal)	I.C.N.P	I.C.N.P
12.5 (41)	680 L (180 gal)	680 L (180 gal)	680 L (180 gal)	680 L (180 gal)	705 L (190 gal)	1800 L (480 gal)	18,900+ L (5,000+ gal)
15 (49)	40 L (10 gal)	40 L (10 gal)	40 L (10 gal)	40 L (10 gal)	40 L (10 gal)	40 L (10 gal)	40 L (10 gal)
15.2 (50)	none	none	none	none	none	none	none

+over 18,900 L (5,000 gal) condition

Key:

I.C.N.P – Internal aircraft ignition cannot be prevented under the assumed conditions.

Green: Time Region I

Blue: Time Region II

Red: Time Region III or IV

Black: Time Region V

Table 10. Suppression Agent Amount Needed to Allow Passengers to Egress to a Safe Area for Scenario Group 2†

Initial Fuel Spill Offset (m (ft))	ARFF Arrival Time (min)						
	1.0	1.5	2.0	2.5	3.0	3.5	4.0
0.5 (1.6)	12,000 L (3,170 gal)	16,020 L (4,240 gal)‡	16,030 L (4,240 gal)	16,030 L (4,240 gal)	16,030 L (4,240 gal)	16,030 L (4,240 gal)	16,030 L (4,240 gal)
1 (3.3)	12,040 L (3,190 gal)	15,890 L (4,200 gal)‡	15,890 L (4,200 gal)	15,890 L (4,200 gal)	15,890 L (4,200 gal)	15,890 L (4,200 gal)	15,890 L (4,200 gal)
2 (6.6)	12,200 L (3,220 gal)	15,630 L (4,140 gal)‡	15,630 L (4,140 gal)	15,630 L (4,140 gal)	15,630 L (4,140 gal)	15,630 L (4,140 gal)	15,630 L (4,140 gal)
3 (9.8)	12,260 L (3,240 gal)	5,700 L (1,510 gal)	15,380 L (4,070 gal)	15,380 L (4,070 gal)	15,380 L (4,070 gal)	15,380 L (4,070 gal)	15,380 L (4,070 gal)
5 (16.4)	12,260 L (3,240 gal)	12,260 L (3,240 gal)	14,860 L (3,930 gal)‡	14,860 L (3,930 gal)	14,860 L (3,930 gal)	14,860 L (3,930 gal)	14,860 L (3,930 gal)
7.5 (25)	12,260 L (3,240 gal)	12,260 L (3,240 gal)	10,440 L (2,762 gal)	14,220 L (3,760 gal)‡	14,220 L (3,760 gal)	14,220 L (3,760 gal)	14,220 L (3,760 gal)
10 (33)	12,260 L (3,240 gal)	12,260 L (3,240 gal)	12,260 L (3,240 gal)	11,340 L (3,000 gal)	13,580 L (3,590 gal)‡	13,580 L (3,590 gal)	13,580 L (3,590 gal)
12.5 (41)	12,260 L (3,240 gal)	12,260 L (3,240 gal)	12,260 L (3,240 gal)	12,260 L (3,240 gal)	12,240 L (3,240 gal)	11,150 L (2,950 gal)	12,940 L (3,420 gal)‡

Table 10. Suppression Agent Amount Needed to Allow Passengers to Egress to a Safe Area for Scenario Group 2† (Continued)

Initial Fuel Spill Offset (m (ft))	ARFF Arrival Time (min)						
	1.0	1.5	2.0	2.5	3.0	3.5	4.0
15 (49)	12,260 L (3,240 gal)	12,260 L (3,240 gal)	12,260 L (3,240 gal)	12,260 L (3,240 gal)	12,260 L (3,240 gal)	12,260 L (3,240 gal)	12,260 L (3,240 gal)
15.2 (50)	12,260 L (3,240 gal)	12,260 L (3,240 gal)	12,260 L (3,240 gal)	12,260 L (3,240 gal)	12,260 L (3,240 gal)	12,260 L (3,240 gal)	12,260 L (3,240 gal)
17.5 (57)	11,660 L (3,090 gal)						
20 (66)	11,020 L (2,920 gal)						
25 (82)	9,740 L (2,580 gal)						
30 (98)	8,460 L (2,240 gal)						
35 (115)	7,170 L (1,900 gal)						
40 (131)	5,890 L (1,560 gal)						
45 (148)	4,610 L (1,220 gal)						
50 (164)	3,330 L (880 gal)						
55 (180)	2,050 L (540 gal)						
60 (197)	770 L (200 gal)						
63 (207)	none						

†No initial agent assumed for table 9 I.C.N.P and 18,900$^+$ L (5,000$^+$ gal) cases.
‡Table 9 18,900$^+$ L (5,000$^+$ gal) case.
Key:
I.C.N.P – Internal aircraft ignition cannot be prevented under the assumed conditions.
Green: Time Region I
Blue: Time Region II
Red: Time Region III or IV
Black: Time Region V

7.3 SCENARIO GROUP 3.

Scenario Group 3 involves a 27-m (89-ft)-long aircraft with a 0.5-mm (0.02-in.) aluminum skin. The wind speed is assumed to be zero. Some key features of this scenario group are as follows:

- Fire width/diameter: 27 m (89 ft)
- Maximum flame height: 41.9 m (137 ft) (line fire correlation)
- Maximum flame emissive power: 24.6 kW/m² (2.17 Btu/s-ft²)
- Heat release rate per unit width of the source fire: 63 MW/m (18,200 Btu/ft)
- Offset distance at which view factor reaches one: 1.03 m (3.4 ft)
- Distance at which heat flux is equal to 9.59 kW/m² (0.84 Btu/s-ft²): 13.4 m (44 ft)

- Distance at which heat flux is equal to 2.5 kW/m² (0.22 Btu/s-ft²): 45 m (148 ft)
- Maximum separation that can be developed using 18,900 L (5,000 gal) of suppression agent: 132 m (433 ft)

Figure 48 shows the possible outcomes for different ARFF arrival times as a function of the initial fire offsets. Tables 11 and 12 summarize the agent amount needed to prevent interior ignition and allow for safe passenger egress.

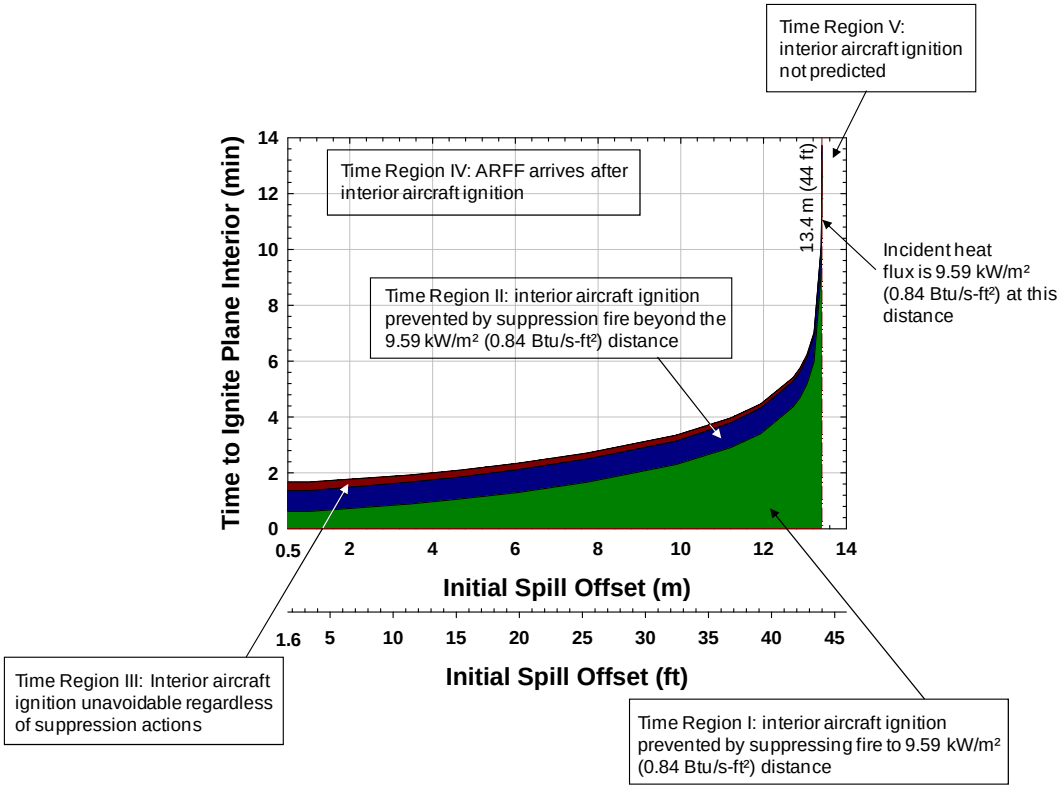

Figure 48. Response Time Regions for Scenario Group 3

Table 11. Suppression Agent Amount Needed to Prevent Interior Aircraft Ignition for Scenario Group 3

Initial Fuel Spill Offset (m (ft))	ARFF Arrival Time (min)						
	1.0	1.5	2.0	2.5	3.0	3.5	4.0
0.5 (1.6)	3520 L (930 gal)	I.C.N.P	I.C.N.P	I.C.N.P	I.C.N.P	I.C.N.P	I.C.N.P
1 (3.3)	3330 L (880 gal)	I.C.N.P	I.C.N.P	I.C.N.P	I.C.N.P	I.C.N.P	I.C.N.P
2 (6.6)	2220 L (590 gal)	I.C.N.P	I.C.N.P	I.C.N.P	I.C.N.P	I.C.N.P	I.C.N.P
3 (9.8)	1610 L (430 gal)	18,900^{+} L (5,000^{+} gal)	I.C.N.P	I.C.N.P	I.C.N.P	I.C.N.P	I.C.N.P

Table 11. Suppression Agent Amount Needed to Prevent Interior Aircraft Ignition for Scenario Group 3 (Continued)

Initial Fuel Spill Offset (m (ft))	ARFF Arrival Time (min)						
	1.0	1.5	2.0	2.5	3.0	3.5	4.0
4 (13)	1360 L (360 gal)	5,200 L (1,380 gal)	I.C.N.P	I.C.N.P	I.C.N.P	I.C.N.P	I.C.N.P
5 (16)	1210 L (320 gal)	2,330 L (620 gal)	I.C.N.P	I.C.N.P	I.C.N.P	I.C.N.P	I.C.N.P
6 (20)	1060 L (280 gal)	1,330 L (350 gal)	18,900+ L (5,000+ gal)	I.C.N.P	I.C.N.P	I.C.N.P	I.C.N.P
8 (26)	770 L (210 gal)	770 L (210 gal)	1,220 L (320 gal)	18,900+ L (5,000+ gal)	I.C.N.P	I.C.N.P	I.C.N.P
10 (33)	490 L (130 gal)	490 L (130 gal)	490 L (130 gal)	610 L (160 gal)	8,180 L (2,160 gal)	I.C.N.P	I.C.N.P
12 (39)	200 L (50 gal)	200 L (50 gal)	200 L (50 gal)	200 L (50 gal)	200 L (50 gal)	200 L (50 gal)	750 L (200 gal)
13.4 (44)	none	none	none	none	none	none	none

+over 18,900 L (5,000 gal) condition

Key:

I.C.N.P – Internal aircraft ignition cannot be prevented under the assumed conditions.

Green: Time Region I

Blue: Time Region II

Red: Time Region III or IV

Black: Time Region V

Table 12. Suppression Agent Amount Needed to Allow Passengers to Egress to a Safe Area for Scenario Group 3†

Initial Fuel Spill Offset (m (ft))	ARFF Arrival Time (min)						
	1.0	1.5	2.0	2.5	3.0	3.5	4.0
0.5 (1.6)	2870 L (760 gal)	6380 L (1690 gal)	6380 L (1690 gal)	6380 L (1690 gal)	6380 L (1690 gal)	6380 L (1690 gal)	6380 L (1690 gal)
1 (3.3)	2980 L (790 gal)	6310 L (1670 gal)	6310 L (1670 gal)	6310 L (1670 gal)	6310 L (1670 gal)	6310 L (1670 gal)	6310 L (1670 gal)
2 (6.6)	3950 L (1040 gal)	6170 L (1630 gal)	6170 L (1630 gal)	6170 L (1630 gal)	6170 L (1630 gal)	6170 L (1630 gal)	6170 L (1630 gal)
3 (9.8)	4410 L (1170 gal)	6030 L (1590 gal)‡	6030 L (1590 gal)	6030 L (1590 gal)	6030 L (1590 gal)	6030 L (1590 gal)	6030 L (1590 gal)
4 (13)	4520 L (1200 gal)	680 L (180 gal)	5880 L (1560 gal)	5880 L (1560 gal)	5880 L (1560 gal)	5880 L (1560 gal)	5880 L (1560 gal)
5 (16)	4530 L (1200 gal)	3410 L (900 gal)	5740 L (1520 gal)	5740 L (1520 gal)	5740 L (1520 gal)	5740 L (1520 gal)	5740 L (1520 gal)
6 (20)	4530 L (1200 gal)	4270 L (1129 gal)	5590 L (1480 gal)‡	5590 L (1480 gal)	5590 L (1480 gal)	5590 L (1480 gal)	5590 L (1480 gal)

Table 12. Suppression Agent Amount Needed to Allow Passengers to Egress to a Safe Area for Scenario Group 3[†] (Continued)

Initial Fuel Spill Offset (m (ft))	ARFF Arrival Time (min)						
	1.0	1.5	2.0	2.5	3.0	3.5	4.0
8 (26)	4530 L (1200 gal)	4530 L (1200 gal)	4090 L (1080 gal)	5310 L (1400 gal)[‡]	5310 L (1400 gal)	5310 L (1400 gal)	5310 L (1400 gal)
10 (33)	4530 L (1200 gal)	4530 L (1200 gal)	4530 L (1200 gal)	4410 L (1170 gal)	none	5020 L (1330 gal)	5020 L (1330 gal)
12 (39)	4530 L (1200 gal)	4530 L (1200 gal)	4530 L (1200 gal)	4530 L (1200 gal)	4530 L (1200 gal)	4530 L (1200 gal)	3980 L (1050 gal)
13.4 (44)	4530 L (1200 gal)	4530 L (1200 gal)	4530 L (1200 gal)	4530 L (1200 gal)	4530 L (1200 gal)	4530 L (1200 gal)	4530 L (1200 gal)
15 (50)	4,300 L (1138 gal)						
20 (66)	3,590 L (949 gal)						
25 (82)	2,870 L (759 gal)						
30 (98)	2,150 L (569 gal)						
35 (115)	1,430 L (379 gal)						
40 (131)	720 L (190 gal)						
45 (148)	none						

[†]No initial agent assumed for Table 11 I.C.N.P and 18,900[+] L (5,000[+] gal) cases.
[‡]Table 11 18,900[+] L (5,000[+] gal) case.
Key:
I.C.N.P – Internal aircraft ignition cannot be prevented under the assumed conditions.
Green: Time Region I
Blue: Time Region II
Red: Time Region III or IV
Black: Time Region V

7.4 SCENARIO GROUP 4.

Scenario Group 4 involves a 73-m (240-ft)-long aircraft with a 2.5-mm (0.1-in.) aluminum skin. The wind speed is assumed to be zero. Some key features of this scenario group are as follows:

- Fire width/diameter: 73 m (240 ft)
- Maximum flame height: 81.2 m (266 ft) (line fire correlation)
- Maximum flame emissive power: 20.0 kW/m² (1.8 Btu/s-ft²)
- Heat release rate per unit width of the source fire: 170 MW/m (49,400 Btu/ft)
- Offset distance at which view factor reaches one: 2.15 m (7.1 ft)
- Distance at which heat flux is equal to 9.59 kW/m² (0.84 Btu/s-ft²): 19.1 m (63 ft)

- Distance at which heat flux is equal to 2.5 kW/m² (0.22 Btu/s-ft²): 87.5 m (287 ft)
- Maximum separation that can be developed using 18,900 L (5,000 gal) of suppression agent: 48.8 m (160 ft)

Figure 49 shows the possible outcomes for different ARFF arrival times as a function of the initial fire offsets. Tables 13 and 14 summarize the agent amount needed to prevent interior ignition and allow for safe passenger egress.

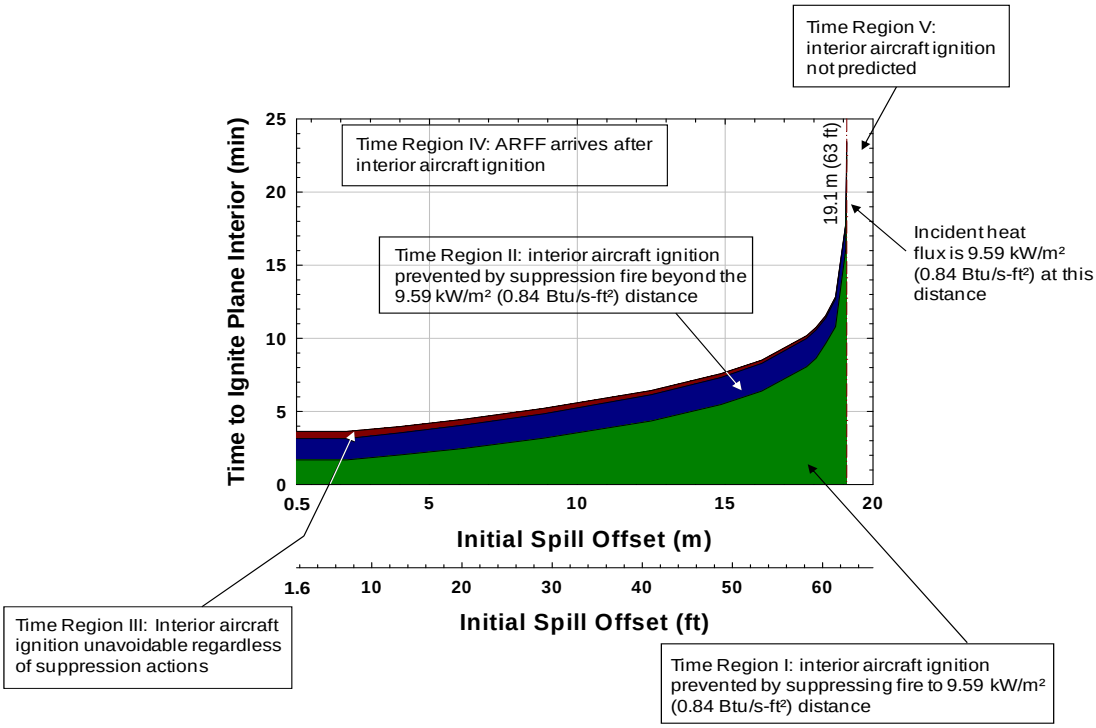

Figure 49. Response Time Regions for Scenario Group 4

Table 13. Suppression Agent Amount Needed to Prevent Interior Aircraft Ignition for Scenario Group 4

Initial Fuel Spill Offset (m (ft))	ARFF Arrival Time (min)						
	1.0	1.5	2.0	2.5	3.0	3.5	4.0
0.5 (1.6)	7200 L (1900 gal)	7200 L (1900 gal)	7540 L (2000 gal)	11,900 L (3,150 gal)	18,900^{+} L (5,000^{+} gal)	I.C.N.P	I.C.N.P
1 (3.3)	7000 L (1850 gal)	7000 L (1850 gal)	7250 L (1920 gal)	11,510 L (3,040 gal)	18,900^{+} L (5,000^{+} gal)	I.C.N.P	I.C.N.P
2 (6.6)	6620 L (1750 gal)	6620 L (1750 gal)	6860 L (1820 gal)	10,830 L (2,870 gal)	18,900^{+} L (5,000^{+} gal)	I.C.N.P	I.C.N.P
3 (9.8)	6230 L (1650 gal)	6230 L (1650 gal)	6290 L (1660 gal)	8,220 L (2,180 gal)	18,900^{+} L (5,000^{+} gal)	I.C.N.P	I.C.N.P
5 (16.4)	5460 L (1440 gal)	5460 L (1440 gal)	5460 L (1440 gal)	5,700 L (1,510 gal)	8,320 L (2,200 gal)	18,900^{+} L (5,000^{+} gal)	I.C.N.P

Table 13. Suppression Agent Amount Needed to Prevent Interior Aircraft Ignition for Scenario Group 4 (Continued)

Initial Fuel Spill Offset (m (ft))	ARFF Arrival Time (min)						
	1.0	1.5	2.0	2.5	3.0	3.5	4.0
6 (19.7)	5070 L (1340 gal)	5070 L (1340 gal)	5070 L (1340 gal)	5,070 L (1,340 gal)	6,090 L (1,610 gal)	14,790 L (3,910 gal)	I.C.N.P
8 (26.2)	4300 L (1140 gal)	4300 L (1140 gal)	4300 L (1140 gal)	4,300 L (1,140 gal)	4,350 L (1,150 gal)	5,220 L (1,380 gal)	12,380 L (3,280 gal)
10 (33)	3520 L (930 gal)	3520 L (930 gal)	3520 L (930 gal)	3,520 L (930 gal)	3,520 L (930 gal)	3,520 L (930 gal)	4,160 L (1,100 gal)
12 (39)	2750 L (730 gal)	2750 L (730 gal)	2750 L (730 gal)	2,750 L (730 gal)	2,750 L (730 gal)	2,750 L (730 gal)	2,750 L (730 gal)
14 (46)	1980 L (520 gal)	1980 L (520 gal)	1980 L (520 gal)	1,980 L (520 gal)	1,980 L (520 gal)	1,980 L (520 gal)	1,980 L (520 gal)
16 (52)	1180 L (310 gal)	1180 L (310 gal)	1180 L (310 gal)	1,180 L (310 gal)	1,180 L (310 gal)	1,180 L (310 gal)	1,180 L (310 gal)
18 (59)	430 L (110 gal)	430 L (110 gal)	430 L (110 gal)	430 L (110 gal)	430 L (110 gal)	430 L (110 gal)	430 L (110 gal)
19.1 (63)	none	none	none	none	none	none	none

[+]over 18,900 L (5,000 gal) condition

Key:
I.C.N.P – Internal aircraft ignition cannot be prevented under the assumed conditions.
Green: Time Region I
Blue: Time Region II
Red: Time Region III or IV
Black: Time Region V

Table 14. Suppression Agent Amount Needed to Allow Passengers to Egress to a Safe Area for Scenario Group 4†

Initial Fuel Spill Offset (m (ft))	ARFF Arrival Time (min)						
	1.0	1.5	2.0	2.5	3.0	3.5	4.0
0.5 (1.6)	26,450 L (7,000 gal)	26,450 L (7,000 gal)	26,110 L (6,910 gal)	21,760 L (5,760 gal)	33,650 L (8,900 gal)[‡]	33,650 L (8,900 gal)	33,650 L (8,900 gal)
1 (3.3)	26,450 L (7,000 gal)	26,450 L (7,000 gal)	26,210 L (6,930 gal)	21,960 L (5,810 gal)	33,460 L (8,850 gal)[‡]	33,460 L (8,850 gal)	33,460 L (8,850 gal)
2 (6.6)	26,450 L (7,000 gal)	26,450 L (7,000 gal)	26,210 L (6,930 gal)	22,240 L (5,880 gal)	33,070 L (8,750 gal)[‡]	33,070 L (8,750 gal)	33,070 L (8,750 gal)
3 (9.8)	26,450 L (7,000 gal)	26,450 L (7,000 gal)	26,400 L (6,980 gal)	24,460 L (6,470 gal)	32,690 L (8,650 gal)[‡]	32,690 L (8,650 gal)	32,690 L (8,650 gal)
5 (16.4)	26,450 L (7,000 gal)	26,450 L (7,000 gal)	26,450 L (7,000 gal)	26,210 L (6,930 gal)	23,600 L (6,240 gal)	31,910 L (8,440 gal)[‡]	31,910 L (8,440 gal)
6 (19.7)	26,450 L (7,000 gal)	26,450 L (7,000 gal)	26,450 L (7,000 gal)	26,450 L (7,000 gal)	25,430 L (6,730 gal)	16,730 L (4,430 gal)	31,530 L (8,340 gal)

Table 14. Suppression Agent Amount Needed to Allow Passengers to Egress to a Safe Area for Scenario Group 4† (Continued)

Initial Fuel Spill Offset (m (ft))	ARFF Arrival Time (min)						
	1.0	1.5	2.0	2.5	3.0	3.5	4.0
8 (26.2)	26,450 L (7,000 gal)	26,450 L (7,000 gal)	26,450 L (7,000 gal)	26,450 L (7,000 gal)	26,400 L (6,990 gal)	25,530 L (6,750 gal)	18,370 L (4,860 gal)
10 (33)	26,450 L (7,000 gal)	26,450 L (7,000 gal)	26,450 L (7,000 gal)	26,450 L (7,000 gal)	26,450 L (7,000 gal)	26,450 L (7,000 gal)	25,820 L (6,830 gal)
12 (39)	26,450 L (7,000 gal)	26,450 L (7,000 gal)	26,450 L (7,000 gal)	26,450 L (7,000 gal)	26,450 L (7,000 gal)	26,450 L (7,000 gal)	26,450 L (7,000 gal)
14 (46)	26,450 L (7,000 gal)	26,450 L (7,000 gal)	26,450 L (7,000 gal)	26,450 L (7,000 gal)	26,450 L (7,000 gal)	26,450 L (7,000 gal)	26,450 L (7,000 gal)
16 (52)	26,450 L (7,000 gal)	26,450 L (7,000 gal)	26,450 L (7,000 gal)	26,450 L (7,000 gal)	26,450 L (7,000 gal)	26,450 L (7,000 gal)	26,450 L (7,000 gal)
18 (59)	26,450 L (7,000 gal)	26,450 L (7,000 gal)	26,450 L (7,000 gal)	26,450 L (7,000 gal)	26,450 L (7,000 gal)	26,450 L (7,000 gal)	26,450 L (7,000 gal)
19.1 (63)	26,450 L (7,000 gal)	26,450 L (7,000 gal)	26,450 L (7,000 gal)	26,450 L (7,000 gal)	26,450 L (7,000 gal)	26,450 L (7,000 gal)	26,450 L (7,000 gal)
20 (66)	26,100 L (6,910 gal)						
25 (82)	24,180 L (6,400 gal)						
30 (98)	22,240 L (5,880 gal)						
35 (115)	20,310 L (5,370 gal)						
40 (131)	18,370 L (4,860 gal)						
50 (164)	14,510 L (3,838 gal)						
60 (197)	10,640 L (2,810 gal)						
70 (230)	6,770 L (1,791 gal)						
80 (262)	2,900 L (770 gal)						
85 (279)	970 L (260 gal)						
87.5 (287)	none						

†No initial agent assumed for table 13 I.C.N.P and 18,900+ L (5,000+ gal) cases.
‡Table 13 18,900+ L (5,000+ gal) case.
Key:
I.C.N.P – Internal aircraft ignition cannot be prevented under the assumed conditions.
Green: Time Region I
Blue: Time Region II
Red: Time Region III or IV
Black: Time Region V

7.5 SCENARIO GROUP 5.

Scenario Group 5 involves a 73-m (240-ft)-long aircraft with a 0.5-mm (0.02-in.) aluminum skin. The wind speed is 8.9 m/s (20 mph), and the aircraft is downwind of the source fire. Some key features of this scenario group are as follows:

- Maximum flame impingement offset distance for the aircraft: 6.3 m (21 ft)
- Fire width/diameter: 73 m (240 ft)

- Maximum flame length: 63.3 m (208 ft) (line fire correlation)
- Maximum flame emissive power: 20.0 kW/m² (1.8 Btu/s-ft²)
- Heat release rate per unit width of the source fire: 170 MW/m (49,400 Btu/ft)
- Offset distance at which view factor reaches one: 8.8 m (29 ft)
- Distance at which heat flux is equal to 9.59 kW/m² (0.84 Btu/s-ft²): 31.7 m (104 ft)
- Distance at which heat flux is equal to 2.5 kW/m² (0.22 Btu/s-ft²): 113.3 m (371 ft)
- Maximum separation that can be developed using 18,900 L (5,000 gal) of suppression agent: 48.8 m (160 ft)

Figure 50 shows the possible outcomes for different ARFF arrival times as a function of the initial fire offsets. Tables 15 and 16 summarize the agent amount needed to prevent interior ignition and allow for safe passenger egress.

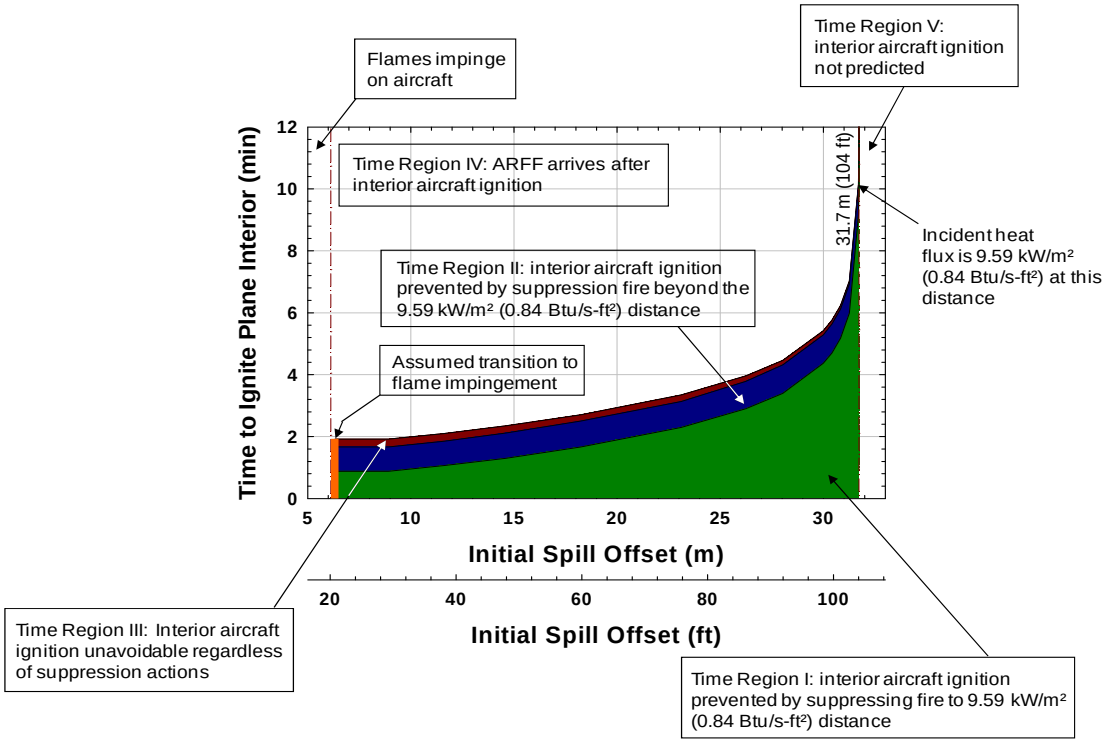

Figure 50. Response Time Regions for Scenario Group 5

Table 15. Suppression Agent Amount Needed to Prevent Interior Aircraft Ignition for Scenario Group 5

Initial Fuel spill Offset (m (ft))	ARFF Arrival Time (min)						
	1.0	1.5	2.0	2.5	3.0	3.5	4.0
8 (26)	9280 L (2460 gal)	18,900+ L (5,000+ gal)	I.C.N.P	I.C.N.P	I.C.N.P	I.C.N.P	I.C.N.P
10 (33)	8410 L (2230 gal)	18,900+ L (5,000+ gal)	I.C.N.P	I.C.N.P	I.C.N.P	I.C.N.P	I.C.N.P
12 (39)	7620 L (2020 gal)	15,280 L (4,040 gal)	I.C.N.P	I.C.N.P	I.C.N.P	I.C.N.P	I.C.N.P
14 (46)	6850 L (1810 gal)	8,710 L (2,300 gal)	18,900+ L (5,000+ gal)	I.C.N.P	I.C.N.P	I.C.N.P	I.C.N.P
16 (52)	6070 L (1610 gal)	6,090 L (1,610 gal)	18,900+ L (5,000+ gal)	I.C.N.P	I.C.N.P	I.C.N.P	I.C.N.P
18 (59)	5300 L (1400 gal)	5,300 L (1,400 gal)	9,570 L (2,530 gal)	I.C.N.P	I.C.N.P	I.C.N.P	I.C.N.P
20 (66)	4520 L (1200 gal)	4,520 L (1,200 gal)	4,930 L (1,310 gal)	18,900+ L (5,000+ gal)	I.C.N.P	I.C.N.P	I.C.N.P
22.5 (74)	3560 L (940 gal)	3,560 L (940 gal)	3,560 L (940 gal)	5420 L (1,430 gal)	18,900+ L (5,000+ gal)	I.C.N.P	I.C.N.P
25 (82)	2590 L (690 gal)	2,590 L (690 gal)	2,590 L (690 gal)	2,590 L (690 gal)	4,740 L (1,250 gal)	I.C.N.P	I.C.N.P
27.5 (90)	1630 L (430 gal)	1,630 L (430 gal)	1,630 L (430 gal)	1,630 L (430 gal)	1,630 L (430 gal)	2,220 L (590 gal)	18,900+ L (5,000+ gal)
30 (98)	660 L (170 gal)	660 L (170 gal)	660 L (170 gal)	660 L (170 gal)	1,630 L (430 gal)	1,630 L (430 gal)	1,630 L (430 gal)
31.7 (104)	none	none	none	none	none	none	none

+over 18,900 L (5,000 gal) condition

Key:
I.C.N.P – Internal aircraft ignition cannot be prevented under the assumed conditions.
Green: Time Region I
Blue: Time Region II
Red: Time Region III or IV
Black: Time Region V

Table 16. Suppression Agent Amount Needed to Allow Passengers to Egress to a Safe Area for Scenario Group 5[†]

Initial Fuel Spill Offset (m (ft))	ARFF Arrival Time (min)						
	1.0	1.5	2.0	2.5	3.0	3.5	4.0
0.5 (1.6)[‖]	43,640 L (11,540 gal)						
1 (3.3)[‖]	43,440 L (11,490 gal)						
2 (6.6)[‖]	43,050 L (11,390 gal)						
3 (10)[‖]	42,670 L (11,290 gal)						
5 (16)[‖]	41,890 L (11,080 gal)						
6 (20)[‖]	41,510 L (10,980 gal)						
8 (26)	31,450 L (8,320 gal)	40,730 L (10,780 gal)[‡]	40,730 L (10,780 gal)	40,730 L (10,780 gal)	40,730 L (10,780 gal)	40,730 L (10,780 gal)	40,730 L (10,780 gal)
10 (33)	31,540 L (8,350 gal)	39960 L (10,570 gal)[‡]	39,960 L (10,570 gal)	39,960 L (10,570 gal)	39,960 L (10,570 gal)	39,960 L (10,570 gal)	39,960 L (10,570 gal)
12 (39)	31,530 L (8,350 gal)	23,910 L (6,340 gal)	39,190 L (10,370 gal)	39,190 L (10,370 gal)	39,190 L (10,370 gal)	39,190 L (10,370 gal)	39,190 L (10,370 gal)
14 (46)	31,530 L (8,350 gal)	29,710 L (7,860 gal)	38,410 L (10,160 gal)[‡]	38,410 L (10,160 gal)	38,410 L (10,160 gal)	38,410 L (10,160 gal)	38,410 L (10,160 gal)
16 (52)	31,530 L (8,350 gal)	31,540 L (8,350 gal)	37,640 L (9,960 gal)[‡]	37,640 L (9,960 gal)	37,640 L (9,960 gal)	37,640 L (9,960 gal)	37,640 L (9,960 gal)
18 (59)	31,530 L (8,350 gal)	31,530 L (8,350 gal)	26,610 L (7,040 gal)	36,870 L (9,750 gal)	36,870 L (9,750 gal)	36,870 L (9,750 gal)	36,870 L (9,750 gal)
20 (66)	31,530 L (8,350 gal)	31,530 L (8,350 gal)	31,160 L (8,240 gal)	36,100 L (9,550 gal)[‡]	36,100 L (9,550 gal)	36,100 L (9,550 gal)	36,100 L (9,550 gal)
22.5 (74)	31,530 L (8,350 gal)	31,530 L (8,350 gal)	31,530 L (8,350 gal)	29,710 L (7,860 gal)	35,120 L (9,290 gal)[‡]	35,120 L (9,290 gal)	35,120 L (9,290 gal)
25 (82)	31,530 L (8,350 gal)	31,530 L (8,350 gal)	31,530 L (8,350 gal)	31,530 L (8,350 gal)	29,420 L (7,780 gal)	34,160 L (9,040 gal)	34,160 L (9,040 gal)
27.5 (90)	31,530 L (8,350 gal)	31,530 L (8,350 gal)	31,530 L (8,350 gal)	31,530 L (8,350 gal)	31,530 L (8,350 gal)	30,970 L (8,190 gal)	33,190 L (8,780 gal)[‡]
30 (98)	31,530 L (8,350 gal)	31,530 L (8,350 gal)	31,530 L (8,350 gal)	31,530 L (8,350 gal)	31,530 L (8,350 gal)	31,530 L (8,350 gal)	31,530 L (8,350 gal)
31.7 (104)	31,530 L (8,350 gal)	31,530 L (8,350 gal)	31,530 L (8,350 gal)	31,530 L (8,350 gal)	31,530 L (8,350 gal)	31,530 L (8,350 gal)	31,530 L (8,350 gal)
35 (114)	30,290 L (8,010 gal)						
40 (131)	28,350 L (7,500 gal)						
50 (164)	24,490 L (6,480 gal)						
60 (197)	20,620 L (5,460 gal)						
70 (230)	16,750 L (4,430 gal)						
80 (262)	12,880 L (3,410 gal)						
90 (295)	9,010 L (2,380 gal)						
100 (330)	5,140 L (1,360 gal)						
110 (361)	1,280 L (340 gal)						
113.3 (372)	None						

[†]No initial agent assumed for table 15 I.C.N.P and 18,900[+] L (5,000[+] gal) cases and for flame impingement (initial offset less than 6.3 m).
[‡]Table 15 18,900[+] L (5,000[+] gal) case.
[‖]Flame impingement on aircraft, interior ignition assumed.
Key:
I.C.N.P – Internal aircraft ignition cannot be prevented under the assumed conditions.
Green: Time Region I
Blue: Time Region II
Red: Time Region III or IV
Black: Time Region V

7.6 SCENARIO GROUP 6.

Scenario Group 6 involves a 73-m (240-ft)-long aircraft with a 2.5-mm (0.1-in.) aluminum skin. The wind speed is 8.9 m/s (20 mph), and the aircraft is downwind of the source fire. Some key features of this scenario group are as follows:

- Maximum flame impingement offset distance for the aircraft: 6.3 m (21 ft)
- Fire width/diameter: 73 m (240 ft)
- Maximum flame length: 63.3 m (208 ft) (line fire correlation)
- Maximum flame emissive power: 20.0 kW/m² (1.8 Btu/s-ft²)
- Heat release rate per unit width of the source fire: 170 MW/m (49,400 Btu/ft)
- Offset distance at which view factor reaches one: 8.8 m (29 ft)
- Distance at which heat flux is equal to 9.59 kW/m² (0.84 Btu/s-ft²): 31.7 m (104 ft)
- Distance at which heat flux is equal to 2.5 kW/m² (0.22 Btu/s-ft²): 113.3 m (371 ft)
- Maximum separation that can be developed using 18,900 L (5,000 gal) of suppression agent: 48.8 m (160 ft)

Figure 51 shows the possible outcomes for different ARFF arrival times as a function of the initial fire offsets. Tables 17 and 18 summarize the agent amounts needed to prevent interior ignition and allow for safe passenger egress.

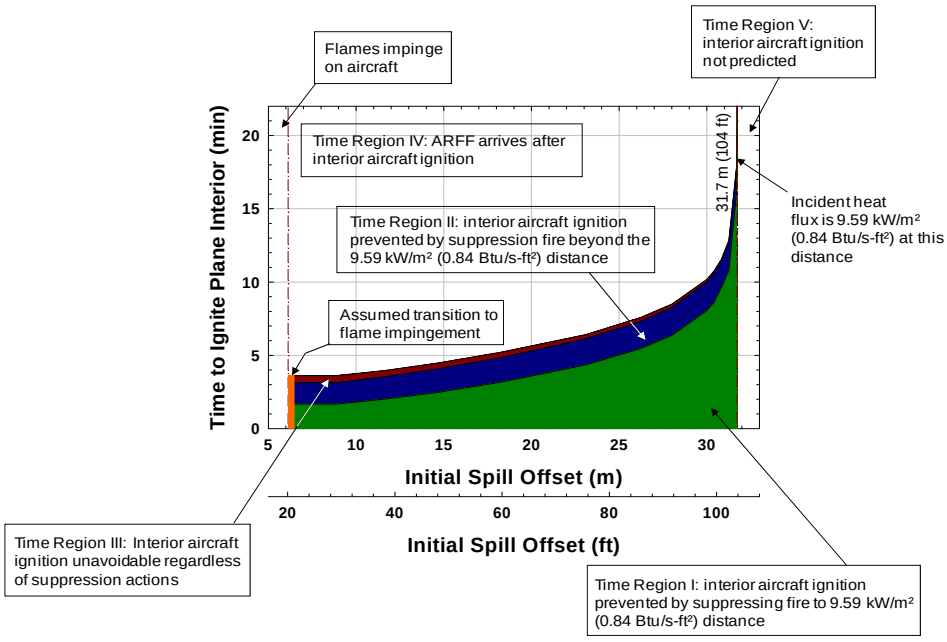

Figure 51. Response Time Regions for Scenario Group 6

Table 17. Suppression Agent Amount Needed to Prevent Interior Aircraft Ignition for Scenario Group 6

Initial Fuel Spill Offset (m (ft))	ARFF Arrival Time (min)						
	1.0	1.5	2.0	2.5	3.0	3.5	4.0
8 (26)	9170 L (2430 gal)	9170 L (2430 gal)	9480 L (2510 gal)	14,700 L (3,890 gal)	18,900+ L (5,000+ gal)	I.C.N.P	I.C.N.P
10 (33)	8400 L (2220 gal)	8400 L (2220 gal)	8510 L (2250 gal)	11,030 L (2,920 gal)	18,900+ L (5,000+ gal)	I.C.N.P	I.C.N.P
12 (39)	7620 L (2020 gal)	7,620 L (2020 gal)	7620 L (2020 gal)	8,120 L (2,150 gal)	14,120 L (3,740 gal)	18,900+ L (5,000+ gal)	I.C.N.P
14 (46)	6850 L (1810 gal)	6850 L (1810 gal)	6850 L (1810 gal)	6,860 L (1,820 gal)	8,220 L (2,180 gal)	18,900+ L (5,000+ gal)	I.C.N.P
16 (52)	6070 L (1610 gal)	6070 L (1610 gal)	6070 L (1610 gal)	6,070 L (1,610 gal)	6,190 L (1,640 gal)	8,320 L (2,200 gal)	18,900+ L (5,000+ gal)
18 (59)	5300 L (1400 gal)	5300 L (1400 gal)	5300 L (1400 gal)	5,300 L (1,400 gal)	5,300 L (1,400 gal)	5,610 L (1,480 gal)	8,320 L (2,200 gal)
20 (66)	4520 L (1200 gal)	4520 L (1200 gal)	4520 L (1200 gal)	4,520 L (1,200 gal)	4,520 L (1,200 gal)	4,520 L (1,200 gal)	4,830 L (1,280 gal)
22.5 (74)	3560 L (940 gal)	3560 L (940 gal)	3560 L (940 gal)	3,560 L (940 gal)	3,560 L (940 gal)	3,560 L (940 gal)	3,560 L (940 gal)
25 (82)	2590 L (690 gal)	2590 L (690 gal)	2590 L (690 gal)	2,590 L (690 gal)	2,590 L (690 gal)	2,590 L (690 gal)	2,590 L (690 gal)
27.5 (90)	1630 L 430 (gal)	1630 L 430 (gal)	1630 L 430 (gal)	1,630 L 430 (gal)	1,630 L 430 (gal)	1,630 L 430 (gal)	1,630 L 430 (gal)
30 (98)	660 L (170 gal)	660 L (170 gal)	660 L (170 gal)	660 L (170 gal)	660 L (170 gal)	660 L (170 gal)	660 L (170 gal)
31.7 (104)	none	none	none	none	none	none	none

+over 18,900 L (5,000 gal) condition

Key:
I.C.N.P – Internal aircraft ignition cannot be prevented under the assumed conditions.
Green: Time Region I
Blue: Time Region II
Red: Time Region III or IV
Black: Time Region V

Table 18. Suppression Agent Amount Needed to Allow Passengers to Egress to a Safe Area for Scenario Group 6[†]

Initial Fuel Spill Offset (m (ft))	ARFF Arrival Time (min)						
	1.0	1.5	2.0	2.5	3.0	3.5	4.0
0.5 (1.6)[‖]	43,640 L (11,540 gal)						
1 (3.3)[‖]	43,440 L (11,490 gal)						
2 (6.6)[‖]	43,050 L (11,390 gal)						
3 (10)[‖]	42,670 L (11,290 gal)						
5 (16)[‖]	41,890 L (11,080 gal)						
6 (20)[‖]	41,510 L (10,980 gal)						
8 (26)	31,530 L (8,350 gal)	31,530 L (8,350 gal)	31,260 L (8,270 gal)	26,030 L (6,890 gal)	40,730 L (10,780 gal)	40,730 L (10,780 gal)	40,730 L (10,780 gal)
10 (33)	31,530 L (8,350 gal)	31,530 L (8,350 gal)	31,450 L (8,320 gal)	28,930 L (7,650 gal)	39,960 L (10,570 gal)	39,960 L (10,570 gal)	39,960 L (10,570 gal)
12 (39)	31,530 L (8,350 gal)	31,530 L (8,350 gal)	31,530 L (8,350 gal)	31,060 L (8,220 gal)	25,070 L (6,630 gal)	39,190 L (10,370 gal)	39,190 L (10,370 gal)
14 (46)	31,530 L (8,350 gal)	31,530 L (8,350 gal)	31,530 L (8,350 gal)	31,550 L (8,350 gal)	30,190 L (7,990 gal)	38,280 L (10,160 gal)	38,280 L (10,160 gal)
16 (52)	31,530 L (8,350 gal)	31,530 L (8,350 gal)	31,530 L (8,350 gal)	31,530 L (8,350 gal)	31,450 L (8,320 gal)	29,320 L (7,760 gal)	37,640 L (9,960 gal)
18 (59)	31,530 L (8,350 gal)	31,530 L (8,350 gal)	31,530 L (8,350 gal)	31,530 L (8,350 gal)	31,530 L (8,350 gal)	31,260 L (8,270 gal)	28,550 L (7,550 gal)
20 (66)	31,530 L (8,350 gal)	31,530 L (8,350 gal)	31,530 L (8,350 gal)	31,530 L (8,350 gal)	31,530 L (8,350 gal)	31,530 L (8,350 gal)	31,260 L (8,270 gal)
22.5 (74)	31,530 L (8,350 gal)	31,530 L (8,350 gal)	31,530 L (8,350 gal)	31,530 L (8,350 gal)	31,530 L (8,350 gal)	31,530 L (8,350 gal)	31,530 L (8,350 gal)
25 (82)	31,530 L (8,350 gal)	31,530 L (8,350 gal)	31,530 L (8,350 gal)	31,530 L (8,350 gal)	31,530 L (8,350 gal)	31,530 L (8,350 gal)	31,530 L (8,350 gal)
27.5 (90)	31,530 L (8,350 gal)	31,530 L (8,350 gal)	31,530 L (8,350 gal)	31,530 L (8,350 gal)	31,530 L (8,350 gal)	31,530 L (8,350 gal)	31,530 L (8,350 gal)
30 (98)	31,530 L (8,350 gal)	31,530 L (8,350 gal)	31,530 L (8,350 gal)	31,530 L (8,350 gal)	31,530 L (8,350 gal)	31,530 L (8,350 gal)	31,530 L (8,350 gal)
31.7 (104)	31,530 L (8,350 gal)	31,530 L (8,350 gal)	31,530 L (8,350 gal)	31,530 L (8,350 gal)	31,530 L (8,350 gal)	31,530 L (8,350 gal)	31,530 L (8,350 gal)
35 (114)	30,290 L (8,010 gal)						
40 (131)	28,350 L (7,500 gal)						
50 (164)	24,490 L (6,480 gal)						
60 (197)	20,620 L (5,460 gal)						
70 (230)	16,750 L (4,430 gal)						
80 (262)	12,880 L (3,410 gal)						
90 (295)	9,010 L (2,380 gal)						
100 (330)	5,140 L (1,360 gal)						
110 (361)	1,280 L (340 gal)						
113.3 (372)	none						

[†]No initial agent assumed for table 17 I.C.N.P and 18,900[+] L (5,000[+] gal) cases and for flame impingement (initial offset less than 6.3 m).
[‡]Table 17 18,900[+] L (5,000[+] gal) case.
[‖]Flame impingement on aircraft, interior ignition assumed.
Key:
I.C.N.P – Internal aircraft ignition cannot be prevented under the assumed conditions.
Green: Time Region I
Blue: Time Region II
Red: Time Region III or IV
Black: Time Region V

7.7 SCENARIO GROUP 7.

Scenario Group 5 involves a 73-m (240-ft)-long aircraft with a 0.5-mm (0.02-in.) aluminum skin. The wind speed is 8.9 m/s (20 mph), and the aircraft is upwind of the source fire. Some key features of this scenario group are as follows:

- Fire width/diameter: 73 m (240 ft)
- Maximum flame length: 63.3 m (208 ft) (line fire correlation)
- Maximum flame emissive power: 20.0 kW/m² (1.8 Btu/s-ft²)
- Heat release rate per unit width of the source fire: 170 MW/m (49,400 Btu/ft)
- Distance at which heat flux is equal to 9.59 kW/m² (0.84 Btu/s-ft²): 2.8 m (9.2 ft)
- Distance at which heat flux is equal to 2.5 kW/m² (0.22 Btu/s-ft²): 33.5 m (110 ft)
- Maximum separation that can be developed using 18,900 L (5,000 gal) of suppression agent: 48.8 m (160 ft)

Figure 52 shows the possible outcomes for different ARFF arrival times as a function of the initial fire offsets. Tables 19 and 20 summarize the agent amount needed to prevent interior ignition and allow for passenger egress.

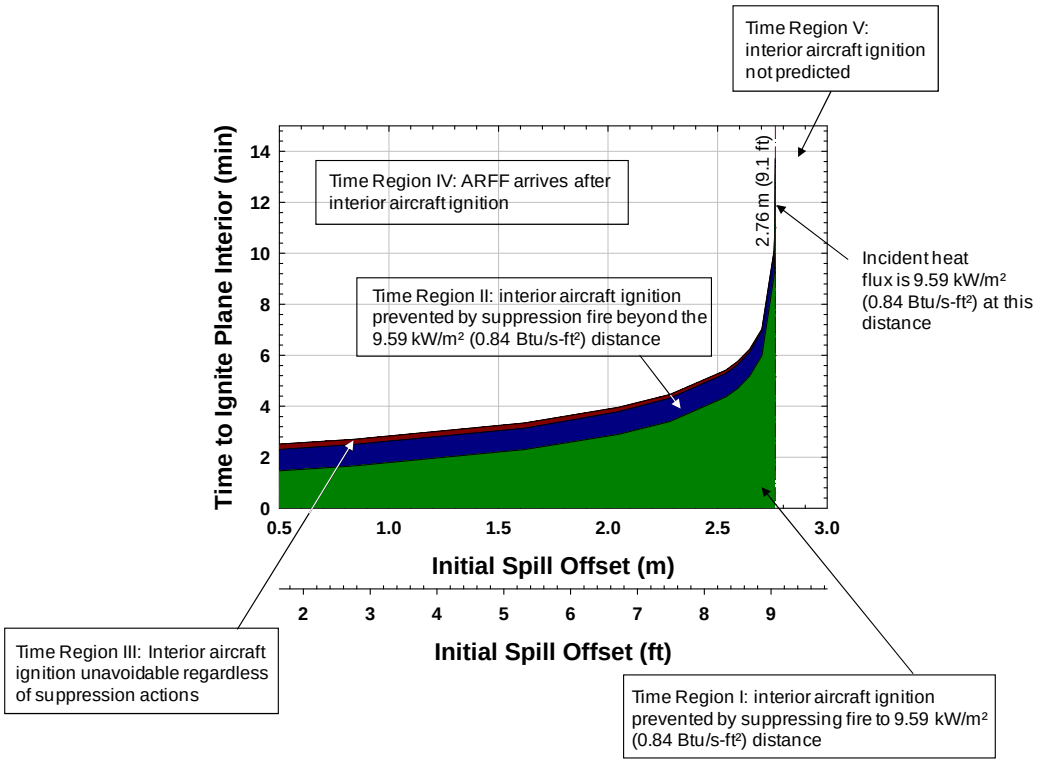

Figure 52. Response Time Regions for Scenario Group 7

Table 19. Suppression Agent Amount Needed to Prevent Interior Aircraft Ignition for Scenario Group 7

Initial Fuel Spill Offset (m (ft))	ARFF Arrival Time (min)						
	1.0	1.5	2.0	2.5	3.0	3.5	4.0
0.5 (1.6)	869 L (230 gal)	869 L (230 gal)	3770 L (1000 gal)	I.C.N.P	I.C.N.P	I.C.N.P	I.C.N.P
1 (3.3)	680 L (180 gal)	680 L (180 gal)	870 L (230 gal)	18,900+ L (5,000+ gal)	I.C.N.P	I.C.N.P	I.C.N.P
1.5 (4.9)	490 L (130 gal)	490 L (130 gal)	490 L (130 gal)	780 L (210 gal)	18,900+ L (5,000+ gal)	I.C.N.P	I.C.N.P
2 (6.6)	290 L (80 gal)	290 L (80 gal)	290 L (80 gal)	290 L (80 gal)	390 L (100 gal)	2,030 L (540 gal)	I.C.N.P
2.5 (8.2)	100 L (30 gal)	100 L (30 gal)	100 L (30 gal)	100 L (30 gal)	100 L (30 gal)	100 L (30 gal)	100 L (30 gal)
2.76 (9.1)	none	none	none	none	none	none	none

+over 18,900 L (5,000 gal) condition

Key:
I.C.N.P – Internal aircraft ignition cannot be prevented under the assumed conditions.
Green: Time Region I
Blue: Time Region II
Red: Time Region III or IV
Black: Time Region V

Table 20. Suppression Agent Amount Needed to Allow Passengers to Egress to a Safe Area for Scenario Group 7†

Initial Fuel Spill Offset (m (ft))	ARFF Arrival Time (min)						
	1.0	1.5	2.0	2.5	3.0	3.5	4.0
0.5 (1.6)	11,890 L (3,150 gal)	11,890 L (3,150 gal)	8,990 L (2,380 gal)	12,770 L (3,380 gal)	12,770 L (3,380 gal)	12,770 L (3,380 gal)	12,770 L (3,380 gal)
1 (3.3)	11,890 L (3,150 gal)	11,890 L (3,150 gal)	11,700 L (3,100 gal)	12,570 L (3,330 gal)‡	12,570 L (3,330 gal)	12,570 L (3,330 gal)	12,570 L (3,330 gal)
1.5 (4.9)	11,890 L (3,150 gal)	11,890 L (3,150 gal)	11,890 L (3,150 gal)	11,600 L (3,070 gal)	12,380 L (3,280 gal)‡	12,380 L (3,280 gal)	12,380 L (3,280 gal)
2 (6.6)	11,890 L (3,150 gal)	11,890 L (3,150 gal)	11,890 L (3,150 gal)	11,890 L (3,150 gal)	11,800 L (3,120 gal)	10,160 L (2,690 gal)	12,190 L (3,220 gal)
2.5 (8.2)	11,890 L (3,150 gal)	11,890 L (3,150 gal)	11,890 L (3,150 gal)	11,890 L (3,150 gal)	11,890 L (3,150 gal)	11,890 L (3,150 gal)	11,890 L (3,150 gal)
2.76 (9.1)	11,890 L (3,150 gal)	11,890 L (3,150 gal)	11,890 L (3,150 gal)	11,890 L (3,150 gal)	11,890 L (3,150 gal)	11,890 L (3,150 gal)	11,890 L (3,150 gal)
3 (9.8)	11,800 L (3,120 gal)						
5 (16)	11,030 L (2,920 gal)						
10 (33)	9,090 L (2,410 gal)						

Table 20. Suppression Agent Amount Needed to Allow Passengers to Egress to a Safe Area for Scenario Group 7† (Continued)

Initial Fuel Spill Offset (m (ft))	ARFF Arrival Time (min)						
	1.0	1.5	2.0	2.5	3.0	3.5	4.0
15 (49)	7,160 L (1,890 gal)						
20 (66)	5,220 L (1,380 gal)						
25 (82)	3,290 L (870 gal)						
30 (98)	1,350 L (360 gal)						
33.5 (110)	none						

†No initial agent assumed for table 19 I.C.N.P and 18,900+ L (5,000+ gal) cases and for flame impingement (initial offset less than 6.3 m).
‡Table 19 18,900+ L (5,000+ gal) case.
Key:
I.C.N.P – Internal aircraft ignition cannot be prevented under the assumed conditions.
Green: Time Region I
Blue: Time Region II
Red: Time Region III or IV
Black: Time Region V

7.8 SCENARIO GROUP 8.

Scenario Group 8 involves a 73-m (240-ft)-long aircraft with a robustly constructed composite skin. The wind speed is assumed to be zero. Some key features of this scenario group are as follows:

- Fire width/diameter: 73 m (240 ft)
- Maximum flame height: 81.2 m (266 ft) (line fire correlation)
- Maximum flame emissive power: 20.0 kW/m² (1.8 Btu/s-ft²)
- Heat release rate per unit width of the source fire: 170 MW/m (49,400 Btu/ft)
- Offset distance at which view factor reaches one: 2.15 m (7.1 ft)
- Distance at which heat flux is equal to 9.59 kW/m² (0.84 Btu/s-ft²): 19.1 m (63 ft)
- Distance at which heat flux is equal to 2.5 kW/m² (0.22 Btu/s-ft²): 87.5 m (287 ft)
- Maximum separation that can be developed using 18,900 L (5,000 gal) of suppression agent: 48.8 m (160 ft).

The time for flame penetration for composite skin aircraft or aluminum with robust insulation can be as high as 4 minutes or more under flame impingement conditions [17]. In this case, it is apparent that any offset that prevents flame impingement would result in even greater interior

ignition times. It is reasonable to assume that a heat flux of 9.59 kW/m² (0.84 Btu/s-ft²) would be a limiting value for interior ignition for the reasons described in section 5. In such a case, the amount of agent necessary to suppress the fire to a distance such that the heat flux is equal to 9.59 kW/m² (0.84 Btu/s-ft²) is all that is required to prevent ignition for ARFF times of 4 minutes or less. Tables 21 and 22 summarize the agent amount needed to prevent interior ignition and allow for passenger egress.

Table 21. Suppression Agent Amount Needed to Prevent Interior Aircraft Ignition for Scenario Group 8

Initial Fuel Spill Offset (m (ft))	ARFF Arrival Time (min)						
	1.0	1.5	2.0	2.5	3.0	3.5	4.0
0.5 (1.6)	7200 L (1900 gal)						
1 (3.3)	7000 L (1850 gal)						
2 (6.6)	6620 L (1750 gal)						
3 (10)	6230 L (1650 gal)						
5 (16)	5450 L (1440 gal)						
6 (20)	5070 L (1340 gal)						
8 (26)	4300 L (1140 gal)						
10 (33)	3520 L (930 gal)						
12 (39)	2750 L (730 gal)						
14 (46)	1980 L (520 gal)						
16 (52)	1180 L (310 gal)						
18 (59)	430 L (110 gal)						
19.1 (63)	none						

Table 22. Suppression Agent Amount Needed to Allow Passengers to Egress to a Safe Area for Scenario Group 8

Initial Fuel Spill Offset (m (ft))	ARFF Arrival Time (min)						
	1.0	1.5	2.0	2.5	3.0	3.5	4.0
0.5-19.1 (1.6-63)	26592 L (7,000 gal)						
20 (66)	26,110 L (6,910 gal)						
25(95)	24,180 L (6,400 gal)						
30 (98)	22,240 L (5,880 gal)						
35 (115)	20,310 L (5,370 gal)						
40 (131)	18,370 L (4,860 gal)						
45 (148)	16,440 L (4,350 gal)						
50 (164)	14,510 L (3,840 gal)						
60 (197)	10,640 L (2,810 gal)						
70 (230)	6,770 L (1,790 gal)						
80 (262)	2,900 L (770 gal)						
85 (279)	968 L (260 gal)						
87.5 (287)	none						

8. DISCUSSION.

For scenarios where some or all of the aircraft is immersed in flames, it is clear the actions of ARFF may not have a significant effect on the prevention of interior ignition. This conclusion is based entirely on the assumption that the heat flux exposure to the aircraft is maximized and that the time for conditions within the aircraft to become untenable is minimized. Practical experience with aircraft fires indicates there may be a subset of scenarios where immersion results, but ARFF can prevent ignition or extend the egress time by suppressing the fire. This is because not all fires will result in a maximum incident heat flux and not all interior ignitions will spread rapidly. These scenario variations were, conservatively, not considered but are acknowledged as being possible. To incorporate such nonconservative assumptions would likely require a risk-based approach, which is beyond the scope of this study.

The agent amount trends for aircraft fire scenarios, where there is an initial offset distance, generally follow expected trends. The results show a marked sensitivity to the agent amount, particularly when ARFF response-initial offset is in Time Region II (see section 7). In these cases, the predicted amount of suppression agent needed to prevent interior aircraft ignition exhibits a rapid drop-off in agent amount with respect to the initial fuel spill offset distance. A typical example is shown in table 7 for a 3-minute ARFF response time. Ignition can be prevented through the application of 4,160 L (1,100 gal) of agent if the initial fuel spill offset from the aircraft is 14 m (46 ft), but more than 18,900 L (5,000 gal) would be required if the initial fuel spill offset was 12 m (40 ft).

This effect can be explained in part by the asymptotic behavior of the time required for the 204°C (400°F) isotherm to penetrate 1.1 cm (0.43 in.) into the aircraft insulation with respect to the incident heat flux, one performance criterion for interior ignition. An example of this is shown in figure 53. As the incident heat flux decreases, the time required to reach the performance criterion asymptotically increases to infinity at the threshold value (9.59 kW/m² (0.84 Btu/s-ft²)). Small changes in the incident heat flux result in large changes in the time required to prevent ignition. In the example shown, scenarios that produce initial incident fluxes less than approximately 30 kW/m² (2.6 Btu/s-ft²) will be very sensitive to the initial fuel spill offset distance since this parameter is correlated to the incident heat flux.

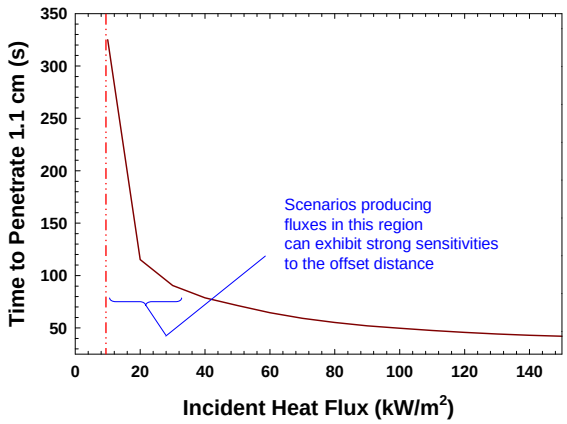

Figure 53. Typical Response of the Time Required to Reach the Ignition Criterion With Respect to the Incident Heat Flux

There is a second and perhaps more significant contributor to the rapid drop-off in agent amount with respect to the initial offset distance. This has to do with the transient response of the skin-insulation system to changes in the incident heat flux and the correlation between the heat flux and the distance between the exposure fire and the aircraft. Provided ignition can be prevented (i.e., a scenario falls within Time Region I or Time Region II as defined in section 7), the nearer the 204°C (400°F) isotherm within the insulation is to the critical distance for ignition (1.1 cm (0.43 in.)), the lower the postsuppression exposure flux must be to prevent ignition (see figures 54 and 55). However, the offset distance necessary to produce low fluxes asymptotically increases to infinity as the flux decreases to zero, as shown in figure 56. Because the agent amount is a linear function of the exposure distance for a given scenario (i.e., 0.05 L agent/m² of fire suppressed (0.13 gal agent/ft² of fire suppressed), the amount of agent will be excessively sensitive to the initial fuel spill fire offset distance if the flux required to prevent ignition is low (~5 kW/m² (~0.44 Btu/s-ft²) or less).

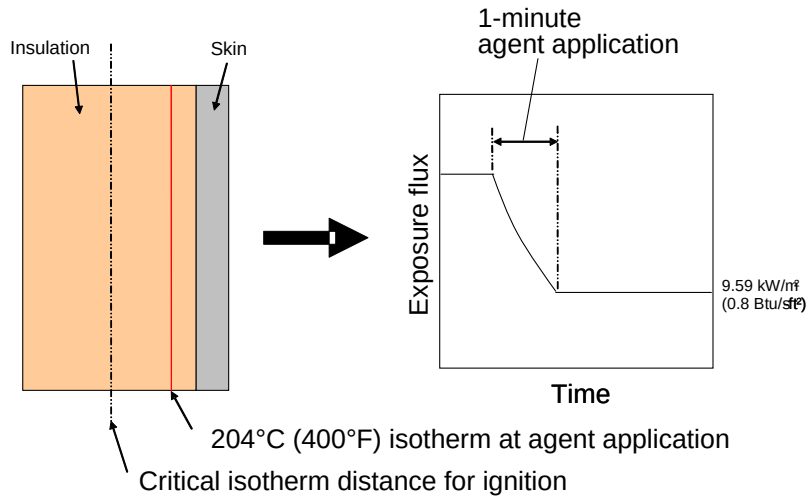

Figure 54. Exposure Flux Profile That Prevents Interior Aircraft Ignition Typical of Time Region I

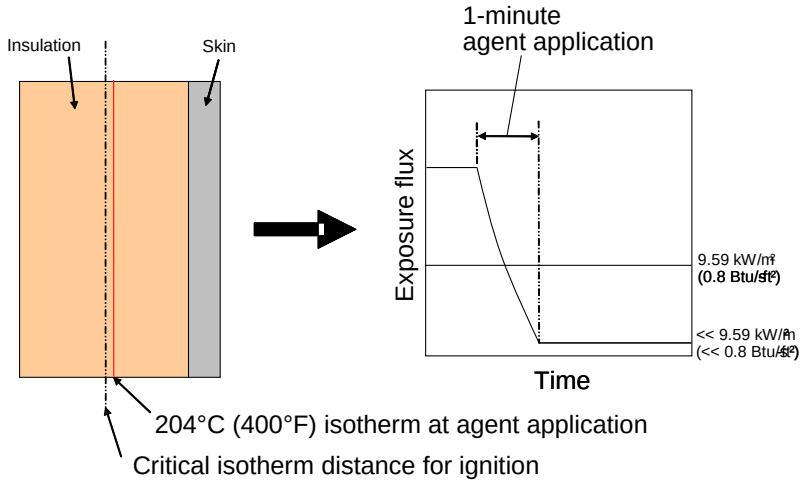

Figure 55. Exposure Flux Profile That Prevents Interior Aircraft Ignition Typical of Time Region II

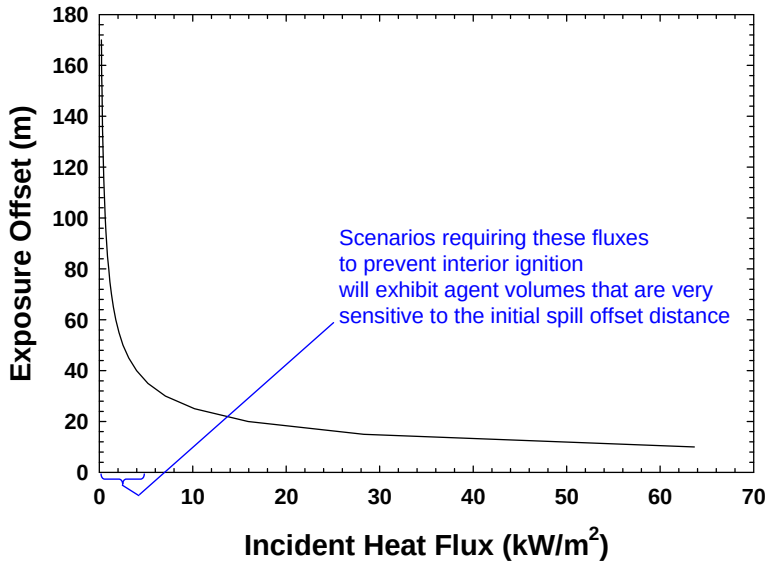

Figure 56. Exposure Offset vs Incident Heat Flux for Large Pool Fire

The agent amounts needed to prevent interior aircraft ignition (shown in tables 7, 9, 11, 13, 15, 17, and 19) indicate another counterintuitive trend. In many instances, the maximum calculated amount of agent needed to prevent interior aircraft ignition decreases as the ARFF arrival time increases regardless of the initial offset distance. Note that the agent amount listed in the tables as 18,900^{+} L (5,000^{+} gal) is not a calculated amount; rather, it indicates that it is theoretically possible for the ARFF to prevent ignition based on the time region, but the agent amount needed would be greater than the maximum agent amount carried. Nevertheless, the intuitive expectation for the calculated agent amounts would be that the amounts either remain constant or steadily increase as the response time increases. The actual result is somewhat different, as shown by the highlighted entries in table 23, for example. Table 23 shows the maximum calculated agent quantities needed to prevent interior ignition decreasing from 13,250 L (3,500 gal) for a 2-minute ARFF response and an 8-m (26.2-ft) initial fire offset distance to 430 L (110 gal) for a 4-minute ARFF response and an 18-m (59-ft) initial fire offset distance. However, this result (decreasing calculated agent quantities) is an artifact of the presentation method, and in particular, the specific offset distances considered. There are two metrics by which to view the results shown in table 23. First, the agent quantity needed to prevent interior ignition remains constant or increases for a fixed spill offset distance. This is true for all scenario groups. Second, the agent quantity increases when the offset distance decreases for a fixed ARFF arrival time. This also is true for all scenario groups. More importantly, it should be recognized that the relationship between the agent amount and the spill offset distance is continuous for a fixed ARFF arrival time and the function will be asymptotic toward infinity if at least one offset distance results in an I.C.N.P (interior ignition cannot be prevented) agent amount. This means that an offset distance can be found that is exactly equal to 18,900 L (5,000 gal), and this distance will be between the offset distance where the quantity is listed as 18,900^{+} L (5,000^{+} gal) and the agent quantity is calculated (i.e., not equal to 18,900^{+} L (5,000^{+} gal). These observations are further illustrated in figure 57.

Table 23. Suppression Agent Amount Needed to Prevent Interior Ignition for Scenario Group 1 (Subset of Table 7)

Initial Fuel Spill Offset (m (ft))	ARFF Arrival Time (min)				
	2.0	2.5	3.0	3.5	4.0
8 (26.2)	13,250 L (3,500 gal)	18,900+ L (5,000+ gal)	I.C.N.P	I.C.N.P	I.C.N.P
10 (33)	4,260 L (1,130 gal)	18,900+ L (5,000+ gal)	I.C.N.P	I.C.N.P	I.C.N.P
12 (39)	2,750 L (730 gal)	4,930 L (1,300 gal)	18,900+ L (5,000+ gal)	I.C.N.P	I.C.N.P
14 (46)	1,980 L (520 gal)	1,980 L (520 gal)	4,160 L (1,100 gal)	18,900+ L (5,000+ gal)	I.C.N.P
16 (52)	1,180 L (310 gal)	1,180 L (310 gal)	1,180 L (310 gal)	1,640 L (440 gal)	18,900+ L (5,000+ gal)
18 (59)	430 L (110 gal)	430 L (110 gal)	430 L (110 gal)	430 L (110 gal)	430 L (110 gal)

Key:
I.C.N.P – Internal aircraft ignition cannot be prevented under the assumed conditions.
Green: Time Region I
Blue: Time Region II
Red: Time Region III or IV
Black: Time Region V

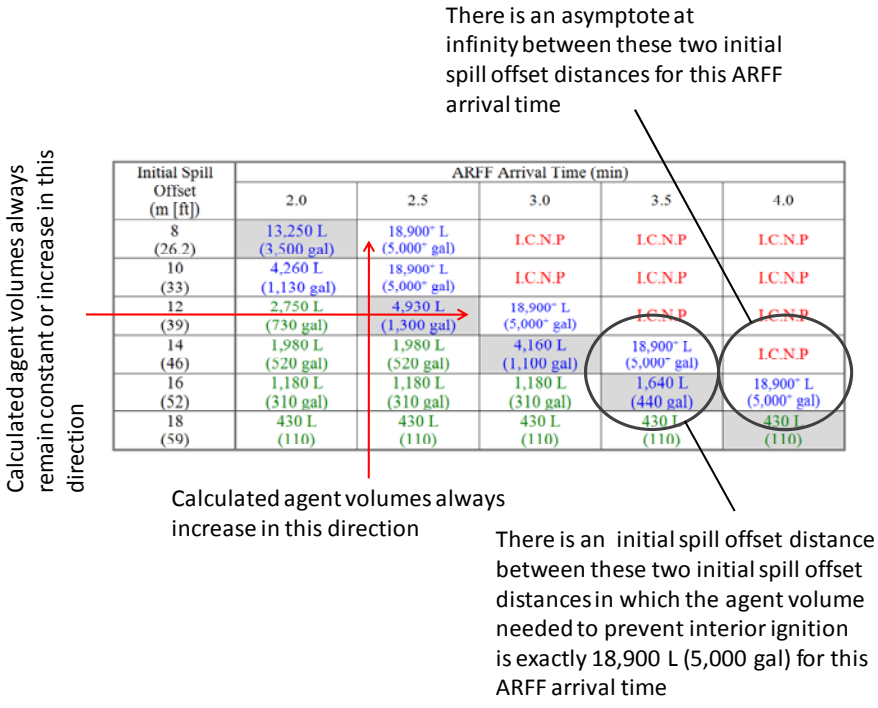

Figure 57. Illustration of the Calculated Agent Amount Trends for Preventing Interior Ignition (Scenario Group 1)

9. SUMMARY.

The amount of suppression agent necessary to prevent interior aircraft ignition and to allow for safe egress on the fire side of an aircraft was presented for representative fuel spill fire scenarios and ARFF arrival times. The scenarios considered wind conditions, aircraft and fuel spill fire sizes, aircraft skin thicknesses, and aircraft insulation/construction. The aircraft was assumed to be intact, and the fuel spill fires were not assumed to immerse any portion of the aircraft. An analysis of fuel spill fire scenarios that immerse portions of the aircraft concluded that interior ignition could occur in as little as 40 seconds, which is shorter than the assumed minimum ARFF arrival time.

Ignition of the aircraft interior was treated as a performance threshold because flashover conditions could develop within 60 seconds after interior ignition. This was consistent with observations from aircraft incidents and fuselage tests as well as with data obtained from interior fire spread in passenger rail cars. Not all interior ignition scenarios resulted in rapid development of flashover conditions, as this depended on the location of ignition, the type, and arrangement of collocated combustible material. Nevertheless, the analysis was based on the ignition time as a conservative performance threshold.

The model used to determine the ignition of the aircraft interior was derived using the minimum of two independent sets of criteria. The first criterion was based on the time required to melt any portion of the aircraft skin and was applicable only to high heat flux boundary conditions, given a melting temperature of approximately 649°C (1200°F). Interior ignition in this case was assumed 10 seconds after the skin melted, consistent with previous analysis approaches. The second criterion was based on the time required for the 204°C (400°F) isotherm to penetrate 1.1 cm (0.43 in.) into the insulation. This heuristic performance threshold was deduced from full-scale aircraft tests and the melting temperature of Tedlar®, a typical moisture barrier for aircraft insulations. This criterion typically applies to low heat flux boundary conditions (i.e., large offset distances or large-diameter fuel spill fires). To determine the melting times and isotherm penetration distances for scenario-specific transient exterior boundary fluxes, the heat transfer model HEATING was used. In this model, the aircraft skin and insulation were treated as a one-dimensional heat transfer system.

The model used to determine safe egress outside the aircraft was based on determining the distance at which the heat flux to a person would be equal to the pain threshold tenability limit, 2.5 kW/m² (0.22 Btu/s-ft²). This was a steady-state tenability limit; transient exposures and dose equivalents were not considered. Higher heat fluxes could result in second-degree burns or blistering in less than 60 seconds.

The heat flux at a target (aircraft skin or person) location was determined by computing the flame shape and view factor under a given wind condition. The fire was assumed to be equal to the plane length and extended indefinitely perpendicular to the plane fuselage. Targets were assumed to be rotated and elevated so that the view factor was maximized. The maximum elevation for a plane target location was 6.1 m (20 ft), and for a person, it was 1.8 m (6 ft). A person was also assumed to move to safety in a direction parallel to and within 1 m (3.3 ft) of the fuselage.

The heat flux was a direct function of the distance between the fire and the target for a given fuel spill fire scenario. The quantity of agent necessary to produce a favorable outcome (i.e., prevent ignition or allow safe egress) was determined, assuming that 5.2 L of agent was necessary to extinguish 1 m² (0.13 gal of agent/ft²) of burning fuel. In practice, the agent amount required to suppress the fire may be as low as 2.8 L of agent/m² (0.07 gal of agent/ft²) of burning fuel. The agent was assumed to consist of two amounts: an initial amount associated with the earliest response team, and an additional amount that arrives later and is tied to the required capacity of the airport ARFF. The initial agent amount was assumed to be used to prevent interior aircraft ignition delivered over a 60-second period, as is presently required. The additional agent amount was assumed to be used to suppress the fire to allow for safe egress outside the aircraft. Because egress was based on a steady-state threshold value, it was not necessary to assume an agent arrival or delivery time for the additional agent amount.

It was determined that an incident heat flux of 9.59 kW/m² (0.84 Btu/s-ft²) was the threshold value for causing the aircraft interior to ignite. The distance at which this flux occurs from the edge of the fire varied with the scenario but ranged from approximately 3 m (9.8 ft) for a downwind fire to 33 m (108 ft) for an upwind fire.

10. REFERENCES.

1. Scheffey, J.L., Darwin, R.L., and Hunt, S., "Methodologies for Calculating Firefighting Agen Quantities Needed to Combat Aircraft Crash Fires," FAA report DOT/FAA/AR-11/29, to be published.

2. National Fire Protection Association (NFPA) 403, "Aircraft Rescue and Fire-Fighting Services at Airports," National Fire Protection Association Standard 403, Quincy, Massachusetts, 2009.

3. Shokri, M. and Beyler, C.L., "Radiation Form Large Pool Fires," *SFPE Journal of Fire Protection Engineering*, Vol. 4, No. 1, pp.141-150, Boston, Massachusetts, 1989.

4. Mudan, K.S., "Thermal Radiation Hazards From Hydrocarbon Pool Fires," "Progress Energy Combustion Science," Vol. 10, 1984, pp. 59-80.

5. Mudan, K.S., "Geometric View Factors for Thermal Radiation Hazard Assessment," *Fire Safety Journal*, Vol. 12, No. 2, October 1, 1987.

6. Muñoz, M., Arnaldos, J., Casal, J., and Planas, E., "Analysis of the Geometric and Radiative Characteristics of Hydrocarbon Pool Fires," *Combustion and Flame*, No. 139, 2004, pp. 263-277.

7. Society of Fire Protection Engineers, "Assessing Flame Radiation to External Targets From Pool Fires," *SFPE Engineering Guide*, Society of Fire Protection Engineers, Bethesda, Maryland, 1999.

8. Childs, K.W., "HEATING 7: Multidimensional, Finite-Difference Heat Conduction Analysis Code System," Technical Report PSR-199, Oak Ridge National Laboratory (ORNL), Oak Ridge, Tennessee, 1998.

9. Webster, H., Geyer, G., Do, D., Wright, J., Collins, J., and Hampton, L., "Full-Scale Air Transport Category Fuselage Burnthrough Tests," FAA report DOT/FAA/CT-TN89/65, February 1990.

10. Webster, H., "Fuel Fire Penetration Test and Destruction of a Transport Aircraft," FAA report DOT/FAA/AR–96/48, December 1996.

11. Conley, E.W., "Post-Crash Fire-Fighting Studies on Transport Category Aircraft," Federal Aviation Agency, Systems Research & Development Service, Atlantic City, NJ, SRDS report No. RD-65-50, May 1965.

12. Society of Fire Protection Engineers, *SFPE Engineering Guide to Performance-Based Fire Protection Analysis and Design of Buildings*, National Fire Protection Association, Quincy, Massachusetts, 2000.

13. NFPA, "NFPA 101 Life Safety Code®," National Fire Protection Association, Quincy, Massachusetts, 2009.

14. Geyer, G.B, "Evaluation of Aircraft Ground Firefighting Agents and Techniques," AGFSRS 71-1, National Aviation Facilities Experimental Center, Atlantic City, New Jersey, February 1972.

15. Welker, J.R., "Prediction of Aircraft Damage Time in Post-Crash Fires," Final Report, University Engineers, Norman, Oklahoma, June 1968.

16. Sarkos, C.P., "Titanium Fuselage Environmental Conditions in Post-Crash Fires," FAA-RD-71-3, National Aviation Facilities Experimental Center, Atlantic City, New Jersey, March 1971.

17. Marker, T.R., "Full-Scale Test Evaluation of Aircraft Fuel Fire Burnthrough Resistance Improvements," FAA report DOT/FAA/AR–98/52, January 1999.

18. Purser, D.A., "Toxicity Assessment of Combustion Products," Section 2-5, *The Society of Fire Protection Engineers (SFPE) Handbook of Fire Protection Engineering*, 3rd Edition, Society of Fire Protection Engineers, Bethesda, Maryland, 2002.

19. Webster, H., "Fuselage Burnthrough from Large Exterior Fuel Fires," FAA report DOT/FAA/CT-90/10, July 1994.

20. Lattimer, B.Y. and Beyler, C.L., "Heat Release Rates of Fully-Developed Fires in Rail Cars," *Fire Safety Science—Proceedings of the Eighth International Symposium*, International Association for Fire Safety Science, London, United Kingdom, 2005.

21. Babrauskas, V., "Technical Note 1103," National Bureau of Standards, Gaithersburg, Maryland, 1979.

22. King, D.F., "Report on the Accident to Boeing 737-236 Series 1, G-GBJL at Manchester International Airport on 22 August 1985," Air Accident Report 8/88, Department of Transport, Air Accidents Investigation Branch, London, United Kingdom, December 15, 1988.

23. Cohn, B.M. and Campbell, J.A., "Minimum Needs for Airport Firefighting and Rescue Services," Report No. AS-71-1, Federal Aviation Administration, Airports Service, Washington, DC, January 1971.

24. Babrauskas, V., "Heat Release Rates," Sections 3-1, *The Society of Fire Protection Engineers (SFPE) Handbook of Fire Protection Engineering*, 3rd Edition, Society of Fire Protection Engineers, Bethesda, Maryland, 2002.

25. DiNenno, P.J., "Fuel Properties and Combustion Data," Appendix C, *The Society of Fire Protection Engineers (SFPE) Handbook of Fire Protection Engineering*, 3rd Edition, Society of Fire Protection Engineers, Bethesda, Maryland, 2002.

26. Gottuk, D.G. and White, D.A., "Liquid Fuel Fires," Sections 2-15, *The Society of Fire Protection Engineers (SFPE) Handbook of Fire Protection Engineering*, 3rd Edition, Society of Fire Protection Engineers, Bethesda, Maryland, 2002.

27. Thomas, P.H., "The Size of Flames From Natural Fires," *Ninth Symposium (International) on Combustion*, Combustion Institute, Pittsburg, Pennsylvania, 1962.

28. Yuan, L. and Cox, F., "An Experimental Study of Some Line Fires," *Fire Safety Journal*, Vol. 27, 1996.

29. Heskestad, G., "Fire Plumes, Flame Height, and Air Entrainment," Section 2-1, *The Society of Fire Protection Engineers (SFPE) Handbook of Fire Protection Engineering*, 3rd Edition, Society of Fire Protection Engineers, Bethesda, Maryland, 2002.

30. SFPE, "The SFPE Engineering Guide for Piloted Ignition of Solid Materials Under Radiant Exposure," Society of Fire Protection Engineers , Bethesda, Maryland, January 2002.

31. AGA, "LNG Safety Research Program," Report IS 3-1, American Gas Association, Washington, DC, 1974.

32. Williamson, R.B., Revenaugh, A., and Mowrer, R.W., "Ignition Sources in Room Fire Tests and Some Implications for Flame Spread Evaluation," *Proceedings of the Third International Symposium on Fire Safety Science*, Elsevier Applied Science, New York, New York, 1991.

33. Lattimer, B.Y., "Heat Fluxes From Fires to Surfaces," Sections 2-14, *The Society of Fire Protection Engineers (SFPE) Handbook of Fire Protection Engineering*, 3rd Edition, Society of Fire Protection Engineers, Bethesda, Maryland, 2002.

34. Siegel, R. and Howell, J.R., *Thermal Radiation Heat Transfer*, Taylor & Francis, New York, New York, 2002.

35. Eklund, T., Wright, J., Fann, F., and Berenotto, J., "Preliminary Evaluation of the Performance of Advanced and Conventional Aircraft Windows in a Model Fire Environment," NAFEC Technical Letter Report NA-80-17-LR, Federal Aviation Administration, National Aviation Facilities Experimental Center, Atlantic City, NJ, May 1980.

36. Holman, J.P., *Heat Transfer*, Seventh Edition, McGraw-Hill Publishing Company, New York, New York, 1990.

37. Incropera, F.P. and De Witt, D.P., *Fundamentals of Heat and Mass Transfer*, Second Edition, John Wiley & Sons, New York, New York, 1985.

38. Bryan, C.B., Childs, K.W., and Giles, G.E., "HEATING6 Verification," Technical Report K/CSD/TM-61, Oak Ridge National Laboratory, Oak Ridge, Tennessee, 1986.

39. Chu, W., "HEATCHEK: A Computer Program to Automate Verification of New Versions of HEATING," Technical Report K/CSD/INF-89/4, Union Carbide Corp., Nuclear Division, Gaseous Diffusion Plant, Oak Ridge, Tennessee, 1989.

40. Tatem, P.A., Budnick, E.K., Hunt, S.P., Trelles, J., Scheffey, J.L., White, D.A., Bailey, J., Hoover, J., and Williams, F.W., "Verification and Validation Final Report for Fire and Smoke Spread Modeling and Simulation Support of T-AKE Test and Evaluation," NRL/MR/6180-04-8746, Naval Research Laboratory, Washington, DC, 2004.

41. Tien, C.L., Lee, K.Y., and Stretton, A.J.,"Convection Heat Transfer," Sections 1-4, *The Society of Fire Protection Engineers (SFPE) Handbook of Fire Protection Engineering*, 4th Edition, Society of Fire Protection Engineers, Bethesda, Maryland, 2002.

42. Quintiere, J.G., "Surface Flame Spread," Sections 2-12, *The Society of Fire Protection Engineers (SFPE) Handbook of Fire Protection Engineering*, 3rd Edition, Society of Fire Protection Engineers, Bethesda, Maryland, 2002.

43. Quintiere, J.Q., *Principles of Fire Behavior*, Delmar Publishers, New York, New York, 1998.

44. DuPont, "Tedlar® SP," Product Information Sheet 234452C, DuPont, Buffalo, New York, January 1996.

45. American Society for Testing and Materials (ASTM) E 119-05, "Standard Test Methods for Fire Tests of Building Construction Materials," American Society for Testing and Materials, West Conshohocken, Pennsylvania, 2005.

46. Farlow, S.J., *Partial Differential Equations for Scientists and Engineers*, Dover Publications, Inc., New York, New York, 1993.